

541.385
1992
AL-*

**A THEORETICAL STUDY OF THE
ELECTROCATALYTIC PHENOMENA
IN FUEL CELLS**

A Thesis Submitted in Partial Fulfillment
of the Requirements for the Degree of
MASTER OF PHILOSOPHY

BY

AL-NAKIB CHOWDHURY



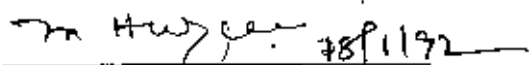
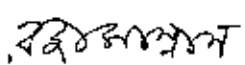
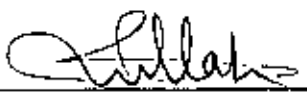
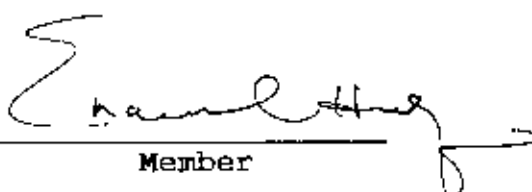
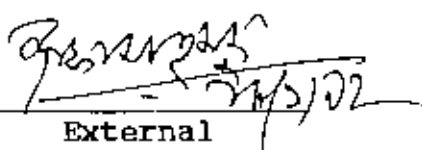
**DEPARTMENT OF CHEMISTRY
BANGLADESH UNIVERSITY OF ENGINEERING & TECHNOLOGY
DHAKA**

JANUARY 1992



THESIS APPROVAL SHEET

Thesis entitled "A Theoretical Study of the Electrocatalytic Phenomena in Fuel Cells" by Al-Nakib Chowdhury is approved for the Degree of Master of Philosophy.

1. Dr. Monimul Huque
Associate Professor
Dept. of Chemistry
BUET, Dhaka.

Supervisor and Chairman
Examination Committee
2. Dr. R. J. Mannan
Professor
Dept. of Chemistry
University of Dhaka.

Co-Supervisor
3. Dr. Md. Rafique Ullah
Assistant Professor
Dept. of Chemistry
BUET, Dhaka.

Member
4. Dr. Enamul Huq
Professor & Head
Dept. of Chemistry
BUET, Dhaka.

Member
5. Dr. A. J. Mahmood
Professor
Dept. of Chemistry
University of Dhaka.

External

ACKNOWLEDGEMENT

It is the greatest opportunity for me to express my sincere gratitude to my reverend teachers Dr. R. J. Mannan, Professor of Chemistry, University of Dhaka and Dr. Monimul Haque, Associate Professor of Chemistry, BUET, for their farsighted guidance and suggestion throughout the progress of the work and during the preparation of the manuscript of this thesis.

I am gratefully indebted to Dr. Enamul Huq, Head and Professor of Chemistry, BUET and Mr. Nurul Islam, Assistant Professor of Chemistry, BUET for their valuable suggestions and providing me with all possible help when required. I would like to express my warmest thanks to Mr. Maniruzzaman, Assistant Professor of Mechanical Engineering, BUET and Dr. Azmal Hossain, for their sincere co-operation and encouragement during the work.

I also thank Mr. Md. Abdul Jalil Sarder, Mech. Engg. Department BUET, for typing this thesis very sincerely.

Finally I would convey my thanks to all of my colleagues of Chemistry Department, BUET, for their co-operation and constant help.

CONTENTS

	Page
CHAPTER 1 INTRODUCTION	
1.1 Sources and Form of Energy	1
1.2 Methods of Direct Energy Conversion	1
1.3 Fuel Cells and Their Classification	10
1.4 Thermodynamic Aspects of Fuel Cell	12
1.5 Efficiency of Electrochemical Energy Conversion	18
1.6 Factor Affecting Efficiency of Electrochemical Energy Conversion	20
1.7 Difference Between Heat Engine and Electrochemical Energy Convertors.....	22
1.8 Electrode Kinetics	27
1.9 Electrocatalysis	36
1.9.1 Distinctive Feature of Electrocatalysis.	39
1.9.2 Factors Affecting Electrocatalysis.....	44
1.9.3 New Types of Electrocatalysts.....	51
CHAPTER 2 SOLID STATE CHEMISTRY	
2.1 Early Works on Semiconductors	54
2.1.1 "Excess" and "Defect" Semiconductors ..	54
2.1.2 Surface and Bulk Effects	55
2.2 Defect Solid	55
2.2.1 Impurities	55

	Page
2.2.2 Interstitial Atoms and Vacancies	56
2.2.3 Dislocations	57
2.2.4 Polygonization and Dislocation Walls ..	57
2.3 Energy-Band Model of Solids	58
2.3.1 Energy bands	58
2.3.2 Density of States	59
2.3.3 Intrinsic Semiconductor	61
2.3.4 Conduction by Electrons and Holes	63
2.4 Extrinsic Semiconductor	64
CHAPTER 3 CHARGE TRANSFER PROCESS	
3.1 Charge Transfer Processes at Metal Electrode.	68
3.2 Charge Transfer processes at Semi-conductr Electrode	74
3.3 Some Principles of Charge Transfer at Semiconductor Electrode and Experimental Techniques	81
3.3.1 Current Potential Curves	83
3.3.2 Injection Process	85
3.3.3 Photocurrents	86
3.4 Charge Transfer Process	87
3.4.1 Charge Exchange	87
3.4.2 Energy Level in Solution Redox Systems..	90
3.4.3 Current-Potential Curves	91
3.4.4 Charge Transfer Process via surface States	97
3.5 Quantum Mechanical Aspects of Charge Transfer	98

	Page
CHAPTER 4	PRESENT WORK ON THE FACTORS AFFECTING ELECTROCATALYSIS
4.1	General..... 107
4.2	General Studies on Electrocatalysis on Various Types of Electrode 107
4.2.1	Types of Metal Electrodes 108
4.2.2	Alloy Electrodes 112
4.2.3	Metal Oxides and Semiconductor Electrodes. 116
4.2.4	Non-metal Electrodes 121
4.3	Phenomena of Oxidation of Organic Compunds used in Fuel Cells 124
4.4	Conclusion 130
	REFERENCES 133

ABSTRACT

The Electrochemical energy convertors known as fuel cells have several advantages over the conventional power sources. They are intrinsically much more efficient than the conventional power sources. In addition, they are noise and pollution free. Theoretically their efficiency can be 100% in contrast to the carnot limitation of heat - mechanical energy - electricity type of power generators.

This work have been undertaken to survey the present state of development of fuel cells, analyse the various factors that are hindering the more efficient performance of fuel cells and indicate where the emphasis for the future trend of research should be given.

The thermodynamic principles of fuel cells, factors effecting the rates of electrochemical reactions occurring in the cells have been discussed.

The role of electrodes in the overall performance of these cells have been found to be of utmost importance. With great technological advancement in the development of new materials which have semiconducting property and are quite stable in the conditions

of electrochemical cells, great advancement in the types and efficiency of fuel cells have began. Principles of electrochemical reactions on semiconducting materials have been discussed. These compounds have tremendous potentials as electrodes in fuel cells of future.

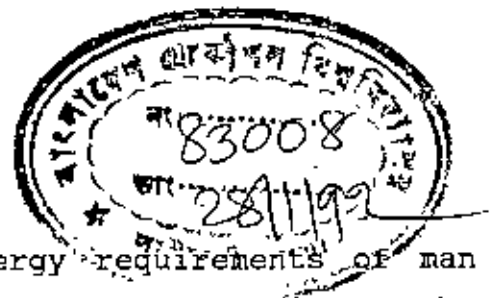
The phenomena of electrocatalysis has great bearing in the improvement of the efficiency of fuel cells. The factors which are influencing this phenomena have been discussed and quantitative expressions were derived which indicate the future trend of research.

Theoretical expressions relating the charge transfer phenomena in solids to a typical electrochemical condition have been developed. Research in this direction will help us to derive more accurate rate expressions.

The current experimental work done in various laboratories around the world have been thoroughly surveyed and it was found that although much of the work dealt with developing new electrode materials and testing their performance in the typical conditions of fuel cells, much more systematic work in reference to a potential indicating a standard state of the electrode surface must be undertaken to make fuel cells as acceptable alternative power sources.

CHAPTER 1

INTRODUCTION



1.1 Sources and Forms of Energy :

With the passage of time, the energy requirements of man increases. Electrical energy is the one and only form which can be easily made, is convenient to transport, and can be used in a controlled manner.

Since the form of energy most frequently required by man is electricity, it is obvious that one would look for direct methods of conversion of energy from its primary sources. The primary sources of energy can be classified as solar, gravitational, geothermal and chemical energy.

The conventional methods for the conversion of energy from their primary forms, pass through the intermediate stage of conversion of heat energy into mechanical energy. Thus, inherent in them is the carnot limitation. On the otherhand direct methods of energy conversion receives more attention because of simplicity, reliability and lessened weight and volume required in these methods. If conversion of energy from a primary source to electricity can be made in one step, the efficiency should be higher than were the conversion to occur in many more steps apart from consideration of the carnot cycle, which limits the efficiency of conventional indirect and of some direct methods.

1.2 Methods for Direct Energy Conversion :

Various methods for direct energy conversion have already been reported. These include :

- (i) **Thermoelectric energy converters :** This method¹⁻³ is based on the Seebeck effect. According to this effect, a potential gradient is set up when junctions of two dissimilar conducting or semi-conducting materials are maintained at different temperatures. Thus when the ends of the materials are connected through a load, a flow of current will be observed.

The efficiency of a thermoelectric generator is given by

$$e = \frac{T_1 - T_2}{T_1} \frac{1}{F(M)} \quad (1.1)$$

Where

$$F(M) = 1 + \frac{Z}{T_1 Z} + \frac{M}{T_1 Z} + \frac{1}{M} \left(\frac{1}{2} \cdot \frac{T_1 + T_2}{T_1} + \frac{1}{T_1 Z} \right) \quad (1.2)$$

M is given by

$$M = \frac{(T_1 - T_2) S - IR_1}{IR_1} \quad (1.3)$$

and Z is given by, $Z = \frac{S}{K\rho}$

T_1 and T_2 are the temperatures at the hot and cold junctions, I is the current flowing through the generator, R_1 is its resistance, S is the thermoelectric voltage per degree due to seebeck effect, K is the thermal conductivity of the material, and ρ is its electrical resistivity. The limiting efficiency (the carnot efficiency) occurs when F(M) in equation (1.1) is unity. F(M) reaches unity when Z is very large. High values of Z are obtained by using materials which have a large value of S and low value of K and ρ .

The terminal voltage, E can be expressed as

$$E = S(T_1 - T_2) - IR_1 \quad (1.4)$$

Therefore the power output is given by

$$P = I[S(T_1 - T_2) - IR_1] \quad (1.5)$$

The energy per unit weight for thermoelectric converter are small, mainly because the required ratios of electrical to thermal conductivity for high figures of merit are found only with the heavy materials. All thermoelectric materials

presently known are unstable. They sublime readily and hence there is an upper limit to the temperature at which these materials may be used. The mechanical properties of the thermoelectric materials are also very poor. Most of these materials are very brittle and difficult to fabricate. Prospects of future applications of thermoelectric devices are not too optimistic because large temperature differences are necessary for high efficiencies, which lead to material instability or diffusion of doping agents across the junction of the two metals. The overall efficiency of thermoelectric generators is of the order of only a few percent. Isotope thermoelectric are currently being designed for space application² such as in SNAP 27.

- (ii) Thermoionic energy converter : Thermoionic energy conversion is the direct conversion of heat to electricity by the heating of an emitter (cathode) to a high temperature and a consequent emission of electrons from it. The electrons reach the collector (anode), which is at a considerably lower temperature and then pass through an external circuit before finally returning to the cathode. Solar, nuclear or chemical energy may be used as the heat source. The use of nuclear fission as a heat source appears attractive since the fuel element may itself be used as the electron emitter (cathode).

The efficiency ϵ of the thermoionic energy converter is defined as the ratio of its power output per unit area of the cathode divided by the heat input into the cathode for the same area. The latter can be calculated if it is assumed that only energy losses from the electrodes are the electrical energies leaving them, together with the thermal energy of these electrons, that is $2kT$ per electron. At a current density of i_a , the number of electrons $\text{sec}^{-1} \text{cm}^{-2}$ is i/e , and hence the loss of energy due to the thermal energy of the escaping electron is $i2kT/e$. Thus the total loss at an

electrode per unit time is $iV + i_2kT/e$. Hence the efficiency is

$$\epsilon = \frac{(i_c - i_a) - (V_c - V_a)}{i_c(V_c + 2kT_2/e) - i_a(V_a + 2kT_2/e)} \quad (1.6)$$

where, i_c represents the current density at which emission occurs from the emitter at a temperature T_1 and i_a is the current density at the collector at temperature T_2 , V_a and V_c are the potentials of the collector and emitter respectively.

Generally the reverse current is small. Hence, when $i_c \gg i_a$ the expression for ϵ in equation (1.6) reduces to

$$\epsilon = \frac{V_c - V_a}{V_c + 2kT_1/e} \quad (1.7)$$

The powder density of a thermionic energy converter is given by

$$P = (i_c - i_a) - (V_c - V_a) \quad (1.8)$$

the closer the values of V_c and V_a to their respective work functions, the better is the performance of the thermionic energy converter.

During the last decade considerable improvements have been made in thermal ionic energy conversion. Devices with lifetime of over 10,000 hr. have been built power densities of the order of 40 Watts cm^{-2} have been attained for some systems using cathodes operating at a temperature of 2000°k. Progress in materials preparation and in an understanding of additives can be expected to lead to long life converters with overall systems efficiencies of about 15%. A disadvantage of the method is that high temperatures are required, which leads to problems of material stability. The area of nuclear-reactor thermionic receiving a great of attention. A combination of a nuclear thermionic and a liquid-metal turbine cycle could lead to systems which might have an overall efficiency about 40% and may be considered for large-scale power generation. Though

somewhat heavy solar thermionic generators are particularly suited for long-space application'.

- (iii) Photovoltaic energy converters : This method unlike the preceding methods, involves conversion of light energy into electricity. It is the only direct-energy conversion method, apart from the electrochemical one, which is free of the carnot limitation. The photovoltaic effect was first discovered by Becqerel, who observed a voltage change on exposing an electrode in solution to light. A photoelectric energy converter is made by exposing light to an n-p junction. A photon with sufficient energy collides with an electron and transfers its energy to the latter. The electron may then have sufficient energy to become free and hence create a hole. This process can occur across the n-p junction. the p type region becomes positive and the n type region negative. When the two regions are connected through an external load, a part of the current I_0 flows through this load.

The current-density-voltage relation at a n-p junction across which a potential drop V exists is

$$i_j = i_L (1 - \exp \frac{V}{RT}) \quad (1.9)$$

Where i_j is the total current due to both hole and electron flow across the junction and i_L is the dark or saturation current density that flows through an external load is given by

$$i = i_p + i_j \quad (1.10)$$

Where i_p is the current density arises due to the transfer of electron across the n-p junction by exposure of the p side of the cell to light.

Combining equation (1.9) and (1.10)
The power density is expressed by

$$i = i_p - i_L \left[\exp\left(\frac{VF}{RT}\right) - 1 \right] \quad (1.11)$$

$$p = iV = V \{ i_p - i_L \left[\exp\left(\frac{VF}{RT}\right) - 1 \right] \} \quad (1.12)$$

The efficiency of conversion is the ratio of the electrical power output to the photon energy input in unit time. Thus

$$\epsilon = \frac{iV}{N_p e E_p} \quad (1.13)$$

Where N_p is the number of incident photons per square centimeter of surface in unit time, e is the electronic charge, and E_p is the average photon energy in electron volts. The maximum efficiency predicted according to this equation for solar cells is of the order of 20%.

The biggest advantage of this type of energy converter is that it converts solar energy directly into electrical energy. The fuel cost is thus zero. This advantage is to a great extent offset by the fact that the large areas of the solar cells are required for any desired power level. An increasing amount of attention is being given to "thin film" photovoltaic cells. A significant advantage of solar cells is that they are relatively light (100 Watts lb^{-1}) compared with some other direct-energy-conversion devices such as thermoelectric one. Solar cells ranging in power levels from a few hundred milliwatts to a kilowatt have been developed for space applications. They have long life, which is another advantage for long duration space missions. They do not require high operating temperatures. During the daytime, the solar cell is used as the power supply for the necessary applications and also regeneration of hydrogen and oxygen from water, which is the fuel cell product formed during the dark periods when the fuel cell is used as the power source. Some of the problems with solar cells are radiation damage and temperature

degradation. There is a considerable amount of work in progress to reduce these effects in solar cells.

- (iv) **Magnetohydrodynamic (MHD) energy converters** : this method involves, a high-temperature plasma, consisting of a mixture of positive and negative ions, moves through a magnetic field and in a direction perpendicular to it. Under these conditions, an electric field is induced in a direction mutually perpendicular to the direction of the magnetic field and the direction of the particles and the positive ions and electrons will be directed toward opposite electrodes. If the two electrodes are connected externally through a load, then a current will flow through this circuit. Thus, in a magnetohydrodynamic generator, the translational energy of the ionized particles is converted to electrical energy.

The electric potential developed across the electrodes under open circuit conditions E_0 is given by

$$E_0 = Bvd \quad (1.14)$$

Where B is the strength of the magnetic field, v is the velocity of the hot ionized gas and d is the distance between the electrodes.

The internal resistance R_i of the generator per square centimeter is given by

$$R_i = \frac{d}{\sigma} \quad (1.15)$$

Where σ is the specific conductivity of the ionized gas between the electrodes. The current density obtained in the external circuit when the external resistance is R_e is expressed by

$$i = \frac{E_0}{R_i + R_e} \quad (1.16)$$

The power density of the MHD generator is given by

Where E is the potential difference across the terminals of

$$P = E_1 \quad (1.17)$$

the electrodes. The efficiency of conversion is the ratio of the power output to the enthalpy flux ΔH into the generator. Thus

$$c = \frac{E_1}{\Delta H} \quad (1.18)$$

Where ΔH is the heat input into the generator in unit time. Since there is a conversion of heat to electricity, the Carnot limitation applies. However, since very high temperatures are used, the maximum efficiencies are high⁵ being from 50 to 60 percents.

Magnetohydrodynamic energy conversion is being mainly considered for large scale power generation. There are no moving parts and thus mechanical problems are eliminated. The higher temperature of the working fluids used here as opposed to those used in conventional power plants makes it possible to attain higher efficiencies. The use of MHD generators is attractive because of the relatively high efficiencies. The hot ionized gases can be recirculated. Under these conditions, MHD generators should prove to be competitive with conventional engine generators. There is a greater enthusiasm about the development of MHD generators in Europe than in the United States⁶.

- (v) Electrochemical energy convertors : Electrochemical energy conversion is the conversion of the free energy change of a chemical reaction directly into electrical energy. The relation between the free energy change of a chemical reaction, ΔG , and the thermodynamic reversible potential of the cell, E_r is given by

$$\Delta G = -nFE_r \quad (1.19)$$

Where n is the number of electrons transferred from the anode

to the cathode during done act of the overall reaction and F is the Faraday constant.

In an electrochemical electricity producer, the anodic and cathodic reactants are fed into their respective chambers. The electrolyte layer is between the two electrodes. The half-cell reaction at the anode yields electrons, which are transported through the external circuit and reach the cathode. These electrons are then transferred to the cathodic reactant. The circuit is completed by the transport of the ions from one electrode to the other through the electrolyte.

In the case of a fuel cell which acts ideally, the terminal-cell potential is constant and is equal to the thermodynamic reversible potential of the cell at any value of the current density drawn from the cell. The ideal efficiency of an electrochemical energy converter is defined by the equation

$$\epsilon = \frac{\Delta G}{\Delta H} = - \frac{nFE_c}{\Delta H} \quad (1.20)$$

Generally, ΔG is quite close to ΔH and hence the efficiency of fuel cell which perform ideally would be close to unity. In case of practically all fuel cells the terminal-cell potential decreases with increasing current density drawn from the cell. This is due to the development of overpotential across the electrode. Under these conditions, the efficiency is expressed as

$$\epsilon = - \frac{nFE}{\Delta H} \quad (1.21)$$

Where E is terminal-cell potential of the non-ideal electrochemical energy converter.

The terminal-cell potential current-density relation from a cell is not fundamental one for a cell. From it, the expression for the efficiency of a cell is obtained using

equation (1.21). Also one can obtain the power-density P -current density i relation for the cell. This relation is given by

$$P = iE \quad (1.22)$$

E is expressed as a function of current density.

The attractive feature of electrochemical energy conversion is the prospect of achieving very high efficiencies. To a large extent, this promise has already been fulfilled, e.g. hydrogen-oxygen, hydrazine-oxygen, lithium-chlorine, and hydrogen-bromine fuel cells. Another advantage is that high energy/weight or energy/volume ratios can be obtained. They are higher than the corresponding ratios of any other mode of converting energy for systems in which energy must be supplied without refueling for the range 10 to 1000 hr. It is this advantage which has made the fuel cell the forerunner for space power system. Besides space applications, many other have been considered, particularly with respect to mobile power, small unit as a source of electric power for homes, industries etc. There are many applications for direct current, as, for example in the case of many manufacturing processes and for some considered forms of future transportation in which trains run in tubes under the influence of linear accelerators. For applications needing alternating current, conversion from direct current can be made without significant loss of efficiency.

1.3 Fuel Cells and Their Classification :

Basically the objective of fuel cells is the conversion of the energy of the chemical reactions directly into electricity.

Several methods of classification of fuel cells have appeared in the literature. In arriving at a systematic classification one of the difficulties is that several operational variables exist.

Fuel cell may be classified according to the temperature range in which they operate- low temperature (25 to 100°C), medium temperature (100 to 500°C), high temperature (500-1000°C), and very high temperature (above 1000°C). Another method would be according to the type of electrolyte, e.g. aqueous, nonaqueous, molten or solid. One could also classify fuel cells according to the physical state of the fuel: gaseous- hydrogen, lower hydrocarbons, liquid; alcohols, hydrazine, higher hydrocarbons; solids; metals; etc.

In the present literature, a broad division is first made according to whether the fuel-cell system is a primary or secondary one. A primary fuel cell may be defined as one in which the reactant is passed through the cell only once, the products of the reaction being discarded. A secondary fuel cell is one in which the reactants are passed through the cell many times because they are regenerated from the products by thermal, electrical photochemical, or radiochemical methods.

Primary fuel cells are further divided into various types depending on the kind of fuel and oxidant used. Oxygen is the most common oxidant, but air is generally substituted for oxygen. Under primary cells, the hydrogen-oxygen system is the most advanced system. The next most researched fuel-cell system is the one using organic fuels (e.g. hydrocarbons, alcohols). The carbon-oxygen system is then dealt with. This was one of the earliest system. A system of interest is carbon monoxide-air. Some work is being carried out with nitrogenous fuels (e.g. ammonia, hydrazine), which come next on the list of primary fuel cells. Metal may be used in a fuel cell although usually regeneratively. In these cases, air or the halogens may be used as the oxidant. Each type is further subdivided into flow, intermediate and high temperature systems. Another fuel cell known as the biochemical fuel cell, is an entirely different type of electrochemical energy converter.

1.4 Thermodynamic Aspects of Fuel Cell :

The basic functions in thermodynamics are internal energy E , enthalpy H , entropy S , Helmholtz free energy A , and Gibbs free energy G .

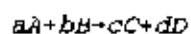
It is more practical to carry out reactions at a constant temperature and pressure rather than at constant temperature and volume and therefore the change in Gibbs free energy is more useful than the change in Helmholtz free energy. The free energy change of a chemical reaction is a measure of the maximum net work obtainable from the reaction. It is equal to enthalpy change of the reaction only if the entropy change of the reaction ΔS is zero, as may be seen from the equation

$$\Delta G = \Delta H - T\Delta S \quad (1.23)$$

The chemical potential of any substance may be expressed by an equation of the form

$$\mu = \mu^\circ + RT \ln a \quad (1.24)$$

Where a is the activity of the substance and μ° when a is unity. The Gibbs free energy change ΔG of the reaction



is given by $\Delta G = c\mu_c + d\mu_d - a\mu_a - b\mu_b$ (1.25)

The standard free energy change ΔG° of the reaction is then given by equation (1.25), with the chemical potentials of all species replaced by their standard chemical potentials.

$$\Delta G^\circ = c\mu_c^\circ + d\mu_d^\circ - a\mu_a^\circ - b\mu_b^\circ \quad (1.26)$$

Substitution of equation (1.24) for each of the reactants and products and equation (1.26) into equation (1.25) gives

$$\Delta G = \Delta G^\circ + RT \ln \frac{a_c^c a_d^d}{a_a^a a_b^b} \quad (1.27)$$

For a process at constant temperature and pressure at equilibrium, the free energy change is zero. Thus with the free energy change as zero in equation (1.27), it follows that

$$\Delta G^\circ = -RT \ln \frac{a_c^c a_d^d}{a_a^a a_b^b} \quad (1.28)$$

$$= -RT \ln K \quad (1.29)$$

Where K is the equilibrium constant for the reaction.

The knowledge of ΔG° allows ΔG to be calculated for any composition of reaction mixture. Knowledge of ΔG indicates whether a reaction will occur or not. If ΔG is positive, a reaction can not occur for the assumed composition of reactant and products. If ΔG is negative a reaction can occur.

The relation between the free-energy change in a cell reaction and the cell potential ; The enthalpy change of a reaction may be written as

$$\Delta H = \Delta E + P\Delta V = Q - W + P\Delta V \quad (1.30)$$

Where ΔE , Q and W are the internal energy, heat absorbed and work done by the system respectively.

If the same reaction is carried out electrochemically, W in equation (1.30) is then, not only the work of expansion but also the electrical work involved in transporting the charges around the circuit from the anode to the cathode at which the potentials are V_a and V_c respectively. The maximum electrical work that can be done per act of an overall reaction (W'_{el}) carried out in a cell and that

$$W'_{el} = ne(V_c - V_a) \quad (1.31)$$

involves transfer of n electrons per act of the overall reaction is for a hypothetical case in which the internal resistance of the cell overpotential losses are negligible. Converting to molar quantities, it is necessary to multiply W'_{el} by N , the Avogadro number; and since the product of electronic charge and Avogadro's number is the Faraday,

$$W_{el} = nF(V_c - V_a) \quad (1.32)$$

Since the only forms of work involved in the working of electrochemical cell are electrical work and work of expansion,

$$W = W_{el} + P\Delta V \quad (1.33)$$

If, in addition, the process is carried out reversibly,

$$Q = T\Delta S \quad (1.34)$$

Using equations (1.30) and (1.32) to (1.34) it follows that

$$\Delta H = T\Delta S - nF(V_c - V_a) \quad (1.35)$$

By comparison of equation (1.35) with equation (1.23), which holds for an isothermal process, the important relation arises is

$$\Delta G = - nF(V_c - V_a) \quad (1.36)$$

Writing $V_c - V_a = E$, equation (1.36) becomes

$$\Delta G = -nFE \quad (1.37)$$

Where E is the electromotive force of the cell.

If the reactants and the products are all in their standard states it follows that

$$\Delta G^\circ = -nFE^\circ \quad (1.38)$$

Standard reversible potentials and their temperature and pressure co-efficient for some Fuel-cell reactions : Calculation of standard thermodynamic reversible cell potentials are relatively simple. It is the first step in determining the usefulness or potential fuels. Temperature and pressure co-efficient of the standard reversible potentials may also be calculated by using appropriate relations. The standard thermodynamic reversible cell potentials and the temperature and pressure co-efficient of the standard thermodynamic reversible potentials for a number of fuel-cell reactions are given in Table-I.1.

Heat change in an ideally operating Fuel Cell : Chemical energy in thermal engines is first released as heat, which then

TABLE 1.1. Thermodynamic Data for Fuel Cell Reaction

Reaction	ΔG° , kcal mole ⁻¹	ΔH° , kcal mole ⁻¹	n	Δn	E° , volts	$\partial E^\circ/\partial T$, mv/°C	$\partial E^\circ/\partial \log P_i$, mv	ϵ_i
Temperature, 25°C								
1. $H_2 + \frac{1}{2}O_2 \rightarrow H_2O$	-56.69	-68.32	2	-1.5	1.229	-0.84	45	0.830
2. $CH_4 + 2O_2 \rightarrow CO_2 + 2H_2O$	-195.50	-212.80	8	-2	1.060	-0.31	15	0.919
3. $C_2H_6 + \frac{7}{2}O_2 \rightarrow 2CO_2 + 3H_2O$	-350.73	-372.82	14	-2.5	1.087	-0.23	10.7	0.941
4. $C_3H_8 + 5O_2 \rightarrow 3CO_2 + 4H_2O$	-503.93	-530.61	20	-3	1.093	-0.19	9	0.950
5. $C_4H_{10} + \frac{13}{2}O_2 \rightarrow 4CO_2 + 5H_2O$	-656.74	-687.99	26	-3.5	1.095	-0.17	8	0.955
6. $C_6H_{12} + 8O_2 \rightarrow 6CO_2 + 6H_2O$	-809.48	-845.17	32	-4	1.097	-0.16	7.5	0.958
7. $C_8H_{18}(g) + \frac{25}{2}O_2 \rightarrow 8CO_2 + 9H_2O$	-1268.43	-1317.46	50	-5.5	1.100	-0.14	6.6	0.963
$C_8H_{18}(l) + \frac{25}{2}O_2 \rightarrow 8CO_2 + 9H_2O$	-1265.87	-1307.54	50	-4.5	1.098	-0.12	5.4	0.968
8. $C_{10}H_{22}(g) + \frac{31}{2}O_2 \rightarrow 10CO_2 + 11H_2O$	-1574.42	-1632.35	62	-6.5	1.101	-0.13	6.3	0.965
$C_{10}H_{22}(l) + \frac{31}{2}O_2 \rightarrow 10CO_2 + 11H_2O$	-1574.42	-1632.35	62	-6.5	1.101	-0.13	6.3	0.965
9. $CH_3OH(g) + \frac{3}{2}O_2 \rightarrow CO_2 + 2H_2O$	-168.05	-182.61	6	-1.5	1.215	-0.35	15	0.920
$CH_3OH(l) + \frac{3}{2}O_2 \rightarrow CO_2 + 2H_2O$	-167.91	-173.67	6	-0.5	1.214	-0.13	5	0.967
10. $NH_3 + \frac{3}{2}O_2 \rightarrow \frac{1}{2}N_2 + \frac{3}{2}H_2O$	-85.04	-91.44	3	-1.25	1.225	-0.31	25	0.930
11. $N_2H_4 + O_2 \rightarrow N_2 + 2H_2O$	-143.81	-148.69	4	-1	1.560	-0.18	15	0.967
12. $C + \frac{1}{2}O_2 \rightarrow CO$	-32.81	-26.42	2	+0.5	0.711	+0.46	-15	1.24
13. $C + O_2 \rightarrow CO_2$	-94.26	-94.05	4	0	1.022	0	0	1.002
14. $CO + \frac{1}{2}O_2 \rightarrow CO_2$	-61.45	-67.63	2	-0.5	1.333	-0.44	15	0.909
15. $Li + \frac{1}{2}Cl_2 \rightarrow LiCl(g)$	-58	-53.00	1	0.5	2.515	-0.72	-30	1.094
Temperature, 150°C								
1. $H_2 + \frac{1}{2}O_2 \rightarrow H_2O$	-52.94	-58.142	2	-0.5	1.14799	-0.25	21	0.911
2. $CH_4 + 2O_2 \rightarrow CO_2 + 2H_2O$	-191.29	-191.42	8	0	1.03702	0	0	0.999
3. $C_2H_6 + \frac{7}{2}O_2 \rightarrow 2CO_2 + 3H_2O$	-346.99	-340.66	14	0.5	1.07491	+0.04	-3	1.019
4. $C_3H_8 + 5O_2 \rightarrow 3CO_2 + 4H_2O$	-499.54	-487.82	20	1	1.08324	+0.05	-4.2	1.024
5. $C_4H_{10} + \frac{13}{2}O_2 \rightarrow 4CO_2 + 5H_2O$	-651.94	-634.29	26	1.5	1.08747	+0.06	-4.9	1.028
6. $C_6H_{12} + 8O_2 \rightarrow 6CO_2 + 6H_2O$	-804.98	-781.19	32	1	1.09099	+0.07	-5.4	1.030
7. $C_8H_{18} + \frac{25}{2}O_2 \rightarrow 8CO_2 + 9H_2O$	-1263.72	-1221.70	50	3.5	1.09614	+0.08	-5.9	1.034
8. $C_{10}H_{22}(g) + \frac{31}{2}O_2 \rightarrow 10CO_2 + 11H_2O$	-1569.62	-1515.37	62	4.5	1.09796	+0.08	-6.2	1.036
9. $NH_3 + \frac{3}{2}O_2 \rightarrow \frac{1}{2}N_2 + \frac{3}{2}H_2O$	-47.28	-77.28	3	0.25	0.6835	-0.96	-7.1	0.612
10. $C + \frac{1}{2}O_2 \rightarrow CO$	-36.09	-26.31	2	0.5	0.782	0.47	-21	1.372
11. $C + O_2 \rightarrow CO_2$	-94.36	-94.08	4	0	1.02309	0	0	1.003
12. $CO + \frac{1}{2}O_2 \rightarrow CO_2$	-58.26	-67.77	2	-0.5	1.26335	-0.46	21	0.860
13. $Li + \frac{1}{2}Cl_2 \rightarrow LiCl(g)$	-81.38	-52.01	1	0.5	3.52442	-1.284	-42	1.565

† Thermodynamic data are presented for the oxidation of one mole of fuel.

causes the expansion of working gases thereby doing mechanical work, and is then transformed into electrical energy by an engine generator. This the normal "hot" combustion. But electrochemical energy conversion avoids the intermediate stage of production of heat in the transformation of chemical energy to electrical energy and this has been called "cold" combustion.

An ideal electrochemical energy converter yields electrical energy to the extent of the free-energy change of the reaction, as given by equation (1.37). However the total energy released in a chemical reaction corresponds to the enthalpy change of the reaction; and so long as the enthalpy change is more negative than the free energy change of the reaction, a part of the total energy change of the reaction which can not be converted to electrical energy is given out as heat. This part is represented by $(\Delta H - \Delta G)$, which is equal to $T\Delta S$. Thus heating effects even in the hypothetical ideal operation of a fuel cell of ΔS is negative. Such heating effects are very small compared to those associated with a heat engine.

There are some reactions that have positive entropy changes. In these cases, the free energy changes of the corresponding reaction are more negative than the enthalpy changes. Under these conditions, the electrochemical energy converter, in which such a reaction occurs, cools and extract heat from the atmosphere, which is also converted into electrical energy.

In most of the fuel cells, the heating effects observed within the electrolyte are due to ohmic losses. The rate of heat liberation is given by I^2R_1 , where I is the current and R_1 is the ohmic resistance of the electrolyte. In an ideal electrochemical energy converter this loss is zero, but there is still heat evolve if the entropy change of the cell reaction is negative. The heat evolved is numerically equal to $T\Delta S$ per mole of fuel consumed. Since ΔS is equal to $nF (dE/dEdT)$, this heat change may be broken up into three components: heat evolved at (1) each of the two metal-solution

junctions and (2) the metal-metal junctions. The major contribution to the heat evolved occurs at the two metal-solution interfaces. Thus the heating effect at the metal-metal junction is small because the potential difference across this junction is equal to the difference in work functions of the two metals and the temperature co-efficient of work functions are small.

1.5 Efficiency of Electrochemical Energy Conversion :

The intrinsic maximum efficiency : In the case of a heat engine, the loss in conversion efficiency has been stressed as being intrinsic. In the case of an electrochemical energy converter working ideally, the free energy change of the reaction may be totally converted to electrical energy. Thus, an electrochemical energy converter has an intrinsic maximum efficiency given by

$$\epsilon_i = \frac{\Delta G}{\Delta H} = 1 - \frac{T\Delta S}{\Delta H} \quad (1.39)$$

It is perhaps not appropriate to regard this equation as indicative of an intrinsic maximum efficiency of less than 100 percent because there is a possibility in the case of some reactions for ΔG to exceed ΔH .

At the present time, overpotential losses reduce the practical efficiencies of some fuel cells to values much less than the intrinsic maximum efficiencies. However, were sufficient advantage in electrocatalysis made (hence, over potential reduced) it might be possible to attain practical efficiencies of over 100 percent and close to maximum intrinsic efficiencies, particularly in situations in which the power density does not have to be high, so that the current density and hence overpotential can be low.

Voltage efficiency : the cell voltage E under load is less than the thermodynamic reversibly potential E_r , calculated according to equation (1.37). The voltage efficiency is defined as

$$\epsilon_r = \frac{E}{E_r} \quad (1.40)$$

Voltage efficiencies observed in some fuel cells (e.g. hydrogen-oxygen) are as high as 0.9 at low current densities and decreases only slowly with increasing current drawn from the cell, until a limiting value is reached.

Faradaic efficiency : The faradaic efficiency is defined as

$$\epsilon_f = \frac{I}{I_m} \quad (1.41)$$

I is the observed current from the fuel cell. I_m is the theoretically expected current on the basis of the amount of reactants consumed. Faradic efficiency is analogous to current efficiency in conventional electrochemical cells.

In most fuel cells ϵ_r is unity. ϵ_r may be less than 1 because of : (1) parallel electrochemical reactions yielding fewer electrons per mole of reactant consumed⁸, (2) chemical reaction of reactants catalyzed by electrodes⁹ and (3) a direct chemical reaction of the two electrode reactants¹⁰.

Overall efficiency : The overall efficiency ϵ in electrochemical energy conversion is the product of the efficiencies worked out in the preceding subsections :

$$\epsilon = \epsilon_1 \epsilon_2 \epsilon_r \quad (1.42)$$

For an electrochemical reaction, under chosen conditions of temperature, pressure, and concentration of reactants and products, ϵ_1 is a definite quantity and the maximum possible value of ϵ is ϵ_1 . A main goal in electrochemical energy conversion is to make both ϵ_1 and ϵ_r tend to unity. It is not difficult to make ϵ_2 tend to unity in the case of many fuel-cell reactions.

1.6 Factor Affecting Efficiency of Electrochemical Energy Conversion :

Activation overpotential : Activation overpotential results from the slowness of one or more of the intermediate steps in either one or both of the electrode reactions.

A typical plot of terminal cell voltage E vs current density i of an operating electrochemical energy converter is shown in Fig. 1.1. The open circuit voltage E_0 is generally less than the thermodynamically reversible potential E_r for the specified conditions of temperature, pressure, activities of reactants and products because of interference caused by adventitious reactions of impurities. When the net current drawn from the cell is small, cell potentials may tend to be controlled by these impurity reactions. However, due to their low concentrations, at higher currents generated from the cell impurity effects are small. Further, it is found that at low current densities there is a very sharp decrease of E with i , as represented by the portion AB of the curve. This type of behaviour is characteristic of highly irreversible processes and is caused by activation overpotential.

Ohmic overpotential: The linear portion in Fig. 1.1. corresponds to a relatively high current density region in which some part of the decrease in cell potential with increase of current density is due to ohmic overpotential. Ohmic overpotential is a result of the resistance of the resistance of the solution and is sometime due to the electric resistance in the electrode. It is given by

$$E_r = i r_i \quad (1.43)$$

where r_i is the internal resistance per square centimeter of cross section of the cell.

The ohmic overpotential is the simplest cause of loss of potential in an electrochemical energy converter. It may be thought that reduction in the thickness of the electrolyte layer between

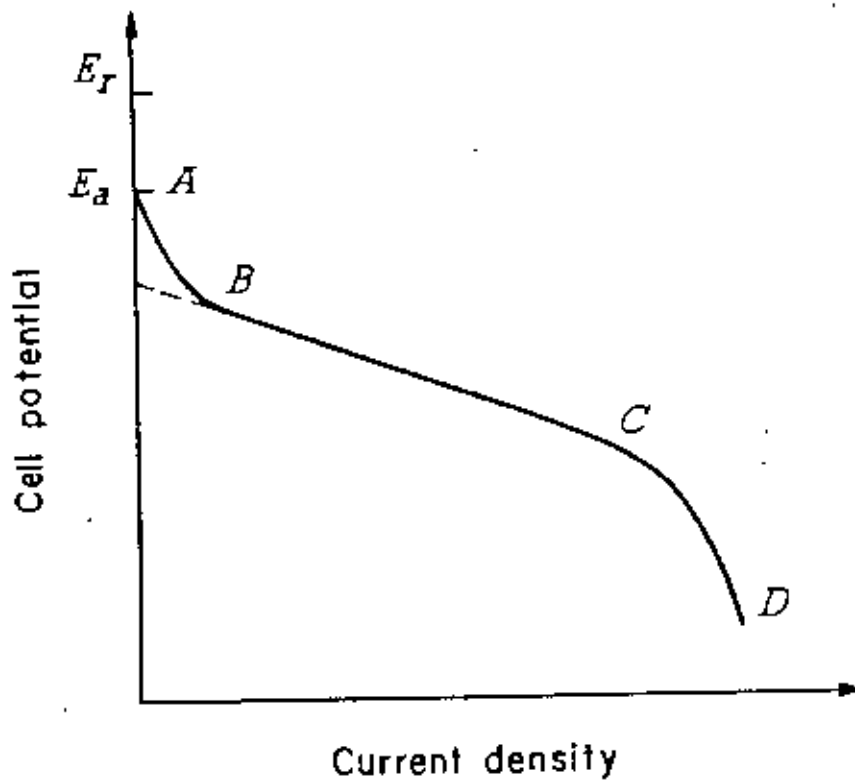


Fig. 1.1 A typical cell-potential-current-density relation for a fuel cell.

anode and cathode would eliminate ohmic overpotential. In the case of high-temperature fuel cells, ohmic overpotential may be a necessary part of the heat balance in the cell.

Mass-transfer overpotential : At sufficiently high rates, most heterogeneous reactions pass over into a region where they are controlled by the rate of transport of reactants to, or products away from, the electrode. This is shown by region CD in Fig. 1.1.

There are two causes of mass-transport control in electrochemical energy converters, which most often use porous electrodes : The potential of one of the electrodes (rarely both together) reaches a value at which it demands a greater rate of supply of its reactant than the rate that diffusional and convectional processes can supply. Under these conditions, the current can no longer increase with change of potential. The other cause of mass transfer polarization is characteristic only of porous gas diffusion electrodes. It is caused by a holdup in the supply of gas to the electrode-electrolyte interface. This occurs when the rate of diffusion of the gas through the electrolyte-free part of the pores becomes equal to or less than the subsequent steps, viz. dissolution of gases reactant in the electrolyte and electrochemical reaction of the dissolved reactant at the electrode-electrolyte interface within the pore.

1.7 Difference Between Heat Engine and Electrochemical Energy :

Heat Engine : The essence of a heat engine is a piston or turbine rotor which is forced to move by the expansion of a gas, which occurs as a consequence of a rise of temperature due to heat that is given out in the chemical reaction between the fuel and oxygen. The combustion process can take place either outside the engine (called external combustion engine) or inside the engine (called internal combustion engine). The feature common to both the external and internal combustion engine is that the chemical energy contained in the fuel is first converted to heat

and then this heat energy is used to produce mechanical power through the force associated with the expansion of a heated gas. Heat is essentially an intermediate form of energy in the conversion of to mechanical work the difference between the energy of the reactants and that of products in chemical reactions and thence its conversion by the generator to electricity.

About 85% of the energy consumed today by man comes from the thermal combustion of coal, oil and natural gas. These hydrocarbon fossil fuels are limited and a gift from natural processes which occurred many millions of years ago. The days must come when the reserves of fossil fuels are exhausted, particularly the easily transportable and usable oil and natural gas. Apart from questions of rationality raised by a continued burning-up of limited oil and natural gas supplies to give man the energy which runs his machines, some direct negative results arise from the present predominates form of energy conversion. Gasoline and diesel oil consumed in present internal combustion engines do not undergo 100% conversion to CO_2 . The organic compounds remaining incompletely burned are several dozens in number and include particularly unsaturated compounds. Carbon oxides, nitrogen oxides, sulphur oxides, and a lead containing compound are also present in significant amounts. Certain of the compounds undergo a photochemical reaction of oxides of nitrogen to produce a complex addition compound which is the origin of smog. There is evidence which suggests that some of the compounds from automobile exhausts are carcinogenic. Again carbon dioxide gas obtained by burning coal and oil, absorbs radiant energy in the infrared. The temperature of the earth's atmosphere is the net consequence of a number of influences which include the amount of solar radiation reflected back to space. The greater the concentration of CO_2 in the atmosphere, the less of this reflected energy escapes, i.e. the more is stored in the earth's atmosphere. The energy thus absorbed degrades to heat, the average temperature of the atmosphere is expected to increase.

Carnot showed that all engines which convert heat to mechanical work operate by transferring heat from a source at a temperature T_1 to a sink at a lower temperature T_2 and that the efficiency ϵ of such an engine is given by

$$\epsilon = \frac{T_1 - T_2}{T_1} \quad (1.44)$$

Since $T_1 - T_2 < T_1$, then $\epsilon < 1$, i.e. the efficiency is less than 100%. Hence for a given source and sink temperature, the maximum possible efficiency is prescribed by what is called the Carnot limitation on the conversion of heat into mechanical work. This limitation is intrinsic; it cannot be avoided by improvement of the engine. In a real engine with moving parts, nonideal materials of construction, etc. extrinsic efficiency losses come in and reduce the efficiency to values below the theoretical maximum efficiency for a heat engine as derived by Carnot. Thus the most mobile combustion engines have in practice percentage efficiencies of 10 to 20%. The intrinsic limitation of the heat engine method of obtaining mechanical energy from chemical reaction is that some 60 to 90% of the energy contained in the reaction of the fossil fuels to oxygen is being wasted, i.e. lost in heat and not converted to mechanical work. Thus the present method of providing available mechanical and electrical energy not only uses up the limited store of hydrocarbons but wastes in doing so and at the same time, it pollutes the atmosphere and may even within decades cause a significant reduction in land area throughout the world.

Electrochemical energy conversion : It would be preferable to attempt to devise a means of converting directly to electricity the energy released during most chemical reactions without involving a second machine and also preferably without moving parts for these are subject to erosion and mechanical failure. Several such methods, called direct energy conversion methods. It includes thermionic converter, thermoelectric converter, magnetohydrodynamic converters etc. In each of these methods, heat is directly converted to electricity without an intermediate stage of

mechanical work or a machine with moving parts. The direct energy producer is a spontaneously working, self-driving electrochemical system. In it, there is the spontaneous occurrence of a de-electronation reaction-sink electrode and an electronation reaction at the electron-source electrode. If an external loads is connected to the two electrodes, a current of electrons flows in the external circuit. Thus the electrodic reactions at the two electrodes bring about the conversion of the difference in the chemical energy of the reactants and products directly into a flow of electricity. There is no intermediate step in which the energy has to bring itself to power by expansion of a gas converting thereby only part of its thermal energy to mechanical work.

To obtain the maximum intrinsic efficiency in electrochemical energy conversion of a chemical reaction to electrical energy let us consider an essential thermodynamic equation,

$$-\Delta G = W_{rev} - P\Delta V \quad \dots(1.45)$$

i.e. the change in free energy in a reaction is equal to the total reversible work obtainable from the reaction diminished by the work of expansion, $P\Delta V$. Hence

$$-\Delta G = W_{rev} \quad (1.46)$$

Where W'_{rev} is all the work obtainable from the reaction exclusive of any work which can be obtained from a possible volume change in the system.

Now once a chemical reaction is carried out in an electrochemical way, the transport of electrical charge will occur across a total potential difference of V , the cell potential. Thus the general expression for the change of free energy in one act of an electrochemical reaction, in which the number of electrons transported externally for each act of the equivalent electrode reaction is n , is nFV_e . F is the Farady and V_e is the thermodynamic equilibrium potential ($=V$). Therefore we can write and hence

$$W_{rev} = nFV_e \quad (1.47)$$

$$-\Delta G = nFV_e \quad (1.48)$$

It is said that, in an electrochemical energy converter, the ideal maximum efficiency is 100% for, if one could carry out reactions in a such way that the electrode potentials were infinitely near the equilibrium values, the electrical energy one could draw from the reaction would be nFV_e and this is all of the free-energy change ΔG , which is the maximum amount of useful work one can obtain from a chemical reaction. However even by the electrochemical method not quite all the energy difference between the reactants and products of a reaction can be made available because some of it is wasted in very fundamental processes connected with the ordering and disordering i.e., the entropy losses and gains, which also occur in chemical reactions. It is the enthalpy change ΔH which is equivalent to the total change in energy between the reactants and the products of a reaction, including the energy lost in entropy increases. Hence a second and better expression for the intrinsic maximum efficiency of an ideal electrochemical converter is

$$\epsilon_{max} = \frac{\Delta G}{\Delta H} = \frac{-nFV_e}{\Delta H} \quad (1.49)$$

However in an electrochemical energy converter, the maximum cell potential is the value V_e obtainable when the reaction in the cell is electrically balanced out to equilibrium, i.e., when no current is being drawn from the cell. As soon as the cell drives a current through the external circuit, the cell potential falls from the equilibrium value V_e to V . The value of the actual potential V at which the cell works when delivering a current i is always less than the equilibrium potential V_e . Hence we can write

$$\epsilon_o = \frac{nFV_e \cdot V}{\Delta H} \quad (1.50)$$

where ϵ_{max} is the maximum efficiency given by equation (1.49) and ϵ_p is known as the voltage efficiency given by

$$\text{or } e_o = e_{\max} e_p \quad (1.51)$$

$$e_p = \frac{V}{V_*} \quad (1.52)$$

This picture is true only if the reactants are completely converted to final reaction products and none of the electrons take part in some alternative reaction. To allow for the possibility that such a wastage does occur, we must consider the current or faradic efficiency ϵ_f to take into account the incomplete conversion of reactants into products. The overall efficiency will be

$$e_o = (e_{\max} e_p) \epsilon_f \quad (1.53)$$

In many reactions, ϵ_f is virtually unity.

1.8 Electrode Kinetics :

The ideal or maximum efficiency of an electrochemical energy converter depends upon electrochemical thermodynamics whereas the real efficiency depends on electrode kinetics.

A term frequently used in chemical kinetics is the "rate-determining step" of an overall reaction. In general terms, it may be defined as the step which determines the velocity of the overall reactions. Further, since many electrochemical reactions proceed by a consecutive mechanism (and few by a parallel-path mechanism), one should expect this concept to apply equally in these cases. The velocity of the rate determining step is the primary factor which determines the power and efficiency of electrochemical energy conversion.

Types of rate-determining steps in electrochemical reactions:

(i) Mass-transport control : The rate determining steps in this classification include mass transport under pure diffusion or diffusion-convection conditions. In addition, when the rate determining step is the transport of an ion or electron through a solid phase, this type of control is also considered under mass transport. (ii) Homogeneous-step control: These refer to situations in which the rate-determining steps occur in solution before the particles reach the electrode. (iii) Heterogeneous-step control : Under this classification is included rate-determining charge-transfer control which is most commonly observed in electrode kinetics. however it could embrace all other kinds of rate-determining surface reactions, e.g. combination of radicals, nucleation, crystal growth, surface diffusion. The present classification of types of rate control in electrochemical reactions is illustrated in Table 1.2.

Table 1.2 : Classification of Electrode Processes ¹¹.

Types of rate-determining steps		
Mass-transport control	Heterogeneous-step control	Homogeneous-step control
1. Diffusion 2. Diffusion-convection 3. Ohmic	1. Charge transfer 2. Adsorption and desorption 3. Nucleation 4. Crystal growth 5. Surface diffusion	1. Chemical reactions in solution

Charge Transfer Process

Comparison of chemical reactions with electrochemical reactions : The velocity of an ordinary chemical reaction can be increased by either an increase in concentrations of reactants or an increase of temperature. The dependence of velocity on concentrations of the reactant is small, since reaction rates depend on a simple power of the concentration. The variation of reaction rates with temperature is significant.

The essential feature of an electrochemical reaction is that it involves interfacial charge transfer process. The various aspects of charge transfer will be discussed in chapter 3.

Adsorption Isotherms and Their Influence On Electrode Kinetics :

Reaction at electrodes may be considered as heterogeneous catalysis with one additional intensive variable - the potential drop at the interface. The nature of the surface plays an important role in two respects. First, the rate of an intermediate step may depend on the heat of adsorption of the reactant and products on the surface. Second, the rate of this step may also depend on the available or free surface on the electrode. The intermediate steps may be charge transfer or chemical steps. The adsorption characteristics of the metal may also change the path of a complex reaction. Adsorption kinetics strongly depends on the type of isotherm governing the adsorption of a particular species.

With the advent of interest in electrochemical energy conversion, particularly using organic fuels, considerable attention has been drawn towards determining the electroadsorption behavior of organic compounds used as fuels. A knowledge of this electroadsorption behaviour is required at two levels-one at a simple level where it is necessary to know the extent to which the organic compound is adsorbed as a function of potential for a certain concentration of the species in solution. Generally this relation

is parabolic. If a fuel is poorly adsorbed, the rate of the overall charge-transfer reaction involving it will tend to be low. The second is at a more sophisticated level. Interpretation of variation of current density with potential depends strongly on the type of these adsorption isotherms.

Langmuir Isotherm : The langmuir isotherm¹² was first derived from a kinetic view point. Suppose a reaction of the type



is considered. The rate of the forward reaction is given by

$$V_1 = k_1 C_A^+ (1-\theta) \exp\left(-\frac{\beta VF}{RT}\right) \quad (1.54)$$

Since, the forward velocity depends on the free surface in addition to the concentration of the reactant. Similarly, the velocity of the reverse reaction is given by

$$V_{-1} = k_{-1} \theta \exp\left[(1-\beta) \frac{VF}{RT}\right] \quad (1.55)$$

k_1 and k_{-1} are the rate constants of the forward and reverse reactions when the metal-solution potential difference is zero. θ is the degree of coverage of the adsorbed species A on the electrode. θ is related to the surface concentration C_A by the relation

$$C_A = k' \theta \quad (1.56)$$

where k' is the surface concentration when $\theta = 1$. At equilibrium

$$\frac{\theta}{1-\theta} = \frac{k_1 C_A^+}{k_{-1}} \exp\left(-\frac{VF}{RT}\right) \quad (1.57)$$

Equation (1.57) reduces to a linear variation of θ with C_A^+ (Henry's isotherm¹³) when $\theta \ll 1$. This model ignores lateral interactions. It assumes that all sites on the surface are equivalent and adsorbed species are immobile on the surface.

Isotherms of Frumkin and of Temkin : the Langmuir isotherms may be written in the more general form

$$KC \exp\left(-\frac{VF}{RT}\right) = \frac{\theta}{1-\theta} = C \exp\left(\frac{-\Delta G^{\circ}}{RT}\right) \exp\left(\frac{-VF}{RT}\right) \quad (1.58)$$

where $K = k_1/k_{-1}$. By considering lateral interactions and by analogy with Van der Waals' equations for gases, Frumkin¹⁴ modified the above equation to

$$KC \exp\left(\frac{-VF}{RT}\right) = \frac{\theta}{1-\theta} \exp\left(\frac{r\theta}{RT}\right) \quad (1.59)$$

The interaction energy parameter r is negative when lateral interaction is attractive, and it is positive when there is repulsion between the adsorbed species.

Temkin¹⁵ considered the more general case of lateral interactions and nonuniformity of surface arising from knowledge of gas-adsorption studies. Using these conditions, Temkin derived an equation of the same form as that of Frumkin.

A simple way of obtaining equation (1.59) is as follows. In the case of most adsorbents, the heat of adsorption, and hence the free energy of adsorption, decreases linearly with coverage. The standard free energy of adsorption (with $V=0$) when the coverage is θ may then be expressed as

$$\Delta G_{\theta}^{\circ} = \Delta G_0^{\circ} + r\theta \quad (1.60)$$

where ΔG_0° is the standard free energy of adsorption at zero coverage and r is an interaction energy parameter. On introducing equation (1.60) into equation (1.58), equation (1.59) results.

At intermediate values of coverage ($0.2 < \theta < 0.8$), when $\theta/(1-\theta)$ is unimportant relative to $\exp(r\theta/RT)$ in equation (1.59), one obtains an equation, sometimes called the Temkin isotherm :

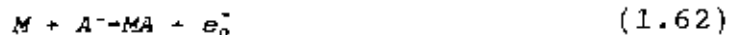
$$r\theta = -VF + RT \ln K + RT \ln C \quad (1.61)$$

when r is very small or at very small coverages, equation (1.59) reduces to the Langmuir equation.

The variation of free energy of adsorption with coverage equation (1.60) may be due to intrinsic heterogeneity of the surface, lateral interaction effects, or induced heterogeneity effects.

Influence of type of isotherms on electrode kinetics

Langmuir conditions : A reaction of the type



can be considered where the product A_2 is a gas. The rates of the forward (V_1) and reverse reactions (V_{-1}) of step (1.62) assuming Langmuir conditions, are

$$V_1 = k_1 C_{A^-} (1-\theta) \exp\left(\frac{\beta VF}{RT}\right) \quad (1.64)$$

$$V_{-1} = k_{-1} \theta \exp\left[-(1-\beta) \frac{VF}{RT}\right] \quad (1.65)$$

and similarly for step (1.63),

$$V_2 = k_2 \theta^2 \quad (1.67)$$

$$V_{-2} = k_{-2} (1-\theta)^2 P_{A_2} \quad (1.68)$$

where C_{A^-} is the concentration of the ion A^- in solution; θ is the degree of coverage of the surface with MA; P_{A_2} is the partial pressure of A_2 and k 's are the respective rate constants indicated by the appropriate suffixes. If the desorption step is rate determining, the discharge step may be considered to be virtually in equilibrium. thus from equations (1.64) and (1.65) it follows that

$$\theta = \frac{k_1 C_{A^-} \exp(VF/RT)}{1 + k_1 C_{A^-} \exp(VF/RT)} \quad (1.69)$$

when $k_1 \exp(VF/RT) \ll 1$, $\theta \rightarrow 0$ and is given by

$$\theta = k_1 C_A \exp\left(\frac{VF}{RT}\right) \quad (1.70)$$

Under these conditions,

$$1 - \theta = 1 \quad (1.71)$$

Thus equations (1.67) and (1.68) reduce to

$$V_2 = k_2 k_1^2 C_A^{-2} \exp\left(\frac{2VF}{RT}\right) \quad (1.72)$$

$$V_{-2} = k_{-2} P_{A_2} \quad (1.73)$$

From equations (1.72) and (1.73) the net current density i may be expressed in the form

$$i = i_0 \left[\exp\left(\frac{2\eta F}{RT}\right) - 1 \right] \quad (1.74)$$

Where,

$$i = 2Fk_2 k_1^2 C_A^{-2} \exp\left(\frac{2V_R F}{RT}\right) - 2Fk_{-2} P_{A_2} \quad (1.75)$$

and η is the overpotential. When $k_1 \exp(VF/RT) \gg 1$, $\theta \rightarrow 1$, and

$$1 - \theta = \frac{1}{k_1 C_A \exp(VF/RT)} \quad (1.76)$$

Under these conditions, it is possible to write

$$i = i_0 \left[1 - \exp\left(\frac{-2\eta F}{RT}\right) \right] \quad (1.77)$$

Where

$$i = 2Fk_2 = 2F \frac{k_{-2}}{k_1^2 C_A^{-2}} P_{A_2} \exp\left(-\frac{2V_R F}{RT}\right) \quad (1.78)$$

It is seen from these limiting conditions of $\theta \rightarrow 0$ or $\theta \rightarrow 1$ that either the forward or the reverse of step (1.63), respectively proceeds at a limiting current density determined by some activation-controlled process at the electrode.

Tamkin Conditions : Temkin, isotherm for the adsorption of the species MA in the reaction sequence (1.62) and (1.63) which was formally treated according to the Langmuir adsorption - one may find out how the kinetic parameters are affected. Thus, taking into consideration the variation of free energy of adsorption of the intermediate MA with coverage,

$$V_1 = k_1 (1-\theta) C_2 \exp\left(\frac{\beta FV}{RT}\right) \exp\left(-\frac{\gamma r\theta}{RT}\right) \quad (1.79)$$

$$V_{-1} = k_{-1} \theta \exp\left(-\frac{VF}{RT}(1-\beta)\right) \exp\left[(1-\gamma) \frac{r\theta}{RT}\right] \quad (1.80)$$

The exponential terms in equations (1.79) and (1.80) may be visualized in the same way as the exponential term in V . The term γ is analogous to a symmetry factor. In the intermediate coverage range, the variation of linear terms in θ is considerably less than the exponential terms in θ . Hence equations (1.79) and (1.80) may be reduced to

$$V_1 = k_1 C_2 \exp\left(\frac{\beta VF}{RT}\right) \exp\left(-\frac{\gamma r\theta}{RT}\right) \quad (1.81)$$

$$V_{-1} = k_{-1} \exp\left[-(1-\beta) \frac{VF}{RT}\right] \exp\left[(1-\gamma) \frac{\gamma\theta}{RT}\right] \quad (1.82)$$

The forward and reverse velocities of the second step, represented by equation (1.63) remembering again that the adsorption energy of the species MA depends on coverage are given by

$$V_2 = k_2 \theta^2 \exp\left(\frac{2\gamma r\theta}{RT}\right) \approx k_2 \exp\left(\frac{2\gamma r\theta}{RT}\right) \quad (1.83)$$

$$V_{-2} = k_{-2} (1-\theta)^2 \exp\left[-2(1-\gamma) \frac{r\theta}{RT}\right] \approx k_{-2} \exp\left[-2(1-\gamma) \frac{r\theta}{RT}\right] \quad (1.84)$$

Under Temkin conditions, where $0.2 < \theta < 0.8$, in equations (1.83) and (1.84) the variations of the preexponential terms in θ are small compared to those of the exponential ones and thus the approximate forms of the equations are found on the second line of

each equation. Again assuming that the first step is virtually in equilibrium, when the second step is rate-determining, it follows from equations (1.81) to (1.84) that

$$V_2 = k_2 (k_1 C_A^-)^{2\gamma} \exp\left\{\frac{2\gamma V F}{RT}\right\} \quad (1.85)$$

$$V_{-2} = k_{-2} \left(\frac{1}{k_1 C_A^-}\right)^{-2(1-\gamma)} \exp\left[-2(1-\gamma) \frac{V F}{RT}\right] \quad (1.86)$$

Since the currents are proportional to the velocities, it follows, from equation (1.85), that for the cathodic reaction

$$\frac{\partial V}{\partial \ln i_2} = \frac{RT}{2\gamma F} \quad (1.87)$$

and from equation (1.86), that for the anodic reaction

$$\frac{\partial V}{\partial \ln i_{-2}} = \frac{RT}{2(1-\gamma)F} \quad (1.88)$$

Thus it is seen from equations (1.74), (1.77), (1.87), and (1.88) that the rate of variation of overpotential with current density of a reaction depends on the type of isotherm which governs the adsorption of reactants (e.g. the fuel in an electrochemical electricity producer). In mechanism determinations, the slope $dV/d \ln i$ is one of the most useful mechanisms indicating criteria but only under the condition that prior knowledge about the type of adsorption isotherm is available.

Photoelectrode Kinetics : The effect of light on electrode reactions is akin to its effect on chemical reactions ¹⁶.

The number of electrons n_v emitted in a second by a metal in vacuum per unit of incident light energy is given by¹⁷

$$n_v = \frac{m c^2}{h^2 \nu^2} \left(1 - \frac{\phi_w}{h\nu}\right) \quad (1.89)$$

Where m is the mass of the electron, c is the velocity of light, ϕ_w is the work function of the metal, and ν is the frequency of light of standard intensity I_0 .

If the metal is immersed in an electrolyte, the effective work function becomes $\phi_m + x$, where x is the surface potential difference at the metal solution interface¹⁸. Under these conditions, the number of electrons emitted per second becomes

$$n_s = \frac{mc^2}{h^2 v^2} \left(1 - \frac{\phi_m + x}{hv}\right) \quad (1.90)$$

Role of dyes in photoelectrode processes : It has been known for long that electrodes that are sensitive to light are affected even more when they are coated with dyes¹⁹. It was subsequently shown that similar effects are observed even when the dyes are present in solution²⁰.

When dyes of a certain type (D) are illuminated, they may be promoted to a singlet state. From this state, the dye may undergo a radiationless transfer to a triplet state, which is metastable. It can then undergo reaction with some reducing agent in solution. Reduction of the dye D to DH changes its concentration and thereby alters the potential of an electrode in solution²¹.

1.9 Electrocatalysis :

Electrocatalysis may be defined as the acceleration of an electrodic reaction by a substance which is not consumed in the overall reaction. The substance is generally the electrode, though, to a lesser extent, the catalytic activities of the solvent may also be envisaged. Further electrocatalysis is analogous to heterogeneous catalysis since at least one step of the electrochemical reaction occurs at the electrode-solution interface and at a given electrode-solution potential difference, it is specifically the property of the electrode surface that affects the overall reaction rates.

The electrolytic hydrogen-evolution reaction has received most attention²². It is seen that the exchange current densities for the hydrogen electrode reaction on a number of metals in acid solution

gives different values which indicates that for this reaction the electrocatalytic activity of the metals varies. The noble metals have the highest catalytic power. The transition metals have an intermediate catalytic power. A knowledge of electrocatalysis is particularly important in the case of electroorganic oxidation. The electrochemical reactivity of ethylene in its oxidation to CO_2 is low²⁹ compared with that of hydrogen. Hence, the rate at which it can be converted with high efficiency, and the corresponding power, is relatively small. The products of the overall reaction here depend on the catalyst²⁴: complete oxidation to CO_2 occurs on Pt, Rh, and Ir, whereas partial oxidation to aldehydes occurs on Pd and Au. From free energy considerations it is important to oxidize a fuel completely as it is to reduce overpotential to obtain the maximum efficiency of electrochemical energy conversion. In some cases, the electrocatalyst may also function as a chemical catalyst and may interfere with or aid the following electrocatalysis. An example is the electrooxidation of propane to CO_2 using Pt as a catalyst²⁵. Alloys often have considerably higher activity than the constituent metals. A good example is in the enhanced activity of Pt-Rh-Mo ternary alloys, which are better catalysts in the oxidation of methanol than are any of the constituent metals²⁶.

Electrocatalysis is mainly concerned with the search for materials which have high exchange current density for electroodic reactions. These studies are far more significant on smooth electrodes in the form of wires, foils, or spheres than on porous electrodes. This is because in the former case, one is able to study only under conditions of activation overpotential without interferences from concentration and ohmic overpotential.

The two important parameters to be considered in electrochemical energy conversion are voltage efficiency and the power density. The voltage efficiency of an electrochemical energy converter is given by

$$e_s = \frac{E_R - \eta_a - \eta_c}{E_R} \quad (1.91)$$

where E_R is the reversible potential of the cell and η_a and η_c are the numerical values of the total overpotentials at the anode and cathode, respectively, when a current density of i is drawn from the cell.

The maximum power density P_M per square centimeter, for several fuel cell reaction, is given by

$$P_M = i_L (E_R - \eta_a - \eta_c) \quad (1.92)$$

where i_L is the limiting current density.

A reduction in overpotential increases both the efficiency and maximum power density. There is a possibility to reducing overpotential by working at higher temperature. It would also be possible to reduce the overpotential considerably by going to still higher temperatures, which would be feasible, were it possible to use molten instead of aqueous electrolytes.

The decrease in overpotential can be brought about by increasing the effective or true area of the catalyst. The best possible manner to increase the effective area is by using suspended catalysts²⁷.

As in heterogeneous catalysis, impurities from the solution or in some cases intermediate or products of the reaction adsorb on the electrode and block the active sites. Thus the activity of the electrocatalyst may decrease with time. A solution to the problem of maintaining a constant activity of the catalyst appears more hopeful in electrochemical reactions than in chemical reactions.

1.9.1 Distinctive Features of Electrocatalysis :

Electrocatalysis may be considered as a special case of heterogeneous chemical catalysis but with one major difference, namely that one or more of the intermediate steps in the overall reaction is a charge transfer one. In heterogeneous catalysis, the reaction rate is measured by the number of moles of reactant consumed in unit time per unit area of the catalyst. By analogy, in electrocatalysis the current density at the electrode is a measure of the reaction rate. The relation between current density i and velocity V is given by

$$i = nFV \quad (1.93)$$

where i is expressed in amperes per square centimeter and V in moles per square centimeter per second. Electrocatalysis has several novel features which will be considered in the following subsections.

Dependence of reaction rate on potential : The forms of equations relating reaction rate to temperature are the same in heterogeneous and electrocatalysis but with one fundamental difference. In heterogeneous catalysis, the velocity V is expressed by the well known Arrhenius equation

$$v = A \exp\left(-\frac{E^\ddagger}{RT}\right) \quad (1.94)$$

where A is a product of certain constants and activities of the reactants and E is the activation energy. In electrocatalysis, the current density is given by

$$i = C \exp\left(-\frac{E^\ddagger}{RT}\right) \exp\frac{eV}{RT} \quad (1.95)$$

In equations (1.94) and (1.95), A , B , C are either independent of temperature or depend on it little compared with the exponential term.

Again the potential V may be expressed by

$$V = V_p + \eta \quad (1.96)$$

where V_p is the reversible potential for the overall reaction and η is the overpotential. Introducing equation (1.96) into (1.95)

$$i = C \exp\left(-\frac{E}{RT}\right) \exp\left(\frac{BV_p}{RT}\right) \exp\left(\frac{B\eta}{RT}\right) \quad (1.97)$$

Equation (1.94) and (1.97) shows the essential difference between electrocatalysis and catalysis, i.e. the electrocatalytic velocity depends exponentially upon the overpotential, the difference between the electrode potential at which the reaction takes place at the rate corresponding to a current density i and the reversible electrode potential. Thus overpotential is a kind of variable component of the activation energy.

The energy of activation in heterogeneous catalysis E^\ddagger is given by

$$E^\ddagger = -R \frac{\partial \ln v}{\partial (1/T)} \quad (1.98)$$

from equation (1.94).

By analogy, the energy of activation for the electrochemical reaction E_η is given by

$$E_\eta = -R \frac{\partial \ln i}{\partial (1/T)} = E^\ddagger - BV_p = E^\ddagger - BV_R - B\eta \quad (1.99)$$

as obtained from equations (1.95) and (1.97).

Equation (1.99) shows that the energy of activation of the reaction at an overpotential η is linearly reduced by the overpotential. At a high enough overpotential (η_L) it should then be possible to reduce the activation energy to zero.

The possibility of carrying out chemical reactions electrochemically: It is not widely realized that many chemical

reactions can be formulated electrochemically. For example, the oxidation of propane to carbondioxide may be represented as an overall process from a chemical point of view as:



In the chemical path the important step occurs by collision between reactant particles either in gas phase or heterogeneously on a catalyst. In the electrochemical path the reaction occurs in two quite distinct partial reactions:



which occurs on two spatially separated electrodes. In addition, some so-called heterogeneous chemical reactions are probably electrochemical in nature, i.e. they occur at two separated locations on the same catalyst. A heterogeneous chemical reaction would then be analogous to a corrosion reaction in which two partial electrochemical reactions occur in an overall reaction with no net electron transfer.

Large variations in reaction rates : A significant advantage of electrocatalysis is that the effective energy of activation, and hence the reaction rate, can be controlled by change of applied potential in the case of a driven cell. Thus, it is possible to change the reaction rate by many orders of magnitude. It is possible to bring about such change easily. A much increased potency in range of reaction rate variation and also control, compared with there of chemical reactions, is possible.

The dependence of the overall reaction on the region of potential : The potential at which reaction commences at an appreciable rate depends on the reversible potential for the overall reaction under the conditions of the experiment and also on the degree of irreversibility of the reaction. Thus depending on the region of the applied potential, it should be possible to study

more than on reaction on an electrocatalyst. In some cases a stepwise oxidation or reduction of a reactant occurs depending on the potential²⁸. An example is the stepwise reduction of nitrobenzene as follows :



The desired product is obtained by a control of the potential of the electrode.

Use of low temperature : A significant advantage of electrochemical reaction is that most of them can be carried out at low and intermediate temperatures. For example it is quite simple to carry out the electrochemical oxidation of hydrogen to water at room temperature. The chemical oxidation of hydrogen to water over catalysts like Pt occurs at significant rates only at temperatures over 200°C. Further it is possible to oxidize many hydrocarbons to carbons to carbondioxide at temperatures less than 100°C. In the chemical oxidation of unsaturated hydrocarbon it is necessary to have temperatures of at least 200°C, and in case of saturated hydrocarbons over 300°C.

Identification of intermediates and variation of their concentrations with potential : One of the major reasons why progress in heterogeneous catalysis has been hindered is because it has not been possible to identify intermediates in reactions. In electrochemical catalysis, it has been possible for a few years in the case of some reaction, e.g. hydrogen evolution, oxygen evolution, Kolbe reaction to identify intermediates, e.g. adsorbed hydrogen, chemisorbed oxygen, carboxylate radical, respectively and to determine their concentrations as a function of potential. These are useful mechanism-determining criteria for the reactions.

Maintenance of constant catalytic activity : One of the difficulties in heterogeneous catalysis is the maintenance of a constant activity of the catalytic surface. The loss in activity of the surface is generally caused by the adsorption of impurities. In

some cases, the poisoning of the surface is caused by adsorption of intermediates or products of the reaction. The same type of loss of activity of the surface occurs in electrochemical reactions as well and should be considered as more probable. Thus impurities may be present in large concentration in solution than are found in the gas phase where the reaction vessels are evacuated and then the purified reactants introduced. In solution it is more difficult to reduce impurity concentration to very low levels. However it is possible to renew the surface of an electrocatalyst by the application of suitable pulse.

Change of paths of reactions using redox systems : It is well known that the oxygen dissolution reaction is highly irreversible on most electrodes and thus reduces the efficiency of electrochemical energy conversion. A way out of the difficulty may be by the use of redox system. In this method, there is a change in the path of reaction. The electrode reaction is the reduction of nitric acid to nitric oxide instead of the electrochemical reduction of oxygen. The oxygen then oxidizes the nitric oxide to nitric acid²⁹. thus though the overall reaction is still the same, the path of the reaction is considerably altered. Further, the electrochemical reduction of nitric acid is fast. The chemical oxidation of the nitric oxide is also rapid. Thus problems of overpotential losses are considerably reduced.

Electrochemical nature of biological reactions : Many biological reactions also occur by an electrochemical path³⁰. It may be that enzymes, which are catalysts for many biological reactions, serves as "poly electrodes" (electrodes at which two or more electrochemical reactions occurs as in a corrosion reaction). For example many enzymes show high catalytic activity when they are wet³¹ and conduct electronically only when wet, as required by such a model. Correspondingly heats of activation of enzymatic reactions are sometimes very low, a fact most easily interpreted in terms of rate-determining electron tunneling as part of the enzymatic reaction path.

1.9.2 Factors Affecting Electrocatalysis :

The three main processes in which the catalyst plays a role in electrochemical reactions are adsorption, charge transfer, and surface reactions. Adsorption and surface reactions, are common to chemical catalysis. By analogy with chemical catalysis, one may expect geometric and electronic factors also to be important in electrochemical catalysis. Since there is an additional process in electrocatalysis -charge transfer - the potential at the metal-solution interface is an additional important factor for electrochemical reactions. One may also expect electronic factors to influence the charge transfer step besides their effect on the other processes.

Before dealing with the influence of the three main factors in electrocatalysis, it will be worthwhile to discuss the nature of the catalysts. From such a discussion, the factors affecting catalytic activity will be seen readily.

Since the catalysts usually employed are metals, alloys, and semiconductors, it is best to deal with the nature of catalysts in this order.

Metals : Metals are characterized by the presence of free electrons and each ion in the bulk of a metallic lattice is equally attracted to all its nearest neighbours. In covalent crystals, directed bonds are present. Due to the absence of directed valencies in metallic crystals, a close-packed structure is expected. The surface of a metal is not homogeneous at temperatures above the absolute zero. The reason for this is due to the presence of steps, kinks and edge vacancies. There are three types of imperfections, which depend on the number of dimension, are commonly found in real crystals. They are (i) point defects (ii) line defects, (iii) plane defects.

The surface of any polycrystalline metal generally contains grains, which exhibit, predominantly, plans of low index. The essential characteristics of such planes is the arrangement of atoms in them, e.g., the internuclear distance of the atoms are characteristic of that which would be expected for the plane concerned. This assumption is not exactly correct for surface atoms but the deviation is quite small.

Alloys : An alloy is defined as a homogeneous substance which consists of two or more elements. The elements are generally metals though in some cases even nonmetals like hydrogen, boron, or nitrogen maybe one of the constituents. There are two types of alloys :

(i) Substitutional alloys (ii) Interstitial alloys.

Substitutional alloys are those in which atoms of one element replace those of another in a regular lattice. One of the necessary criteria for substitutional alloy formation over a wide range of concentration of each of the constituents is that their lattice structures and parameters must be similar.

Interstitial alloys are those in which atoms of one of the components are so small that they occupy interstitial positions in a regular network of the other component without disturbing (or only slightly so) the latter.

The defects in the surface structure of substitutional alloys are similar to that of metals. However, it is found that the surface and bulk compositions are not the same in composition. Further, the compositions at grain boundaries and in crystallites are also not identical. These differences cause a difference in the number of active sites on the surface of an alloy, compared with that which would exist were the surface and bulk concentrations the same.

Semiconductors : Semiconductors may broadly be divided into three types depending on whether they are composed of single

elements, intermetallic compounds, or inorganic compounds. Further they may also be classified under intrinsic semiconductors and extrinsic semiconductors.

The elements silicon, germanium, and tin which are intrinsic semiconductors have the diamond type of structure. In this structure, each atom is tetrahedrally surrounded by four other atoms. With increasing interatomic spacing, as in the series Si, Ge, and Sn, the semiconductivity increases. This is as expected since with increasing interatomic spacing, there is a weakening of the binding between the atoms as well as an increase in the sizes of the atoms. Intern, the forces binding the electrons to the metals become weaker with increase of interatomic distances, causing an increase of semi-conductivity with increase of atomic weight.

The intermetallic semi-conductors are similar to alloys in that they are both composed of two or more elements. In the case of alloys, the elements are metals and metalloids. The main difference between the two types is that in alloys, the bond formation is of the metallic type, but in intermetallic semi-conductors, the bonding is predominantly covalent.

The most common compounds, which are semi-conductors, are oxides, sulfides and some times these compounds modified by the presence of defects. Mixture of oxides or sulfides are often better semiconductors than the component oxides or sulfides :

Generally, in oxides the oxygen atoms are arranged in the hexagonal or cubic close packing and the cations place themselves at octahedral or tetrahedral sites. The bonding between the metal and oxygen atoms is mainly ionic in character and hence electronic conductivity of oxides is low. The introduction of very small quantities of a second compound causes the semiconductivity of oxides. Two types of defects may be introduced : one of which (n - type) gives electrons in excess of those available to the

conductivity band in the original substance and electron-defect semiconductors (p-type) where the added substance absorbs electrons and creates electron vacancies (holes) in the lattice. Many complex oxides and sulfides, for example the spinels, are also semiconductors. The structure of these compounds are quite variable.

Geometric Factors :

- (i) Lattice spacing in crystals : If there is more than one point of attachment of the reactant, the energy of activation for the adsorption process is affected by the internuclear distance. For dissociative adsorption, the activation energy is a minimum for an optimum spacing. At larger spacings, the activation energy is higher because dissociation has to occur before adsorption, and at smaller distances, the same result arises because repulsive forces retard adsorption. Sherman and Eyring³² showed by a theoretical calculation that the optimum internuclear distance for the adsorption of hydrogen on carbon is 3.5 Å.
- (ii) Intersite distance in crystal : It is commonly assumed that the adsorption of reactant atoms occur on the atoms of the catalyst. This assumption may not always be correct since with small atoms a more probable adsorption site is an interstitial position on the surface. Thus if there is more than a one-point attachment the intersite (adsorption) distance is more critical than the interlattice spacing. Some evidence for this prediction follows from the adsorption of hydrogen on W single crystals³³.
- (iii) The effect of grain size has also been studied using platinized-platinum electrodes. It was found that in the oxidation of formic acid on platinized platinum electrodes, the only effect of platinization is to increase the roughness factor³⁴.

- (iv) Presence of steps, kinks, and surface vacancies : In a perfect crystal the surface may contain edges, steps, and kinks. An atom at a plane has the highest number of neighbors which is followed by the atoms at a step and then by atoms at a kink. Thus, due to the variation in number of free valencies available at the different possible adsorption sites, one could expect that adsorption, the preliminary step of the reaction, is easiest at a kink, then at a step, and finally at a plane.

There are other considerations. Adsorption at defects is not always easy. From potential-energy calculations for metal-deposition reactions, it was shown that transfer of the hydrated metal ion from the solution occurs more easily at a site on a crystal plane rather than on a kink site because of energy necessary to distort the ionic hydration shell during transfer to a kink site³⁴.

- (v) Presence of point defects : Introduction of point defects increases the rates of some electrode reactions. For example, the exchange current density for hydrogen evolution on iron containing 0.2% impurities (carbon) is higher than on zone refined iron containing 0.01% impurities by a factor of ten³⁵. One of the difficulties of investigating the effect of trace inclusions in a substrate is that its bulk concentration only is known and Gibbs adsorption will cause the concentration of the trace substance to be different on the surface than in the bulk.

It is also probable that the introduction of point defects may influence electronic factors as well- the work function is lowered in the region of the defect³⁶. This may be one cause of the effect of the effect of traces as exemplified here for hydrogen evolution on iron.

- (vi) Presence of line defects : The presence of dislocations in the substrate should affect the rate of an electrochemical reaction because atoms in the region of the dislocation have a higher energy than the atoms on a plane surface. Thus one can expect energies of adsorption of reactants at defects to be higher which in turn accelerates reaction rates.

Electronic Factors :

The transition metals are the most active catalysts for a variety of reactions. These metals are known to adsorb atomic hydrogen and oxygen as well as molecules and fragments of hydrocarbons. The bond between the adsorbent and adsorbate are as strong as chemical bonds. Thus it would be necessary to consider the electronic structure of the adsorbent atoms. Electronic structures of surface atoms have not been studied directly. The alternate course is to understand the electronic structure of the bulk atoms and make the assumption that the surface atoms have similar electronic structures.

There are two approaches to the electronic structure of transition metals :

- (i) Electron-bond theory of metals and d-vacancies : The transition metals have partially filled d-shells and, in the gas phase, the number of electrons in these shells increases from one to nine in each of the long periods of the periodic table. If the same electronic structure were maintained in the case of the solid metals (as opposed to the individual atoms), one would have 6, 7 and 8 electrons in the d-shells of the atoms Fe, Co, and Ni respectively. Thus since by the Pauli exclusion principle, the number of unpaired electrons are 4, 3 and 2 Bohr magnetons, respectively. However, the measured values of the magnetic moments are 2.22, 1.61 and 0.61 Bohr magnetons, respectively. The discrepancy is due to a difference in the electronic structure of these metals in the

solid state, from that which would exist if the atoms maintained the same electronic structure as for individual atoms in the gas phase.

- (ii) Valence-bond Theory : The electron bond theory is quantitatively satisfactory only for the group VIII metals and not for the transition elements preceding it. Pauling put forward an alternate theory - Valence -bond theory³⁷ which is of more general applicability than the electron band theory and is thus more useful for an interpretation of the electronic structure of the transition metals. In this theory, promotion of several electrons to higher orbitals (e.g. 3d to 4s) is suggested as playing a basic role in the bonding of metals.

Effect of Potential :

A change in potential across the double layer at the electrode-solution interface has two effects. It affects (i) the rate constants of any of the intermediate steps involving a charge transfer and (ii) adsorption characteristics of most reactants, intermediates and products.

A considerably greater variation in reaction rate is obtained by changing the potential than by change of concentration or temperature.

The rate of an electrochemical reaction (i.e. current density at any desired potential) is also affected by the adsorption characteristics of reactants, intermediates or products which may be a function of potential.

The rate of an electrochemical reaction may be expressed by the equation

$$i = k_0 e^{VF/RT} \quad (1.104)$$

When the activities of the reactants are taken as unity. In equation (1.104), k_0 is the rate of the reaction when the metal solution potential difference is zero.

1.9.3 New Types of Electrocatalysts :

Chelate catalysts : Recently chelates have been used as catalysts in the electrochemical oxidation of soluble (e.g. formic acid, hydrazine) and some insoluble (hydrogen, propane) fuels²³. Since electrocatalysis is markedly affected by the co-ordination characteristics of the substrate, surrounding a metal atom with electron donor groups of varying ligand strengths should change both the stereochemistry and the co-ordination characteristics of the metal and hence its electrocatalytic activity. Some ligands, their structure and relative field strength are given in Table-1.3.

Stable metal chelates, having square planar configurations, can react with molecules (e.g. fuels, catalyst support molecules) above and below the plane of the metal ion forming an octahedral configuration. Thus square planar chelates may arrange themselves parallel to the plane of the catalyst support with an open-bonding position available above the plane of the complex to react with the fuel and a bonding position below the plane of the complex to interact with the catalyst support. By a suitable choice of metal ions and ligand, a series of chelates of varying co-ordinating tendency may be prepared for different types of fuels.

The use of metal chelates for the oxidation of insoluble fuels (hydrogen, hydrocarbons) requires careful design of the electrode assembly to maximize the three-phase contact of fuel-electrode-electrolyte, chelates have been found to be active in oxidation of hydrocarbons using cesium carbonate as electrolyte at 150°C. In a few cases, concentrated phosphoric acid was used with phthalocyanines and chlorophthalocyanines as electrocatalysts.

<i>Ligand</i>	<i>Structure</i>	<i>Relative field strength</i>
1. Hexafluoroacetylacetonone (HFAA)		Weak
2. Acetylacetonone (AA)		Weak
3. Bisacetylacetonone-ethylenediimine (BAAEDI)		Moderate
4. Bissalicylaldehyde-ethylenediimine (BSAEDI)		Moderate

TABLE 1.3 Some Ligands Used in Preparation of Chelate Electrocatalysts.

Sodium tungsten bronzes : The desired region of potential in which a fuel cell oxygen cathode should operate is 0.8 to 1.2 volts (NHE) in acid solutions. Due to oxide formation or metal dissolution in this region in the case of most metals or alloys, it is only possible to use noble metal catalysts. In alkaline solutions, conditions are more favourable. However, in the case of organic compound- air fuel cells, it is necessary to develop acid electrolyte fuel cells since carbondioxide rejection is immediate in this medium.

Three basic requirements for an oxygen electrode material are that it must be highly conducting (electronic), be corrosion resistant, and have good catalytic properties for the electrode reaction. Recently, the sodium tungsten bronzes, of general formula $\text{Na}_x \text{WO}_3$, with x varying from 0.2 to 0.93, were found by Sepa, Danjanovic, and Bockris³⁰ to satisfy all these requirements.

A curious aspect of the bronzes is the presence of a type of promotor activity. Small traces of metals, for example 1 ppm of nickel, promote the reduction of O_2 by $10^2 - 10^3$ times in rate. A negative aspect arises from the fact that oxide films form at higher potentials on bronzes. If single crystals are used, these films have little importance for the resistance. However for porous electrode use, the oxide layers are in series through all the small crystal catalysts in contact, and hence there is considerable diminution in activity in porous electrodes. Investigation of the replacement of Pt by the cheap bronze as electrocatalysts is an important and worthwhile research objective.

CHAPTER 2

SOLID STATE CHEMISTRY

2.1 Early Work on Semiconductors :

The history of research on the substances now generally known as semiconductors is a long one, extending over more than a century. Much of the early work was carried out under very great difficulties. The purity of the materials available to the early workers fell far below the very high standards which we now know to be necessary if unambiguous results are to be obtained. It is, nevertheless, a high tribute to the skill and care of many experimenters that, in spite of this, semiconductors had been recognized as a distinct class of substances and their main properties appreciated long before a comprehensive theory was available to account for them. That mistakes were is not surprising. A few substances included once in the class have now been shown to be metals, and a number of substances thought to show metallic behaviour have now been shown, when pure, to be semiconductors.

2.1.1 'Excess' and 'Defect' Semiconductors :

A considerable amount of work on a large variety of substances thought to be semiconductors was carried out between 1910 and 1930 but not a great deal of fundamental progress was made. Increased interest in these substance was aroused about 1930 largely due to the stimulus of technological applications. Hall effect, conductivity and thermoelectric power measurements were mainly used for their study and it was shown that the sign of the Hall effect, at low temperatures, and of the thermoelectric power are generally the same. A study of the chemistry of a number of semiconducting compounds to identify two distinct types of semiconductor - 'defect' and 'excess' semiconductors. The substances concerned were mainly metallic oxides and sulphides and the 'defect' semiconductors were those with a metallic content less than that corresponding to stoichiometric composition, i.e. oxydized compounds. They generally showed a positive Hall coefficient at low temperatures and a positive thermo electric power. The 'excess'

semiconductors were 'reduced' compounds and had an excess of metal. They had generally a negative Hall coefficient at all temperatures. For the 'defect' semiconductors the Hall coefficient sometimes became negative at high temperatures. These are what we now call respectively p-type (p for positive) and n-type (n for negative) semiconductors.

2.1.2 Surface and Bulk Effects :

Much of the uncertainty of the early work on semiconductors arose through a failure to differentiate between effects which arise in the bulk of the material and those which are characteristic of the surface or of the interface between two different materials. Extensive use of compressed powder samples accentuated the surface effects. It was later thought that a negative temperature coefficient of resistance is always a bulk effect but it is now known that this is by no means so. Rectification was rightly classed as a surface or interface effect but a great deal of confusion arose over photovoltaic and photoconductive effects.

2.2 Defect Solid :

In a perfect crystal it is assumed to have all their atoms at sites which lie on a perfect periodic lattice. This condition does not hold for real crystals. The thermal vibrations of the atoms about their positions of equilibrium destroy the perfect periodicity. We shall consider various other types of imperfection or defect.

2.2.1 Impurities :

the most obvious type of imperfection is due to the presence of foreign atoms in the crystal. No substance can be made perfectly pure, and although great strides have recently been made in this direction, mainly through research on semiconductors, even the

purest crystals contain many foreign atoms. An impurity content of '1 part in 10^9 ', still leaves about 10^{14} impurity atoms per cm^3 . The bulk of the atoms making up the crystal we call atom of the host crystal. The foreign atoms are generally called impurities, and they play, as we shall see, a vital part in determining the properties of semiconductors. We must distinguish two types of impurity, substitutional impurities, which replace atoms of the host crystal on their lattice sites, and interstitial impurities which occupy positions in between the lattice sites.

2.2.2 Interstitial Atoms and Vacancies :

Another type of imperfection occurs when an atom of the host crystal is displaced from a lattice site into an interstitial position. Such an imperfection is called an interstitial atom. When this occurs, a vacant lattice site may be left, and this forms another type of imperfection generally called a vacancy. More complex configurations may exist in which two or more vacancies occur at neighbouring lattice sites.

If the atoms removed from lattice sites migrate to the surface of the crystal, they may extend the crystal by occupying regular lattice sites on the surface. Thus we may have vacancies without corresponding interstitial atoms; such defects are known as Schottky defects. On the other hand, vacancies and interstitial atoms may be formed in pairs, these defects are known as Frenkel defects. All the above imperfection may also have variations according to their electrical charge, i.e. they may in some cases trap one or more electrons or positive holes and may exist in different states.

At high temperatures these imperfections will be mobile, and a thermodynamic equilibrium may be set up between the various types of imperfection. The smaller the energy of formation the larger the number of defects of a particular type.

Although thermodynamic equilibrium may exist at temperatures not far below the melting point of a crystal, the time required for the establishment of such equilibrium at lower temperatures may be very long, and the imperfections may be 'frozen in'. Thus the number of imperfections will depend on the thermal history of the crystal. By holding the crystal for some time at an intermediate temperature the number of imperfections may be considerably reduced. This process is known as annealing.

2.2.3 Dislocations :

The imperfections discussed above are all mainly point imperfections. A small number of neighbouring imperfections may group to form a cluster or short line of imperfections but these are generally sharply localized. We must now consider imperfections which run as lines (not necessarily straight, but frequently so) through the crystal. Such imperfections are known as dislocations. When a crystal is subject to stress it generally yields by crystal planes slipping over one another. The whole plane does not slip at once but does so along a curve which spreads gradually over the plane. The line separating the slipped from the unslipped portion is called a dislocation. When the direction of slip is at right angles to the line, the imperfection is called an edge dislocation. When the direction of the slip is along the line the imperfection is called a screw dislocation. Where a dislocation line meets the surface of a crystal the regular order of the atom is disturbed and the surface may be differently attracted by an etching solution. Under proper conditions small pits, known as etch pits, are formed at the intersection of the dislocation with the surface.

2.2.4 Polygonization and Dislocation Walls :

Dislocation may be spread in a fairly random array throughout a crystal, but it is found that, on annealing the crystal, they frequently tend to line up to form dislocation walls. These walls

sometimes form a net work throughout the crystal. When intersected by a plane they show up a network of polygons.

A particularly striking form of a walls of parallel edge dislocations is formed at a small angle grain boundary. This is common form of rather more gross imperfection which occurs in crystals.

2.3 Energy-band Model of Solids :

The understanding of semiconductor is based almost entirely on the energy-band model of solids. The energy-band model most conveniently represents the distribution of electrons in a semiconductor under various conditions. It also has contributed greatly to the understanding of other solids for which the quantitative agreement may not be as satisfactory. It should be understood, however, that the band model is an approximation, and certain semiconductor properties cannot be fully explained on this basis.

2.3.1 Energy-bands :

The energy-band model of a semiconductor is quite similar to that of an insulator and consists, at absolute zero, of a filled valence band that is separated from the empty conduction band by a forbidden energy region called the forbidden-energy gap. This gap is usually quite narrow in semiconductors, so that as the temperature of the semiconductor is increased, some of the electrons occupying states near the top of the valence band can transfer to empty states near the bottom of the conduction band, after absorbing sufficient energy. This process is usually described by saying that some of the valence electrons have been "excited" to states in the conduction band. Let us consider the periodically varying potential energy of an electron along some row of atoms in a crystal. The allowed-energy values for the inner electrons are localized in the vicinity of their respective nuclei.

The outermost electrons do not appear to be localized at any particular atom rather form a quasi-continuous band extending through the entire crystal. If a foreign atom is substituted into a crystal structure it introduces new energy levels in the vicinity of each foreign atom. Such localized levels play an important role in semiconductors.

The relative positions of the energy-band maxima and minima vary with crystallographic direction in the crystal and a complete, quantitative accurate description of a semiconductor therefore requires a three dimensional band model. It turns out, however, that most properties of semiconductors can be understood quite well by considering a one-dimensional model.

2.3.2 Density of States :

It is necessary to know the density of states in each allowed-energy band in order to determine the electron distribution under various conditions. In principle, this is easily determined because the density of allowed states is governed by the crystal structure, and their occupation at any temperature is determined by the Fermi distribution function.

Each energy level can contain two electrons having opposite spins, the total number of electrons that can be accommodate is given by

$$N = 2 \times \frac{4}{3} \pi k^3 \times \frac{v}{8\pi^3} = \frac{8\pi}{3} \frac{(2mE)^{3/2}}{h^3} v \quad (2.1)$$

where E is the kinetic energy of the electron, m is the mass of electron, v is the volume of the crystal and h is the Planck constant. The number of available states having energy levels lying between E and $E + dE$ is then found by differentiating (2.1):

$$\frac{dN}{dE} = 8\pi m \frac{(2mE)^{1/2}}{h^3} v \quad (2.2)$$

The quantity $\frac{dN}{dE}$ is called the density of states.

The number of electrons in a crystal of volume v , whose energies lie between E and $E + dE$, is determined according to (2.2) by

$$N(E) dE = \frac{dN}{dE} f(E) dE = S(E) f(E) dE \quad (2.3)$$

where $S(E)$ is energy density of available state, $f(E)$ is the Fermi function

The energy density of available states per cubic meter near the bottom of the conduction band can be represent as

$$S(E) = \frac{8\pi m}{h^3} \sqrt{2m(E-E_c)}$$

where E_c is the energy at the conduction-band edge.

The number of electron per cubic meter in the conduction band can be determined as

$$n = \int_{E_c}^{\infty} S(E) f(E) dE \quad (2.4)$$

This equation can be simplified as

$$n = 2 \left(\frac{2\pi m k T}{h^2} \right)^{3/2} e^{-(E_c - E_0)/kT} \quad (2.5)$$

Since the exponentaila in (2.5) represents the Fermi function, the quantity multiplying the exponential is called the effective density of state in the conduction band,

$$N_c = 2 \left(\frac{2\pi m k T}{h^2} \right)^{3/2} \quad (2.6)$$

Finally the electron density is simply

$$n = N_c e^{-(E_c - E_0)/kT} \quad (2.7)$$

Similarly the number of holes per cubic meter in the valence band may be found and for the hole density is

$$P = N_v e^{-(E_c - E_v)/kT}$$

$$\text{where } N_v = 2 \left(\frac{2\pi m_p kT}{h^2} \right)^{3/2} \quad (2.9)$$

is the effective density of states in the valence band.

2.3.3 Intrinsic Semiconductors :

A perfect crystal structure which contains no chemical impurities and in which there are no atoms displaced from their proper sites, the properties of such a solid are thus characteristic of the ideal structure, and such a material is called an intrinsic semiconductor. In an intrinsic semiconductor the number of electrons occupying states in the conduction band is equal to the number of holes in the valence band. In order to calculate the actual hole and electron densities, the position of the Fermi level E_c first must be determined. Since $n = p$, this can be done by equating (2.7) and (2.8). The result is

$$N_v/N_c = e^{-(E_c + E_v - 2E_0)/kT} \quad (2.10)$$

which may be solved for the Fermi energy

$$E_c = \frac{E_c + E_v}{2} + \frac{3kT}{4} \ln \frac{m_c^*}{m_p^*} \quad (2.11)$$

Here m_c^* is the effective mass of electrons in the conduction band, and m_p^* is the effective mass of the electrons in the valence band, often called the effective mass of the holes.

If $m_c^* = m_p^*$, then the Fermi level lies midway between the valence and conduction-band edges as indicated in Fig. 2.1. In any event, E_c does not deviate appreciably from the centre of the gap because the logarithm in the second term of (2.11) is small. For

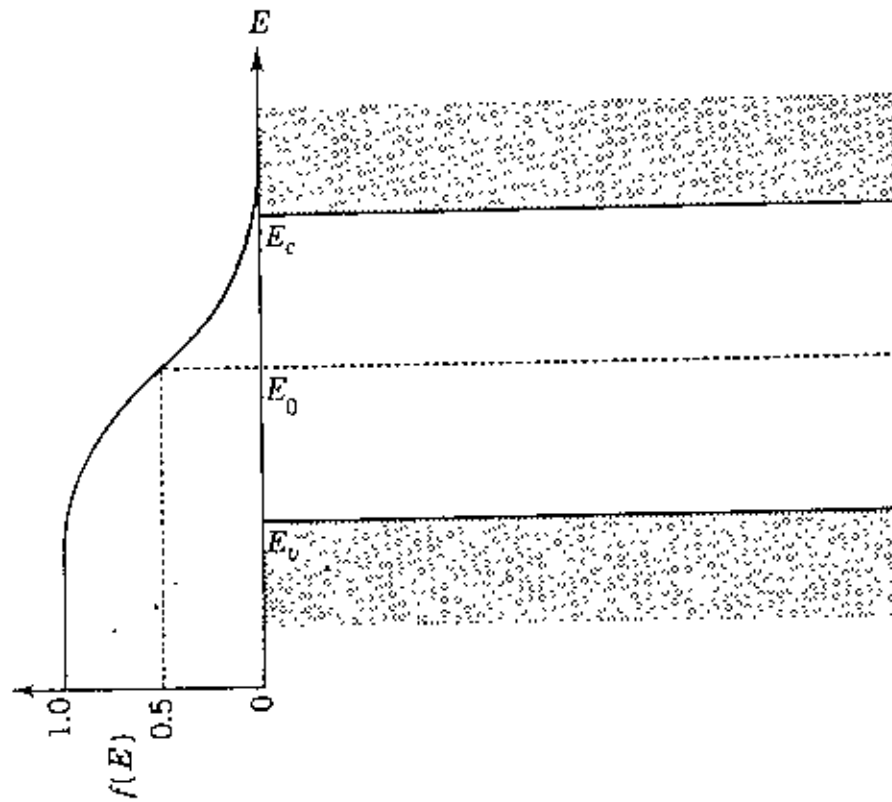


Fig.2.1 Position of the Fermi level and the Fermi distribution for an intrinsic semiconductor.

convenience, therefore, the Fermi level is usually assumed to be midway between the bands in an intrinsic semiconductor.

2.3.4 Conduction by Electrons and Holes :

Any electrons occupying states in the conduction band are free to respond to an applied electric field. The energy they gain in the direction of the field results in motion that constitutes an electric current. The conductivity of a material is defined by Ohm's law to be the current density J per applied field, so that

$$\sigma = \frac{J}{E} \quad (2.12)$$

The current density due to n electrons per cubic meter moving at a resultant or average velocity \bar{v} is simply $J = n e \bar{v}$, which gives, for the conductivity due to electrons in the conduction band,

$$\sigma = n e \mu \quad (2.13)$$

Here, $\mu = \bar{v}/E$ is the average velocity of an electron per applied field, and is called the mobility of the electron.

The conductivity produced by the holes is given by an expression identical with (2.13). Therefore, the total conductivity of a semiconductor crystal is the sum of the conductivity by electrons and holes,

$$\sigma = n e \mu_e + p e \mu_h \quad (2.14)$$

where μ_e and μ_h are the electron and hole mobilities, respectively.

Since $n = p$, the conductivity of an intrinsic semiconductor can be obtained by combining equation (2.7), (2.8), and (2.11). Introducing $E_g = E_c - E_v$, where E_g is the width of the forbidden-energy gap, the result is (for $N_c = N_v$)

83008

$$\sigma = N_c e (\mu_p + \mu_n) e^{-E_g/2kT} \quad (2.15)$$

Equation (2.15) shows that the conductivity of an intrinsic semiconductor increases exponentially with temperature. Such a conductivity variation is a characteristic of semi conductors and distinguishes them from metallic conductors. The width of the forbidden-energy gap can be determined from (2.15) by experimentally measuring the temperature dependence of conductivity. Taking the natural logarithm of both sides,

$$\ln \sigma = \ln N_c e (\mu_p + \mu_n) - \frac{E_g}{2k} \cdot \frac{1}{T} \quad (2.16)$$

This is the expression for a straight line, since the first term on the right does not vary appreciably with temperature. Thus, a plot of $\ln \sigma$ versus $1/T$ yields a straight line of slope $-E_g/2kT$, and E_g can be evaluated directly.

2.4 Extrinsic Semiconductor :

Impurity Levels :

When foreign, or impurity, atoms are incorporated into the structure, the available quantum states are altered and this introduces significant changes in the properties of the semiconductor. Since these properties now depend strongly upon the impurity content, the solid is called an extrinsic semiconductor. Because the number of electrons and holes normally present in an intrinsic semiconductor is small, small additions of impurity atoms are significant to produce major change.

Consider a single crystal of silicon. Each silicon atom has four valence electrons with which it forms four electron-pair bonds with four Si neighbors. If a pentavalent atom, for example phosphorous, arsenic, or antimony, substitutes for a silicon atom, only four of its electrons are required to complete the covalent bonding in this structure. The extra electron is constrained to remain in the neighborhood of the impurity atom, however, because it is attracted by the extra positive charge on the nucleus.

Thermal energies are sufficient to overcome this binding even at quite low temperatures, so that the electron is excited to empty states in the conduction band, where it behaves like a nearly free electron. Chemical additions from the fifth column of the periodic table thus are able to "donate" electrons to the conduction band, and they are called donor impurities for this reason. Since this increases the density of conduction electrons in the crystal, it is called an n-type extrinsic semiconductor.

The extra electron of a donor atom is primarily influenced by the excess positive charge of the ion's nucleus. Its motion near the donor atom, therefore, is quite analogous to that of the electron in a hydrogen atom.

The quantum state of this electron, called a donor level, is located below the bottom of the conduction band for pentavalent substitutional impurities in silicon. Since the donor level has a specific energy, it is called a discrete state, and since it exists only in the vicinity of the donor atom, it is also said to be localized. One such discrete, localized donor level exists for each impurity atom, and these are usually indicated by short lines on an energy-level diagram, as shown in Fig. 2.2(A).

By comparison, when a trivalent atom like boron, aluminium, gallium or indium substitutes for a silicon atom, one of the covalent bonds in the structure can not be satisfied. This unsatisfied electron-pair bond can be completed by the transfer of another valence electron from a nearby silicon atom. The loss of a valence electron by this silicon atom is represented in the energy-band model by the appearance of a hole in the valence band. The foreign atom is thus said to have accepted a Valence electron from the crystal, and such impurities are termed acceptors. The inclusion of acceptor in a crystal, therefore, creates hole in the valence band and leads to p-type extrinsic conductivity.

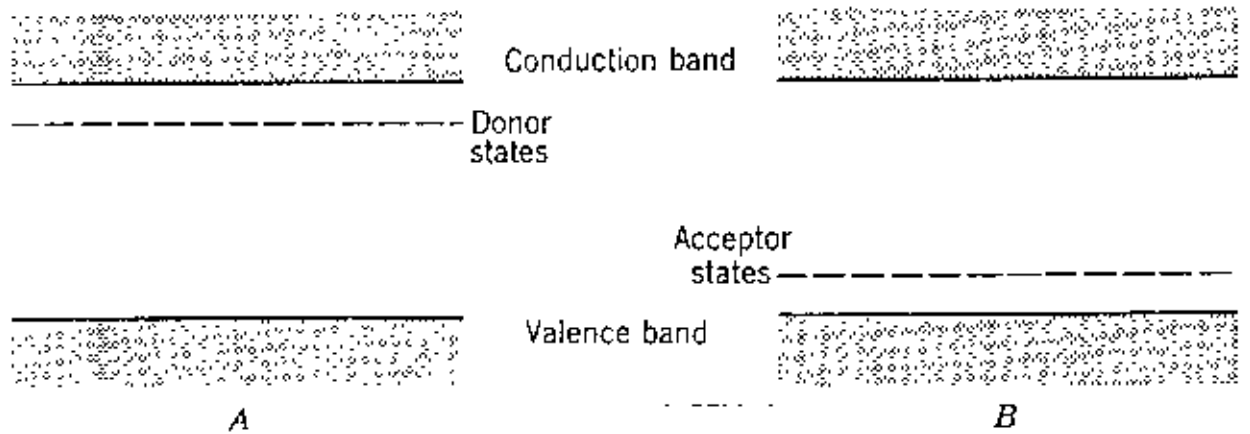


Fig.2.2 Representation of discrete, localized impurity levels in an energy-level diagram for the case of A, donor, and B, acceptor, impurities.

The motion of the hole near the acceptor impurity is analogous to that of an electron near a donor. The hole has an effective positive charge, while the acceptor has an effective negative charge, since it has one less nuclear charge than the other atoms in the solid. Acceptor states are also discrete and localized and are located above the top of the Valence band as shown in Fig. 2.2(B).

Other types of chemical impurities produce different kinds of impurity levels, depending on their valence-electron structure and how they are incorporated into the crystal structure. Metals such as iron, nickel, cobalt, and copper in silicon and germanium crystals produce discrete localized levels far removed from the band edges, and are called deep levels. Zinc and gold atoms give rise to three discrete states per impurity atom, each at a different distance from the band edges. On the otherhand, oxygen may be chemically bound in the structure in such a way as to give rise to no discrete states. In addition to chemical impurities, point imperfections may result in localized levels; for example, a vacancy-interstitial pair called a Frenkel defect behaves in many respects like an acceptor level. It is because of the generation of such states by chemical and crystalline imperfections that semiconductor crystals normally must be produced under conditions assuring extreme purity and perfection.

CHAPTER 3

CHARGE TRANSFER PROCESS

3.1 Charge Transfer Process at Metal Electrode Comparison of Chemical Reactions with Electrochemical Reactions :

The essential feature of an electrochemical reaction is that it involves interfacial charge transfer. Thus, its reaction rate would be expected to depend on the electric potential difference at the interface. The rate constant for a chemical reaction may be expressed by the Arrhenius equation, given by

$$k_o = A \exp\left(-\frac{E^\ddagger}{RT}\right) \quad (3.1)$$

where E^\ddagger is the energy of activation for the process, A is a constant (frequency factor), R is the gas constant and T is the absolute temperature. In many electrochemical reactions, the current is found to vary exponentially with potential across the metal-solution interface. Hence, the rate constant for an electrochemical reaction may be empirically expressed by

$$k = k_o \exp KV = A \exp\left(-\frac{E^\ddagger}{RT}\right) \exp KV \quad (3.2)$$

where V is the metal solution potential difference and K is a constant.

Remarkable control is possible through this extra-potential-dependent term⁴⁰ and that it is far in excess of any variation due to concentration or temperature.

Two other characteristics make chemical and electrochemical reactions different. Electrode reactions always are heterogeneous, whereas many chemical reactions are homogeneous. Finally heterogeneous chemical reactions take place on surface principally occupied by the adsorbed reactants. Electrochemical reactions, in aqueous and nonaqueous solutions, occur on substrates which are always covered by solvent molecules and some times anions⁴¹. The concentrations of both the species are potential-dependent. →

Effect of potential difference across electrode-electrolyte interface on electrochemical rate constant : The effect of

potential on electrochemical rate constants may be visualized from potential-energy diagrams⁴². Consider a reaction of the type



in which M is the metal and AB⁺ is a diatomic ion. The potential energy-distance (from the metal) relation for the reaction, assuming a linear transition state, when the metal-solution potential difference is zero (V=0) is shown in curve 1 of Fig. 3.1. In the presence of a metal-solution potential difference V, the additional energy of the ion due to its electrical energy in the region between the two minima is linear and is given by curve 2. Under these conditions, the potential energy-distance relation (curve 3) for the reaction may be obtained by superposition of curve 1 and 2. It is assumed that the electrical potential in the final state is zero, then the superposition of curve 1 and 2 results in a vertical shift of the right-hand minimum (initial state) by VF. At the same time, the maximum of the curve is only shifted by a fraction of VF (because of the linear variation in potential between the metal and the outer Helmholtzj plane), i.e. (1-β) VF, where 0 ≤ β ≤ 1; β depends on the position of maximum and is referred to as the " symmetry factor". The symmetry factor represents the fraction of the contribution of electrical energy to the activation energy of an electron-transfer reaction. Thus, if k₀ and k are the rate constants in the absence (V=0) and in the presence of a metal-solution potential difference (V=V), the relation between the two rate constants is given by

$$k = k_0 \exp\left(-\frac{\beta VF}{RT}\right) \quad (3.4)$$

According to equation (3.4), it is seen that the activation energy of an electrochemical reaction of the type (3.3) varies linearly with the potential drop across the metal-solution interface (i.e., with the electrode potential).

Potential energy calculations for electrochemical reactions:
A method of obtaining the potential energy as a function of the

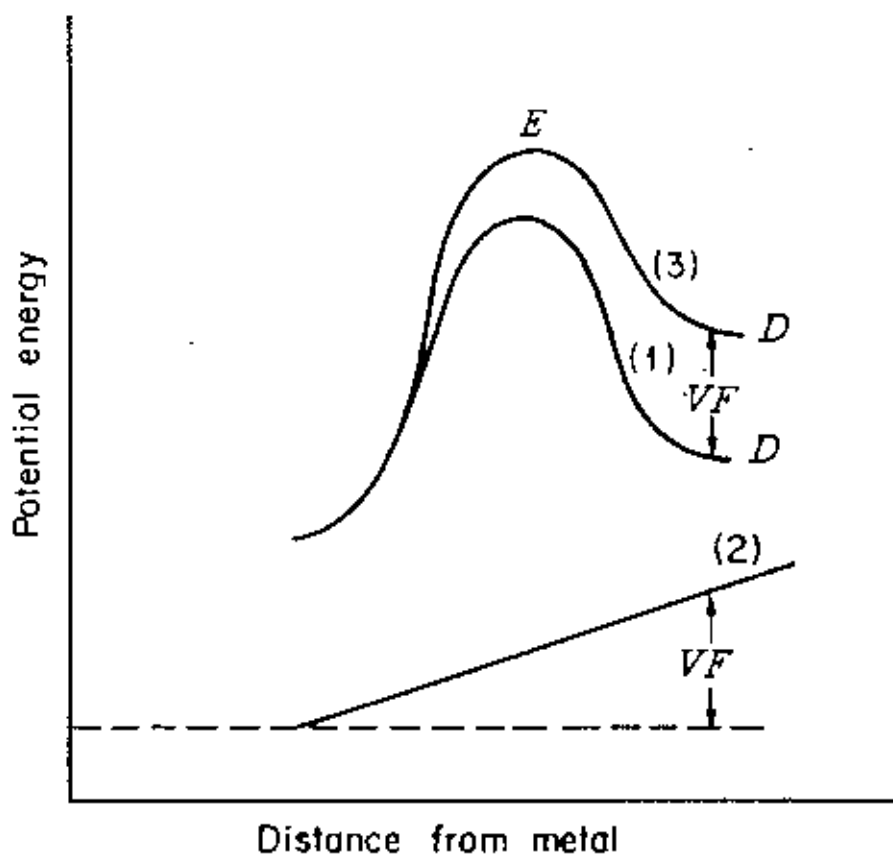


Fig.3.1 The relation of potential energy to distance along the reaction coordinate for a charge-transfer reaction in the absence (curve 1) and in the presence (curve 3) of metal-solution potential difference V — simple picture. Curve 2 represents the electrical energy of charged species as a function of its distance from metal.

distance along the reaction coordinate in the case of the hydrogen-electrode reaction was first introduced by Horiuti and Polanyi⁴³. According to this treatment, the activation energy is represented by the difference in height from the intersection point of the curves of potential energy Vs distance along the reaction coordinate for the stretching of the bond being broken (i.e. between A-B) and that being formed (i.e. between B-C) for a reaction of the type



to the minimum of the potential-energy curve for the bond being broken (i.e. between A-B). For the purpose of constructing this potential-energy profile, it is assumed that the extreme atoms are fixed and the transition state (A.....B.....C) is linear. An analogous electrochemical reaction is represented by equation (3.3). It is necessary in this case to substitute electrochemical energies rather than chemical energies to obtain the potential-energy diagram. The change in height of the barrier with polarization of the electrode was represented by a vertical shift in the potential-energy curve of the initial state. Thus in Fig. 3.2 curve PQR represents the potential energy-distance plots for the reactants for varying B-A' distance when $V = 0$; P Q' R' represents a similar plot when the metal-solution potential difference is V , the difference in height between the two minima being VF ; and XYZ represents the potential energy curve for the stretching of the M-A bond.

A simple picture of the symmetry factor : It has been observed experimentally that the symmetry factor is constant over a wide range of potential. This can at once be shown to follow if the potential energy-distance relations for the initial and final state curves are linear in the region of their point of intersection. According to this treatment⁴⁴, the potential energy-distance relation is as shown in Fig. 3.3. The curves in this figure are the linear analogs of the curves in the previous figure.

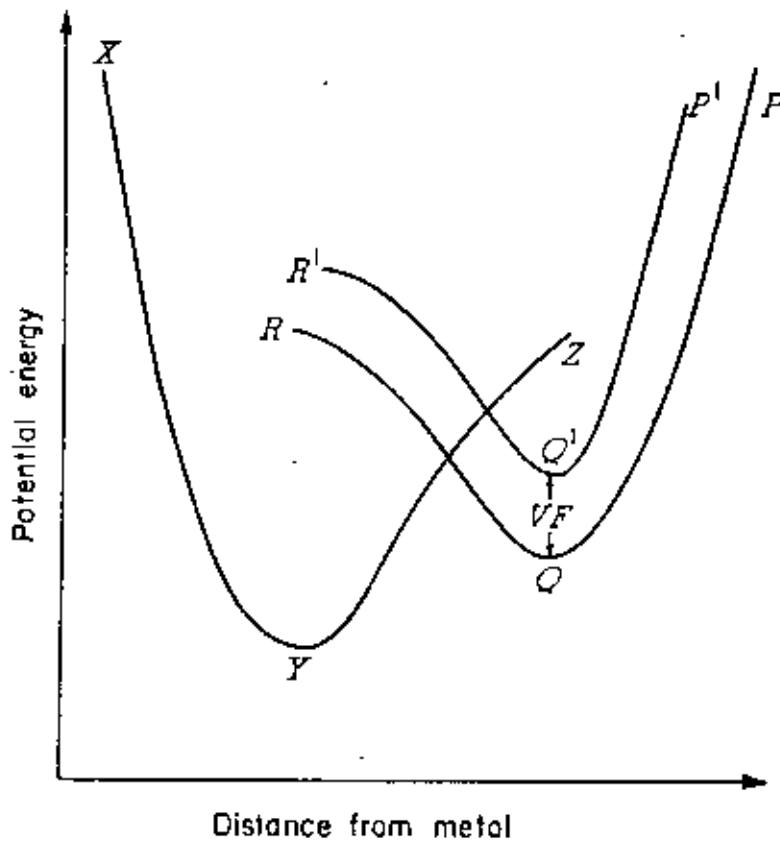


Fig.3.2 Potential-energy-distance relation for charge-transfer reaction in the absence and in the presence of metal-solution potential difference V - a more realistic picture.

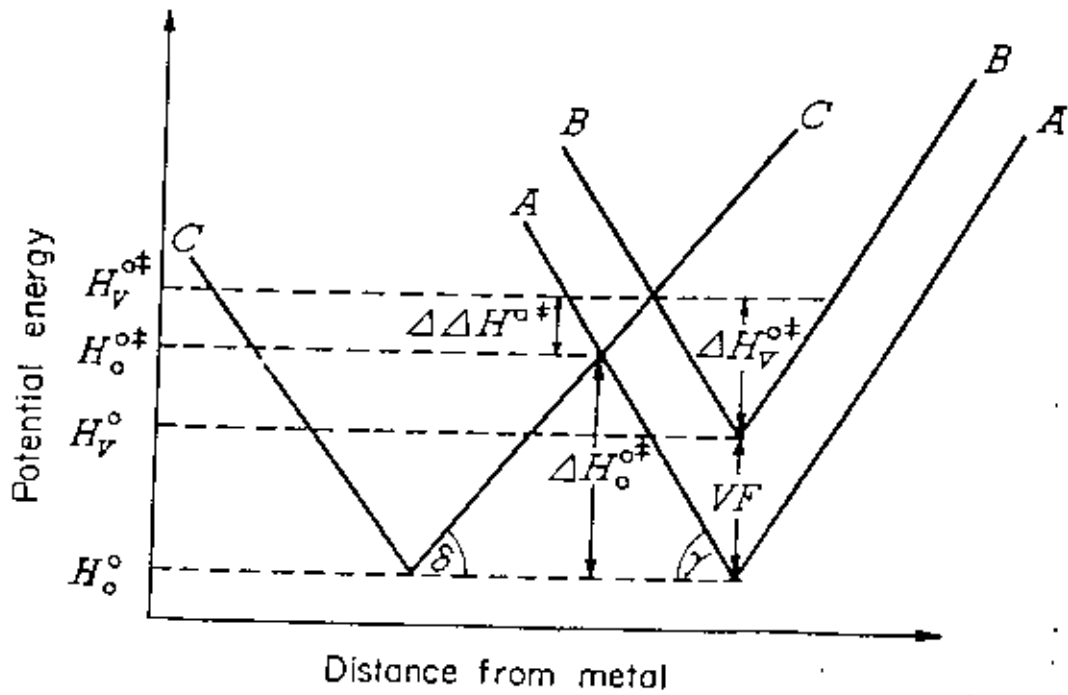


Fig. 3.3 Linear analogs of potential-energy-distance relations in the absence and in the presence of metal-solution potential difference V .

As seen from Fig. 3.3.

$$\Delta H_v^{\ddagger} + VF = \Delta H_o^{\ddagger} + \Delta\Delta H^{\ddagger} \quad (3.6)$$

It can easily be shown¹⁴ that

$$\Delta\Delta H^{\ddagger} = VF \frac{\tan\delta}{\tan\delta + \tan\gamma} \quad (3.7)$$

Thus,

$$\Delta H_v^{\ddagger} = \Delta H_o^{\ddagger} - \beta VF \quad (3.8)$$

Where,

$$\beta = \frac{\tan\gamma}{\tan\delta + \tan\gamma} \quad (3.9)$$

If $\tan \delta = \tan \gamma$, then $\beta = 1/2$. Linearity of potential-energy curves near the point of intersection is a good approximation; thus, by a change of potential, β would remain constant over a range of potential. However, if the applied potential is varied considerably, the approximation may no longer hold, causing changes in β with change of applied potential.

3.2 Charge Transfer Processes at Semiconductor Electrodes :

Problems of semiconductor-electrolyte interface were approached originally from two different fields—from electrochemistry and from solid state physics.

In solid state physics the main interest has been in studies of semiconductor surfaces, since surface effects influence the electrical properties of many semiconductor devices. Investigations of semiconductor-electrolyte interface have solved some of these problem.

From electrochemical investigations information has been obtained not only about the properties of semiconductor electrodes, but also about the basic mechanisms of charge transfer processes between electrodes and molecules in the electrolyte.

There are several advantages in using a semiconductors : (i) In a semiconductor well-defined energy bands exist, their energy separation depending on the type of semiconductor; (ii) The carrier density can be varied by doping over many orders of magnitude; (iii) The occupation of energy levels by electrons or holes can be increased by optical excitation.

Charge and potential distribution at the semiconductor-electrolyte interface:

At the semiconductor-electrolyte interface a double layer is formed in the same way as at the metal electrolyte interface. The double layer consists of charges of opposite signs in both phases and of oriented dipoles at the interface. Between both phases, which are charge-free in the bulk, a potential difference occurs (Galvani potential). The charges on the metal or the semiconductor surface are electrons and in the electrolyte are ions. The interphase distance between charges corresponds to the ionic radius which includes the solvation shell. The compact double layer (Helmholtz layer) may be considered as a charged condenser. Assuming that the charge is distributed homogeneously over the surface, the capacity of the condenser should be constant i.e. it is independent of any applied potential. This model, however, is only applicable for concentrated electrolytes. In dilute solutions the capacity depends on the concentration of ions in the electrolyte. Gouy⁴⁵ and Chapman⁴⁶ improved this model insofar as they assumed a space charge distributed from the interface into the interior of the electrolyte (Gouy layer).

Space-Charge layer in the semiconductor :

Metal and semiconductor electrodes show the same behaviour as far as the double layer and the Gouy layer are concerned. The main difference between these two types of electrode materials consists in the much lower density of mobile charge carriers in the semiconductor. Accordingly, the charges in a space charge are not located directly at the surface, as they are in a metal, but are

distributed within a certain region below the surface (the "space charge region")- similar to the case of a dilute electrolyte. The relation between space-charge density $\rho(x)$ and potential ϕ at the surface is given by the Poisson equation :

$$\Delta^2\phi = \frac{d^2\phi}{dX^2} = \frac{\rho(X)}{e\epsilon_0} \quad (3.10)$$

where ϕ is the electrostatic potential, ϵ is the dielectric constant and X is the distance from the surface. The space charge ρ is given by the charge carrier densities of all mobile and immobile carriers, i.e. of the electrons $n(X)$ and holes $P(X)$ as mobile carriers and of ionized donors n_D and acceptors n_A . Assuming homogeneous doping, the total space charge is given by

$$\rho(X) = e[n_D - n_A - n(X) + P(X)] \quad (3.11)$$

In the interior of the semiconductor the space charge is zero ($\rho = 0$) and the number of electrons and holes is determined only by doping i.e., $n(x) \rightarrow n_0$ and $P(X) \rightarrow P_0$. In this case equation (3.11) is simplified to

$$\rho(X) = 0 = e(n_D - n_A - n_0 - P_0) \quad (3.12)$$

Using the band model for semiconductors, the electron density in the conduction band can be calculated. In the case of nondegenerate semiconductors (i.e. the Fermi level is located below the conduction band and above the valence band) and only those are considered here the electron and hole densities follow the Boltzman distribution. Accordingly, the electron density in the conduction band is given by

$$n = N_c \exp\left(\frac{-(E_c - E_F)}{kT}\right) \quad (E_c > E_F) \quad (3.13)$$

where N_c is density of states in the conduction band, E_c is the lower edge of the conduction band, k is the Boltzman constant and T is the temperature. The density of electrons depends mainly on the relative position of the Fermi level E_F .

A corresponding relation can be derived for holes :

$$P = N_v \exp\left(\frac{-(E_f - E_v)}{KT}\right) \quad (3.14)$$

Where N_v is the density of states in the valence band and E_v is the upper edge of the valence band. In the bulk of the semiconductor thermodynamic equilibrium exists i.e.,

$$n_o P_o = n_i^2 \quad (3.15)$$

where n_i is the intrinsic concentration.

Using equation (3.10) to (3.15), it would be possible in principle to determine the potential distribution within the space-charge region. However, since it is impossible to solve equation (3.10) without any simplifications, the potential distribution shall only be considered qualitatively, as follows.

We assume that equilibrium exists within the bulk and at the surface. In the case, for instance, that the electron density n_s at the surface is lower than in the bulk, the energy distance between conduction band and Fermi level is larger than in the bulk; this corresponds to an upward bending of the energy bands as demonstrated in Fig.3.4. Using equation (3.13) the relation between electron density at the surface n_s and in the bulk n_o can be calculated and one obtains

$$n_s = n_o \exp\left(\frac{-eU_{sc}}{KT}\right) \quad (3.16)$$

in which U_{sc} is the corresponding potential difference between surface and bulk (3.4). By the same procedure the hole density at the surface (P_s) can be determined :

$$P_s = P_o \exp\left(\frac{eU_{sc}}{KT}\right) \quad (3.17)$$

The equilibrium condition is given by

$$n_s P_s = n_o P_o = n_i^2 \quad (3.18)$$

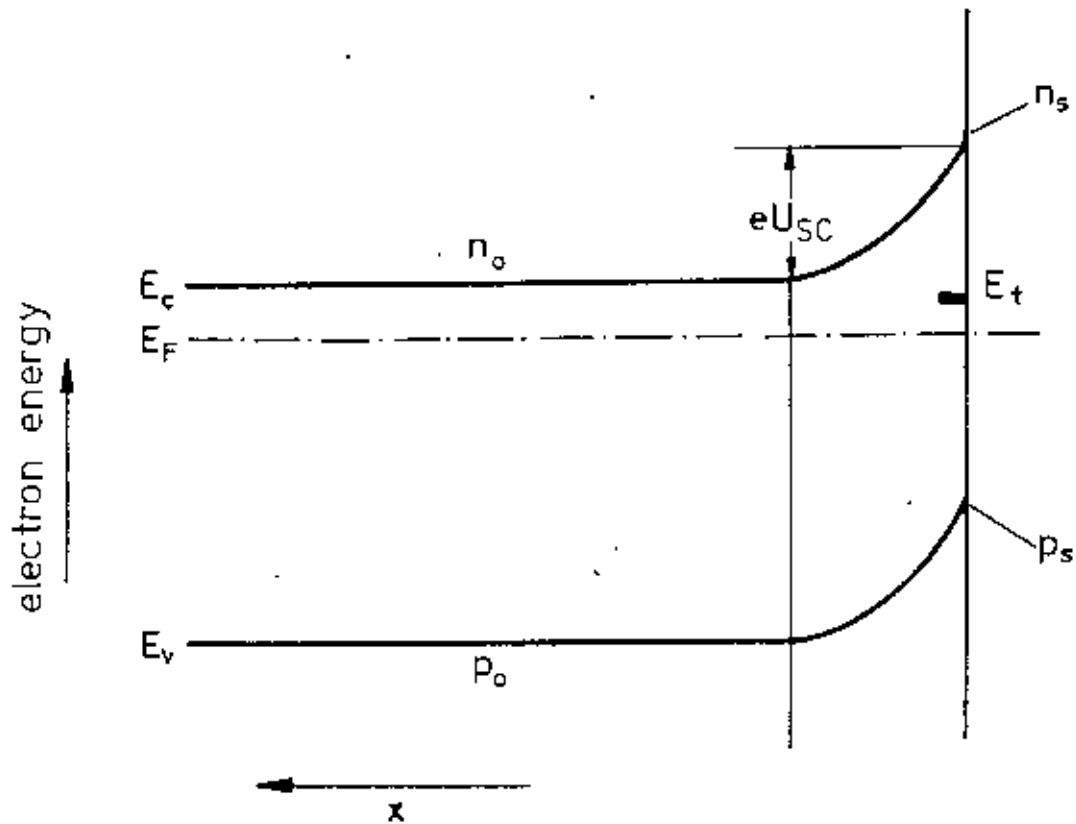


Fig. 3.4 Model of energy bands at semiconductor surface. E_c and E_v , band edges of conduction and valence band, respectively; E_F , Fermi level; n_0 and p_0 , electron and hole densities, respectively, in the bulk; n_s and p_s , electrons and hole densities, respectively, at the surface; eU_{SC} , band bending, E_t , surface state; x , distance from the surface.

If energy bands are bent upward at the surface of an n-type semiconductor, the space-charge region is called a depletion layer ($n_s < n_0$) or an inversion layer ($P_s > n_s$). On the other hand, if $n_s > n_0$ (energy bands bent downward), the space charge is called an accumulation layer.

Surface States :

Charges on the semiconductor sides of the interface must not be only distributed within the space region, but may also exist in surface states. These are energy states E_t at the surface located within the forbidden zone (Fig. 3.4). They can be formed by adsorption of atoms or ions or simply by interruption of lattice periodicity at the interface. Whether these energy levels E_t are occupied by electrons or holes depend, also, on the relative position of the Fermi level at the surface. A variation of the band bending may lead to a change of the occupation of these states.

Potential Distribution :

The charge distribution at the semiconductor-electrolyte interface shows a certain symmetry : The interface surfaces are oppositely charged; the charge separation being of the order of atomic dimensions (Helmholtz layer). Underneath the surface there exist space-charge layers extending into the neutral regions of both phases, as schematically shown in Fig. 3.5. In this example (Fig. 3.5) the charge in the surface states is assumed to be positive. Since their density is small, they do not influence the potential distribution.

Accordingly, the Galvani potential consists of three positions: the potential U_s across the space charge within the semiconductor, the potential U_e across the Gouy layer within the electrolyte, and the potential U_H across the compact double layer (Helmholtz layer):

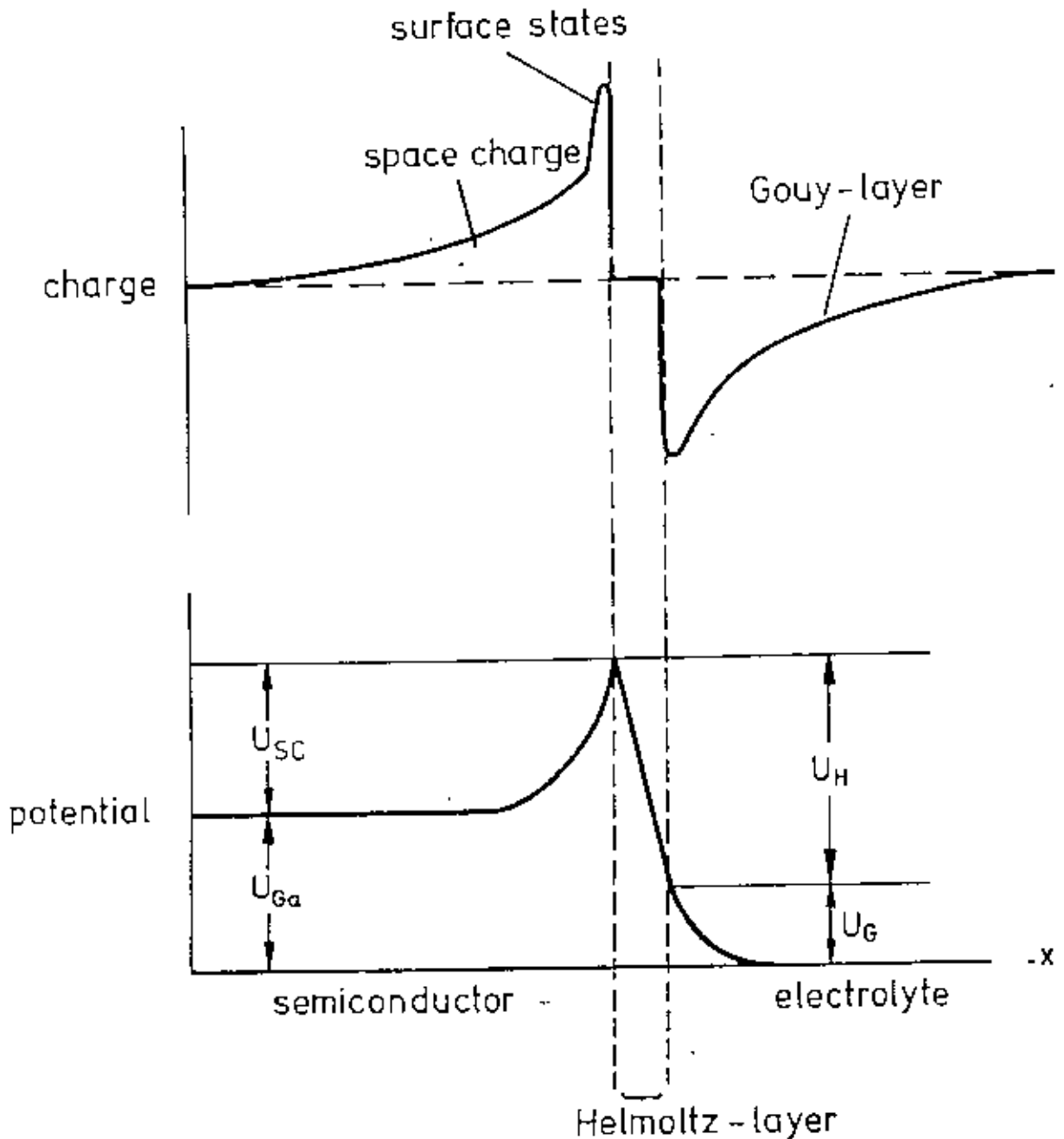


Fig. 3.5 Charge and potential distribution at the semiconductor-electrolyte interface. U_{sc} , potential across the space charge; U_{Ga} , Galvani potential; U_H , potential across the Helmholtz layer; U_G , potential across the Gouy layer; x , distance from the surface.

$$U_{GA} = U_{sc} + U_G + U_H \quad (3.19)$$

Many results are available as far as the potential distribution at semiconductor-electrolyte interfaces are concerned. Quantitative results at germanium electrodes were obtained not only by capacity measurements^{47,63}, but also by surface conductivity measurements⁴⁹. A typical capacity curve as obtained with intrinsic germanium is shown in Fig. 3.6. The experimental values (circles) were determined as a function of the electrode potential U_E (lower scale), whereas the theoretical curves (solid line) was calculated as a function of the potential U_{sc} across the space-charge layer (Upper scale). Since the experimental curve fits the theoretical curve very well, we can conclude that any variation of the electrode potential, ΔU_E , occurs across the space-charge layer, i.e.

$$\Delta U_E = \Delta U_{sc} \quad (3.20)$$

In contradiction to results obtained with metal electrodes the potential across the Helmholtz layer remains unchanged i.e., $\Delta U_H = 0$. Similar results were also obtained with n- and p-Ge^{47,50,51}. Further investigations^{49,50,52} have shown that the potential across the Helmholtz layer, U_H , can be changed by varying the P^H of the electrolyte.

3.3 Some Principles of charge Transfer At Semiconductor Electrodes And Experimental Techniques :

At metal electrodes the charge exchange occurs mainly at the Fermi energy, since only in the region of Fermi level are both occupied and unoccupied energy levels present. In semiconductors the energy levels across which a charge exchange can occur will be widely separated from the Fermi level. This situation must have a decisive influence on the electrode process. In principle, a charge exchange can proceed via the conduction or valence band. Also in certain cases both energy bands can be involved. Various

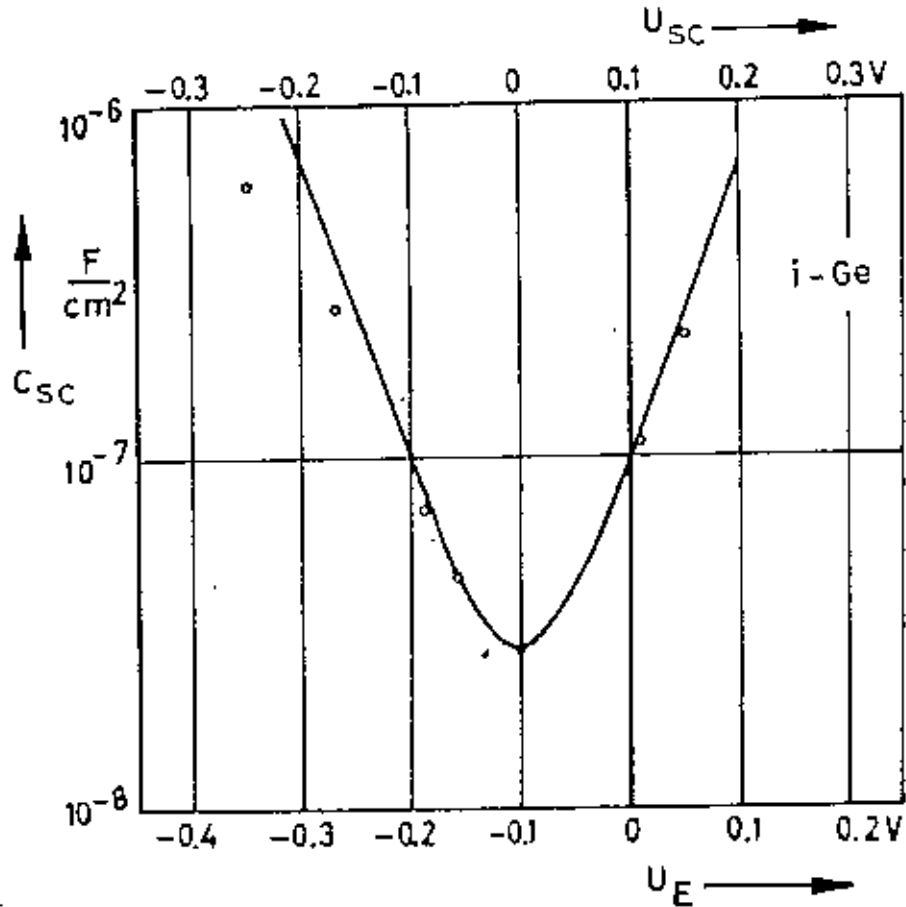


Fig.3.6 Space-charge capacity C_{sc} versus electrode potential U_E for intrinsic germanium in 0.1 N H_2SO_4 . Circles, U_E versus SCE; solid line, theoretical values as a function of U_{sc} (upper scale).

experimental techniques are available to distinguish between a charge transfer across the conduction band and one across the valence band.

3.3.1 Current - Potential Curves :

Qualitative information is readily obtained by measuring the current-potential curves. A typical example is given in fig. 3.7, which represents the current-potential curves as obtained with n- and p-type GaP electrodes⁵³. In the negative potential range the cathodic current, which is due to H_2 evolution, increases exponentially for n-GaP, whereas the current is limited to a rather small value for a P-GaP. From this result it can be immediately concluded that electrons from the conduction band are consumed in the cathodic H_2 evolution- because only in the n-type electrode is a sufficient number of energy states in the conduction band occupied by electrons. For a valence band process one would not expect any current limitation in either P-or n-GaP, because a large number of electrons would be available in the valence bands of both types of electrodes. The limiting current observed with p-GaP, however, can be increased by optical excitation of electrons from the valence band into the conduction band(dashed line in Fig. 3.7).

An equivalent behavior was also found for anodic current at positive potentials. In this case, however, a limiting current was observed with n-GaP whereas it increased for p-GaP. This process, anodic dissolution, obviously occurs via the valence band i.e. electrons can only be transferred if a sufficient number of holes are available. Again light excitation leads to an increase of the hole concentration in n-GaP (dashed line in Fig. 3.7(b)).

These basic properties are found for all semiconductor electrodes and were observed at first by Brattain and Garrett⁵⁴ for germanium electrodes. It must be determined in each case, however, whether a certain electrochemical process proceeds via the conduction or valence band of the semiconductor used in the

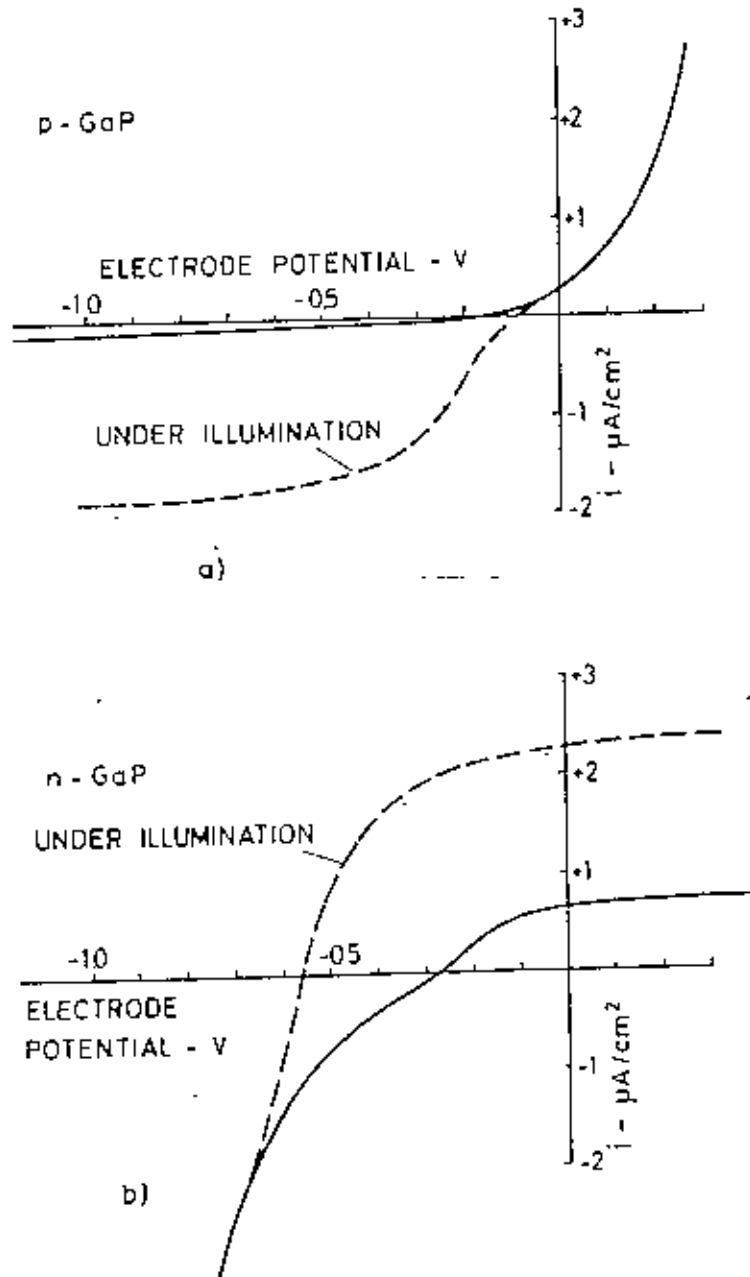


Fig.3.7 Current-potential curves for GaP electrodes in a 1 N KCl solution.

experiment. It should be emphasized that the limiting currents observed in the dark at p-GaP in the cathodic and at n-GaP in the anodic range are theoretically determined by the diffusion of minority carriers towards the surface, i.e., by

$$i_{lim,n} = \frac{eD_n n_p}{L_n} \text{ (for p-type materials)} \quad (3.21)$$

$$i_{lim,p} = \frac{eD_p p_n}{L_p} \text{ (for n-type materials)} \quad (3.22)$$

and in which D_n , D_p are the diffusion constants of electrons and holes; L_n , L_p the diffusion length; and n_p , p_n the densities of electrons and holes in p- and n-type materials, respectively. The relation between limiting current and minority carrier density was quantitatively confirmed by measurements with germanium electrodes⁵⁵. For the case of semiconductors with a large band gap, such as 2.3 eV for GaP, however, the pure diffusion current of electrons or holes would be undetectable ($\sim 10^{-22}$ A cm⁻²) since the minority carrier density is only about 10^{11} cm⁻³ (majority carrier density: 10^{17} cm⁻³). Since limiting currents of the order of 10^{-6} to 10^{-9} A cm⁻² were found, it is generally assumed that generation processes via surface states are involved.

3.3.2 Injection Process :

In some electrochemical reactions in which more than one electron per elementary step is transferred, both energy bands can be involved. Examples are anodic dissolution and two-step processes. In these cases it is difficult to decide from current-potential curves whether only one or both energy bands are involved. Quantitative information, however, can be obtained using the "thin silica method"^{56,58}. This method consists of an electrode with np-junction on its backside. Assuming for example, an anodic process of a p-electrode, the total current consists of two partial currents- one via the conduction band is i_c and the other via the valence band i_v :

$$i_{tot} = i_c + i_v$$

the charge transfer from the electrolyte into the valence band corresponds to a certain hole (majority carrier) current toward the surface. The electrons injected into the conduction band i_c , however, can only diffuse toward the interior of the p-electrode; some recombine and the others reach the pn-junction, where they are forced toward the n-contact by the electric field of the junction. The corresponding short circuit current i_s , measured at the junction, is a direct measure for the injected electrons and is related to the injection current i_c by⁵⁷.

$$i_s = i_c \exp\left(-\frac{d}{L}\right) \quad (3.24)$$

in which d is the thickness of the electrode and L is the diffusion length of the electrons. Using this equation, i_s can be calculated and compared with the total current i_{tot} .

This method has been successfully applied for germanium⁵⁰⁻⁵¹ and silicon⁶² electrodes. However, for semiconductor electrodes with a large band gap, it failed because the diffusion length is too small. It should be mentioned that an electrolyte contact instead of a pn-junction can also be used, as proposed by Pleskov⁵⁸.

3.3.3 Photocurrents :

Much information can also be obtained from photocurrent measurements, as has already been mentioned in connection with the current-potential curves. According to the current-potential curves in Fig. 3.7, the cathodic photocurrents as observed with p-GaP (Fig. 3.7a) sets in at a lower (i.e., less negative) potential than does the corresponding dark current found for n-GaP (Fig. 3.7b). In this case the photocurrent which corresponds to H_2 evolution begins at a potential even more positive than the H_2/H^+ normal potential. This results from the downward bending of the energy bands: The

electrons created by light are forced to move toward the surface because of the field of the space charge. It should be emphasized that in this situation no thermodynamic equilibrium exists. This effect has been observed for many semiconductor electrodes with a large band gap also, for anodic processes such as oxygen evolution⁶³ at n-type electrodes.

3.4 Charge Transfer Process :

In most cases pure charge transfer at the interface is accompanied by chemical reactions. In connection with this problem is of importance whether surface atoms or bands of the semiconductor are or are not involved in the charge transfer process. In the first case we have a strong interaction between surface and a possible reactant. Typical reactions are oxidizing and reducing processes in which the surface is attacked (e.g. anodic dissolution). On the other hand, a large number of charge exchange processes are known in which the interaction between surface and reactant is weak as, for example, in many redox reaction.

3.4.1 Charge Exchange :

Since the work by Gurney⁶⁴ in 1931, a number of theories on electron transfer reactions been published by Hush⁶⁵ Marcus⁶⁶, Levich⁶⁷, and Chizmadzhev⁶⁸, Kuznetsov and Dogonadze⁶⁹, by Gerischer⁷⁰. According to Marcus, electron transfer of the simplest class of electrode reactions, for example, the oxidation of Fe^{2+} , can be described as follows.

A reacting molecule reaches a suitable position at the electrode surface by thermal motion. Energy fluctuations in the solution may result in activation of the molecule and consequently, also in the activation of the reacting electron. Provided that the electron energy in the molecule attains a level which is equivalent to unoccupied states in the electrode, the electron may be

transferred from the molecule to the electrode. This transition is assumed to be fast compared to the relaxation time of the surrounding solvent molecules i.e., the Franck-Condon principle is assumed to be valid.

According to this model, the anodic current can be expressed by

$$i_a = FZC \int_0^{\infty} x(E) \rho(E) [1-f(E)] \left[\exp\left(-\frac{E^*}{KT}\right) \right] dE \quad (3.25)$$

Where ZC is the number of molecules which reaches the electrode surface; $x(E)$ is the transmission coefficient, which strongly depends on the distance of the reacting molecules from the surface; $\rho(E)$ is the distribution function of electron states in the electrode, $[1-f(E)]$ is the probability that these states are occupied (Fermi function); and E^* is the activation energy. This is the energy difference of the whole system between its initial and its transition state. The exponential term refers, therefore, to the number of molecules in the activated state with the electron energy E .

These changes in energy of the complete system consisting of the electrons, the ions, and the surrounding solvent molecules are caused by vibrations and rotations of the particles around their equilibrium position. The thermal energy of such a system can be described by a set of harmonic oscillators. On the basis of this model the activation energy was calculated, as given by

$$E^* = \frac{(E_2^0 - E_1^0 + \lambda)^2}{4\lambda} \quad (3.26)$$

This equation contains an energy term λ , the so-called rearrangement or reorientation energy. This is the energy required to change the orientation of solvent dipoles surrounding, for instance, an Fe^{+2} molecules to their equilibrium positions around the oxidized molecules Fe^{+3} .

In equation (3.26), $E_2^\circ - E_1^\circ$ is the difference between the minimum potential energy of the whole system in its initial state (in which the electron is localized in the ions) and that of its final state (with the electron in the electrode), i.e.,

$$E_2^\circ - E_1^\circ = E - E_{redox}^\circ - kT \ln\left(\frac{C_{ox}}{C_{red}}\right) \quad (3.27)$$

E_{redox}° is the energy equivalent to the redox potential U_{redox}° i.e., $E_{redox}^\circ = eU_{redox}^\circ$, C_{ox} and C_{red} are the concentrations of the oxidized and reduced species, respectively; whereas E is the energy level in the electrode at the electron transfer occurs. To have the same reference point for energy level in the electrolyte and in the solid, E_{redox}° must be defined in the same energy scale as the Fermi level in the solid electrode (i.e., with a reference point of the vacuum level). Consequently,

$$E_{f,el} = E_{redox}^\circ + kT \ln\left(\frac{C_{ox}}{C_{red}}\right) \quad (3.28)$$

can be defined as the Fermi level of a redox system in solution, which differs from the usual redox potential only by an additive constant K :

$$E_{f,el} = eU_{redox}^\circ + K \quad (3.29)$$

Under equilibrium conditions the Fermi levels in the electrode and in the redox system must be equal, i.e.,

$$E_F = E_{f,el} \quad (3.30)$$

Inserting equations (3.27) and (3.28) into equation (3.26), one obtains for the activation energy

$$E^* = \frac{E - E_{f,el} - \lambda}{4\lambda} \quad (3.31)$$

As mentioned above E is the energy level in the electrode across which the charge transfer occurs. In the case of a semiconductor electrode such an energy level could be the conduction or the valence band, while for a metal it involves energy states around the Fermi level. Using equation (3.31), the

anodic current i^+ is then given by

$$i^+ = \frac{FZC}{(\pi kT\lambda)^{1/2}} \int_{-\infty}^{\infty} X(E) \rho(E) [1-f(E)] \left[\exp \frac{-(E-E_{F,eI}-\lambda)^2}{4kT\lambda} \right] dE \quad (3.32)$$

[see equation (3.25)]. the factor $(\pi kT\lambda)^{1/2}$ was introduced to normalize the integral to unity with respect to the activation term. A similar equation can also be derived for a cathodic current i^- , which is given by

$$i^- = \frac{FZC}{(\pi kT\lambda)^{1/2}} \int_{-\infty}^{\infty} X(E) \rho(E) f(E) \left[\exp \frac{-(E-E_{F,eI}+\lambda)^2}{4kT\lambda} \right] dE \quad (3.33)$$

these rather general formulas may be applied for metal electrodes as well as for semiconductor electrodes.

3.4.2 Energy Levels in Solution Redox Systems :

In a weak interaction between electrode and reactant is assumed, the quantum states on both sides of the interface must remain unchanged during the charge transfer, i.e., the charge transfer can only occur via states of equal energy. Moreover, it is required that on one side of the interface occupied energy states exist, whereas on the other side unoccupied states of equal energy are available. Taking, for instance, an electron transfer from a redox system to an electrode, unoccupied states, given by $\rho(E)[1-f(E)]$ in equation (3.32), must be present in the solid. By analogy the exponential term in the same equation can be considered as the distribution function D_{red} of the occupied electron states in the redox system, i.e.,

$$D_{red} = \exp \left\{ \frac{-(E-E_{F,eI}-\lambda)^2}{4kT\lambda} \right\} \quad (3.34)$$

In a similar way, the distribution function of unoccupied states in the redox system can be defined as

$$D_{ox} = \exp\left[\frac{-(E-E_{F,el}+\lambda)^2}{4kT\lambda}\right] \quad (3.35)$$

In a redox system such as Fe^{+2}/Fe^{+3} the occupied states correspond to the solvated Fe^{+2} ions and the unoccupied states to the solvated Fe^{+3} ions. Using these definitions the charge transfer equations (3.32) and (3.33) can be written as⁷¹

$$i^+ = \frac{FZC}{(\pi kT\lambda)^{1/2}} \int_{-e}^{+e} x(E) \rho(E) [1-f(E)] D_{red}(E) dE \quad (3.36)$$

$$i^- = \frac{FZC}{(\pi kT\lambda)^{1/2}} \int_{-e}^{+e} x(E) \rho(E) f(E) D_{ox}(E) dE \quad (3.37)$$

These equations derived from Marcus' theory are identical to the results obtained by Gerischer⁷², who started from a somewhat different point of view. Sometimes the theories by Marcus and Gerischer have been considered to be very different. As concerns semiconductor electrode it is only of importance that they lead quantitatively to the same results.

3.4.3 Current - Potential Curves :

When applying Marcus' theory to semiconductor electrodes, the partial currents via the conduction and the valence band must be formulated separately. According to equation (3.32), the anodic currents are then given by

$$i_c^+ = \frac{FZC}{(\pi kT\lambda)^{1/2}} \int_{E_c}^{+e} x(E) N_c \exp\left[\frac{-(E-E_{F,el}-\lambda)^2}{4kT\lambda}\right] dE \quad (3.38)$$

for the conduction-band mechanism ($E > E_c$); and by

$$i_v^+ = \frac{FZC}{(\pi kT\lambda)^{1/2}} \int_{-e}^{E_v} x(E) P_v \exp\left[\frac{-(E-E_{F,el}-\lambda)^2}{4kT\lambda}\right] dE \quad (3.39)$$

for the valence - band mechanism ($E \leq E_v$).

In equation (3.34) the number of unoccupied states in the conduction band, $\rho(E)[1-f(E)]$, is replaced by the density states N_c at the lower edge of the conduction band because most of these states are unoccupied even in n-type material i.e., $f(E) \approx 0$. In the case of a large transfer via the valence band the unoccupied states are identical with the number of holes P_s at the surface.

The integral can only be analytically solved using certain approximations as follows. Since the distribution functions vary exponentially with E^2 [equation (3.34)] and since in most cases the overlapping between states is limited to a rather small energy range, the charge transfer will occur mainly within kT at the edge of the conduction or valence band. Therefore, it is reasonable approximation to replace the integrals by inserting $\Delta E = kT$ and $E=E_c$ (conduction-band mechanism) or $E=E_v$ (Valence-band mechanism). then from equation (3.38) and (3.39), anodic current is given by

$$i_c^+ = FZC \left(\frac{kT}{\pi\lambda} \right)^{1/2} \alpha(C) N_c \exp \left[-\frac{(E_c - E_{F,el} - \lambda)^2}{4kT\lambda} \right] \quad (3.40)$$

for the conduction-band mechanism ($E=E_c$); and by

$$i_v^- = FZC \left(\frac{kT}{\pi\lambda} \right)^{1/2} \alpha(E_v) P_s \exp \left[-\frac{(E_v - E_{F,el} - \lambda)^2}{4kT\lambda} \right] \quad (3.41)$$

for the Valence-band mechanism ($E=E_v$).

In a similar procedure, the cathodic current is given by

$$i_c^- = FZC \left(\frac{kT}{\pi\lambda} \right)^{1/2} \alpha(E_c) n_s \exp \left[\frac{-(E_c - E_{F,el} + \lambda)^2}{4kT\lambda} \right] \quad (3.42)$$

for the conduction-band mechanism ($E=E_c$); and by

$$i_v^- = FZC \left(\frac{kT}{\pi\lambda} \right)^{1/2} \alpha(E_v) N_v \exp \left[\frac{-(E_v - E_{F,el} + \lambda)^2}{4kT\lambda} \right] \quad (3.43)$$

for the Valence band mechanism ($E=E_v$).

In the first case [equation (3.42)] the number of occupied states is given by the free electrons in the conduction band, N_s ,

and in the second case by the density of states, N_v , at the upper edge of the Valence band.

By way of comparison with semiconductors the current at metal electrodes should also be mentioned. In this case the charge transfer occurs across energy levels close to the Fermi level in the metal i.e., at $E=E_F$. Using the same approximations, one obtains for the anodic current (metals)

$$i_{\text{met}}^+ = FZc\rho(E) \chi(E) \left(\frac{kT}{\lambda\pi}\right)^{1/2} \exp\left[\frac{-(E_F - E_{F,el} - \lambda)^2}{4kT\lambda}\right] \quad (3.44)$$

and for the cathodic current (metals)

$$i_{\text{met}}^- = FZc\rho(E) \chi(E) \left(\frac{kT}{\pi\lambda}\right)^{1/2} \exp\left[\frac{-(E_F - E_{F,el} + \lambda)^2}{4kT\lambda}\right] \quad (3.45)$$

From equation (3.40) to (3.44) the potential dependence of the partial currents can be obtained immediately. Applying an external potential η across interface, then, the Fermi level on each side of the interface is relatively shifted according to

$$E_F = E_{F,el} - e\eta \quad (3.46)$$

This leads to different consequences with respect to the conduction- or valence-band processes. In the case of an anodic current, for instance, the current i_c^- across the conduction band is independent of the potential [equation (3.40)]. This is caused by the fact that any externally applied potential only leads to a potential change across the space charge layer in the semiconductor. Consequently, the relative position of the energy bands at the semiconductor surface and of the energy levels in the redox system remains unchanged. This situation is schematically shown in Fig. 3.8a. In order to illustrate this effect more clearly, the energy bands of the semiconductor are plotted in this figure as a function of distance from the surface. Moreover the density of energy states in the redox system is shown in a logarithmic scale. Comparing the two cases (under polarization and at equilibrium), in Fig. 3.8b it is quite obvious that the relative position of energy level at the interface remains unchanged i.e.,

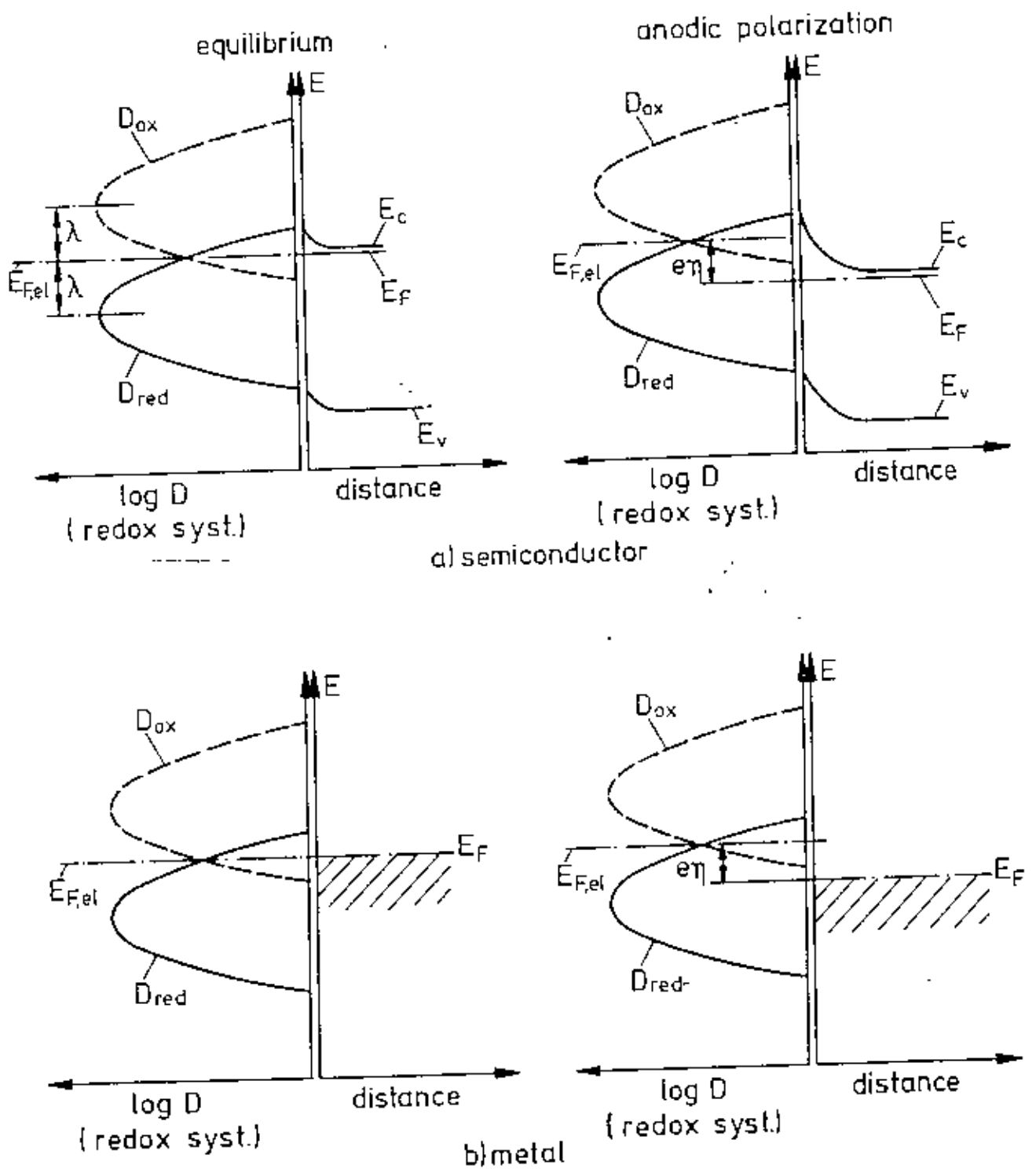


Fig. 3.8 Energy states in the redox system and (a) in the semiconductor, (b) in the metal. Left side, at equilibrium; right side, at anodic polarization.

$E_c - E_{F,el}$ also remain constant. Since an anodic current based on a charge transfer via the conduction band is independent of the potential, it is also identical with the exchange current i_c^0 at equilibrium. The potential dependence of this current is schematically shown ($i_c^+ = i_c^0$) in fig. 3.9. The absolute value of the current depends on the preexponential factor in equation (3.40) and on the reorientation energy λ , which determines the width of the distribution function and its distance from the Fermi level $E_{F,el}$.

Basically the same arguments are used for deriving the potential dependence of a valence-band process, i.e., an electron transfer from the occupied state in the redox system into the valence band. Such a process depends on the hole concentration P_s at the surface, which in turn depends on the relative position of Fermi level and Valence band at the surface. This distance is changed by applying an external potential via a variation of the band bending leading also to a change of the surface hole concentration. Denoting P_{s0} as the hole concentration at surface under equilibrium conditions, the surface hole concentration is given by

$$P_s = P_{s0} \exp\left[\frac{e\Delta U_{sc}}{kT}\right] = P_{s0} \exp\left[\frac{e\eta}{kT}\right] \quad (3.47)$$

Accordingly, an anodic current i_a^+ across the valence band increases exponentially with the electrode potential, as also shown in Fig. 3.9.

The same procedure can be applied for cathodic currents. However in this case it is the partial current i_c^- (via the valence band) which is independent of the potential, whereas the current i_c^- (via the conduction band) increases with negative η -values caused by the potential dependence of the electron concentration n_s at the surface as given by (Fig. 3.8).

$$n_s = n_{s0} \exp\left[\frac{-e\Delta U_{sc}}{kT}\right] = n_{s0} \exp\left[\frac{-e\eta}{kT}\right] \quad (3.48)$$

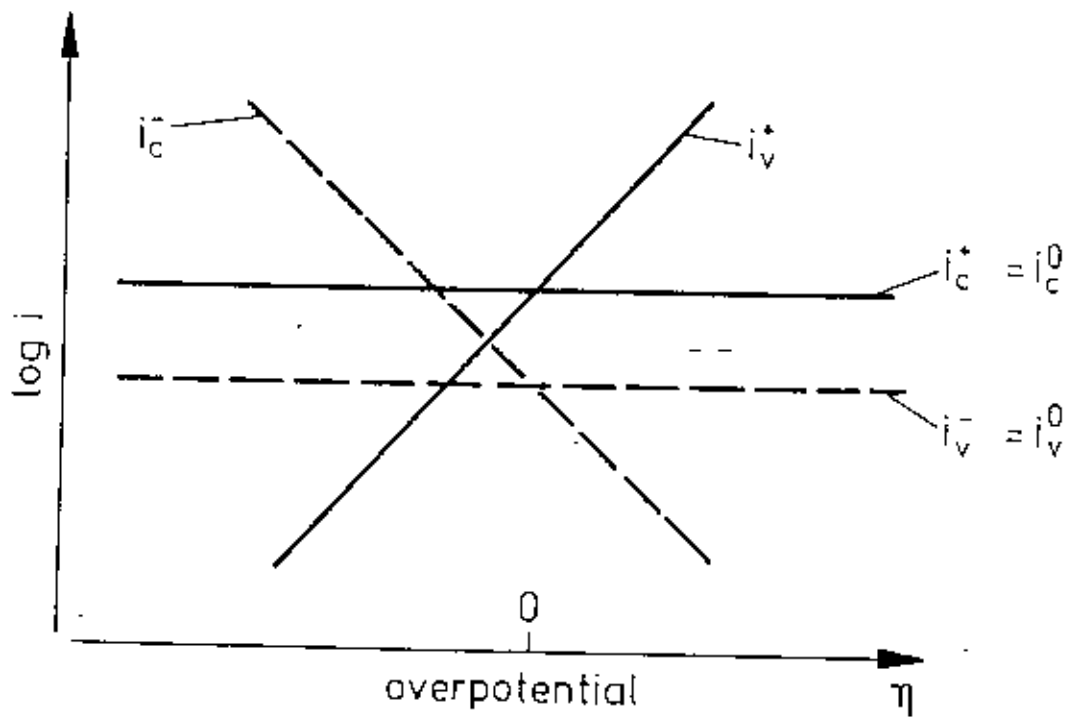


Fig. 3.9 Potential dependence of anodic and cathodic partial currents.

At equilibrium the anodic and cathodic current across each energy band must be equal i.e.,

$$i_c^+ = i_c^- = i_c^0 \text{ and } i_v^+ = i_v^- = i_v^0 \quad (3.49)$$

in which i_c^0 and i_v^0 are the corresponding exchange currents. The two partial currents which become potential dependent due to a variation of the carrier density at the surface, can now be expressed by inserting equation (3.47) into (3.41) and equation (3.48) into (3.42) :

$$i_c^+ = i_c^0 \quad i_v^+ = i_v^0 \exp\left[\frac{e\eta}{kT}\right]$$

$$i_v^- = i_v^0 \quad i_c^- = i_c^0 \exp\left[-\frac{e\eta}{kT}\right] \quad (3.50)$$

in which the exchange currents i_c^0 and i_v^0 are given by

$$i_c^0 = FZC \bar{X}(E) \left(\frac{kT}{\pi\lambda}\right)^{1/2} N_c \exp\left[-\frac{(E_c - E_{F,s1} + \lambda)^2}{4kT\lambda}\right]$$

$$i_v^0 = FZC \bar{X}(E) \left(\frac{kT}{\pi\lambda}\right)^{1/2} N_v \exp\left[-\frac{(E_v - E_{F,s1} - \lambda)^2}{4kT\lambda}\right] \quad (3.51)$$

Metal electrodes differ from semiconductors in that no space charge exists inside the metal and the external applied potential occurs only across the Helmholtz layer. This leads to a change of the relative position of energy levels [Fig. 3.8b]⁷². The exchange current i_{met}^0 ($E_v = E_{F,s1}$) is given, according to equation (3.44), by

$$i_{\text{met}}^0 = FZC \rho(E_F) X(E) \left(\frac{kT}{\pi\lambda}\right)^{1/2} \exp\left[-\frac{\lambda}{4kT}\right] \quad (3.52)$$

3.4.4 Charge Transfer Processes Via Surface States :

The question arises whether all charge transfer process occur only via one of the energy bands or whether surface states within the energy gap could also be involved. Especially in the case of semiconductor electrodes with large band gaps, the exchange currents are sometimes very small because of the poor overlapping

between energy levels of a redox system with the energy bands as discussed above. One might expect that the overlap with surface states is much better-which could also lead to a charge transfer even if the density of surface states is rather low.

Corresponding redox processes in which surface states are involved were actually observed with p-type GaP electrodes⁷³. When such an electrode was polarized cathodically in an electrolyte containing no redox system, only small current was detected, which could be enhanced by optical excitation of an electron from the valence into the conduction band.

Surface states have also been identified in other electrochemical reactions, e.g. in the reduction of germanium surfaces^{74,75}.

3.5 Quantum Mechanical Aspects of Charge Transfer :

The solution of Schrodinger equation for a particle passing through a rectangular potential barrier, when the kinetic energy of the particle is less than the potential energy it has within the barrier, can be represented as

$$P_T = \frac{16E}{U_0} \left(1 - \frac{E}{U_0}\right) \exp(-2k_2a) \quad (3.53)$$

This equation provide proof of the remarkable fact that a material particle of mass m and total energy E , which is incident on a potential barrier having a height U_0 and finite thickness a , actually does have a certain probability P_T of penetrating through the barrier and appearing on the other side. This phenomenon is called barrier penetration or "tunneling" through the barrier.

If the potential energy barrier does not have a simple form (e.g. constant with respect to distance) the solution of the Schodinger equation even in one dimension is quite complicated. The WKB method⁷⁶, named after its originators Wentzel, Kramer and

Brillouin, is a treatment for obtaining an approximate solution of the Schrodinger equation when the potential varies only fairly slowly with distance x .

The expression for the probability of tunneling using WKB method is given by

$$P_T = \exp(-2 \int_a^b \frac{8\pi^2 m}{h^2} [U(x) - E]^{1/2} dx) \quad (3.54)$$

where h is the Plank's constant.

Another tunneling probability expression for the particle incident on a general potential given by Eckart that is neither constant nor slowly varying with position.

Eckart²⁷ considered a particle of mass m moving in the potential that he constructed empirically with an eye to the need to present barriers of different shapes. The expression for the potential he chose is

$$U(x) = \frac{Ae^{2\pi x/d}}{1+e^{2\pi x/d}} + \frac{Be^{2\pi x/d}}{(1+e^{2\pi x/d})^2} \quad (3.55)$$

Where $2d$ is the barrier width, A is the difference between U at $-a$ and U at $+a$, and B is a constant that gives the measure of the barrier height. This potential is illustrated in Fig. 3.10. which shows that the Eckart potential encompasses a variety of forms of potential depending on the ratio of B/A .

An advantage of the Eckart potential and its solution is that the corresponding potential function on which it is based has two variable parameters A and B , respectively. Adjusting their values, one may get a realistic shape for a potential barrier (Fig. 3.10) and not only for the symmetrical shape to which the WKB methods have been applied. The barrier shapes in Fig. 3.10 are those seen in chemical and electrochemical kinetics. Such barriers can be used for the treatment of proton and electron tunneling situation in calculating the rate of charge transfer of electrochemical

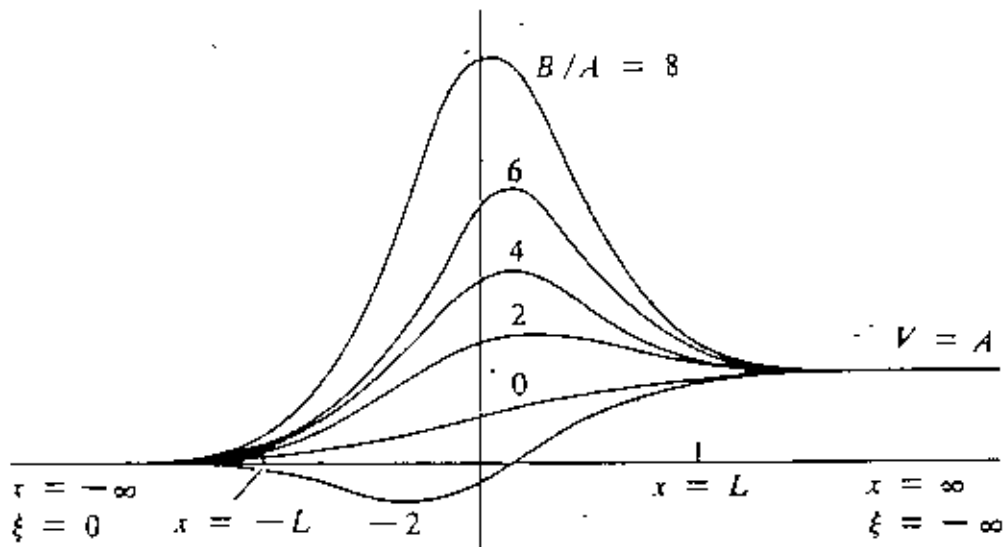


Fig.3.10 The Eckart potential. $V(x) = -A\xi(1-\xi)^{-1} - B\xi(1-\xi)^{-2}$, where $\xi = e^{2x/L}$ for various values of the ratio B/A . If $A=0$, the potential is symmetrical about $x=0$. The Eckart potential varies smoothly from a plateau of $V=0$ at $x = -\infty$ to a plateau of $V = A$ at $x = +\infty$.

reactions. Gurney's tunneling theory of electron transfer at interface : The situation of neutralization of a gaseous^{78,79} by electron tunneling is illustrated in fig. 3.11. in which the potential energy of an electron along a line perpendicular to the surface of the metal is sketched. The work function of the metal is denoted by ϕ and the ionization potential of the ion by I .

Gurney's radiationless tunneling condition for the neutralization of a hydrogen ion in vacuum by an electrode at an electrode is

$$\phi \leq I \quad (3.56)$$

This condition means that the magnitude of electron energy in the metal electrode (with respect to vacuum) must be less than or equal to the magnitude of the electron energy (with respect to vacuum) in the a hydrogen atom in the gas medium. The Fermi level of the electron in a metal electrode and a single electron level in a hydrogen atom in the gas medium are shown in fig.3.11.

When the ion is no longer in the gas phase, but in solution, the situation is more complicated. Consider a hydrogen atom in solution. The work done to ionize it is $+ I$, but now the hydrogen ion is being created in solution and one must immediately add to the energy of the atom the energy of the hydrogen ion in solution, so that the changed energy is $I+L$, where L is the solvation energy. Gurney's radiationless condition is therefore

$$-\phi > -(I+L) \text{ or } \phi \leq (I+L) \quad (3.57)$$

This is illustrated in fig. 3.12.

Effect of electrode potential : If we flow in electrons or extract electrons from the electrode by an outside source of potential, the energy of the outgoing surface electrons changes by e_0V and the work function becomes $\phi + e_0V$.

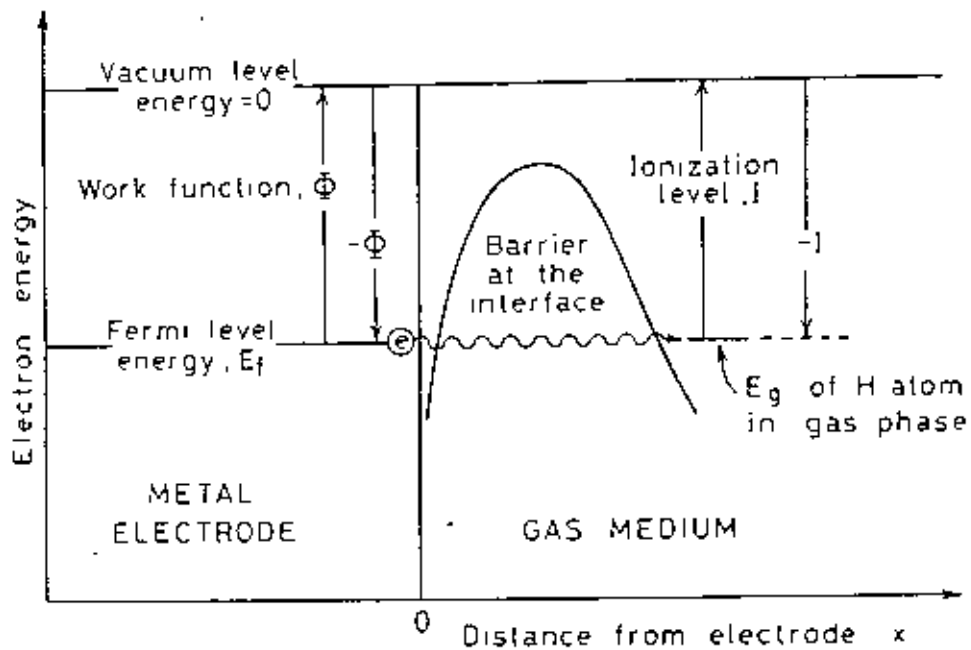


Fig. 3.11 The schematic diagram of the potential energy barrier at the interface of a metal electrode and a gas medium of H^+ ions. The diagram shows also the ground-state hydrogen atom levels, E_g , in the gas phase.

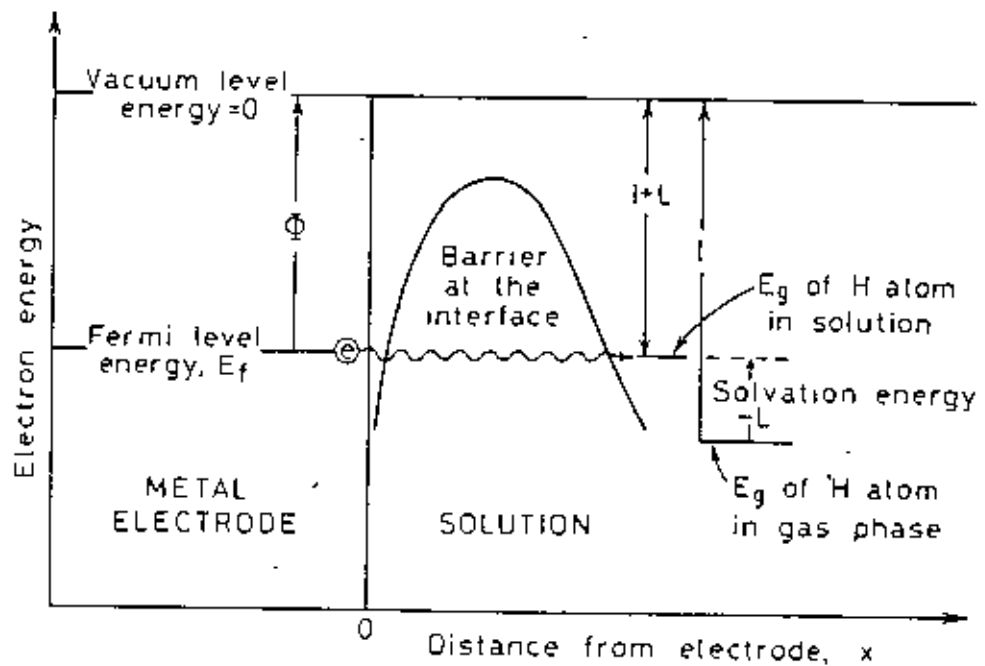


Fig. 3.12 The schematic diagram of the potential energy barrier at the interface of a metal electrode and solution of H^+ . The diagram shows also the effect of solvation energy, L , on the ground-state energy level, E_g , of hydrogen atoms in solution.

Thus, reformulating the Gurney's condition for radiationless transfer with electrode potential V , we have

$$-(\phi + e_0 V) > -(I+L) \text{ or } (\phi + e_0 V) \leq (I+L) \quad (3.58)$$

Where e_0 is the electronic charge and the sign of the potential V should be taken into account.

Effect of the hydrogen atom-water interaction: Gurney was working with the model that the potential energy of interaction of the ion and the adjacent water molecules is equal to $-L$ before neutralization and zero after neutralization. But according to the Franck-Condon principle, the potential energy between hydrogen and water just after neutralization of the $H^+ - H_2O$ ion will have repulsive interaction of some value R . Inclusion of the term R into the energy of the electron in the hydrogen atom means that the electron tunneling condition becomes

$$\phi + e_0 V \leq I + L - R \quad (3.59)$$

R is a repulsive energy and its numerical value is positive.

Effect of metal-Atom interaction : Bulter²⁰ reexamined the theory of Gurney and besides the repulsion between hydrogen and water, he considered attraction energy A between the hydrogen atom and the metal surface, which Gurney had neglected. Inclusion of this metal-atom interaction energy A . Change the workdone in bringing an electron from vacuum to a hydrogen in solution (Fig. 3.13). Hence, the electron tunneling condition becomes

$$\phi + e_0 V \leq I + L - R + A \quad (3.60)$$

Results of making the energy in the hydrogen atom more negative by considering Metal-Hydrogen interaction: It is easy to realize the effect of this process on the likelihood than an electron will transfer from the metal to a proton in solution. In Fig. 3.13 there are shown two cases, one in which the hydrogen atom is supposed to have the zero interaction with the metal, and one in which the interaction energy A is supposed to be high; i.e., a

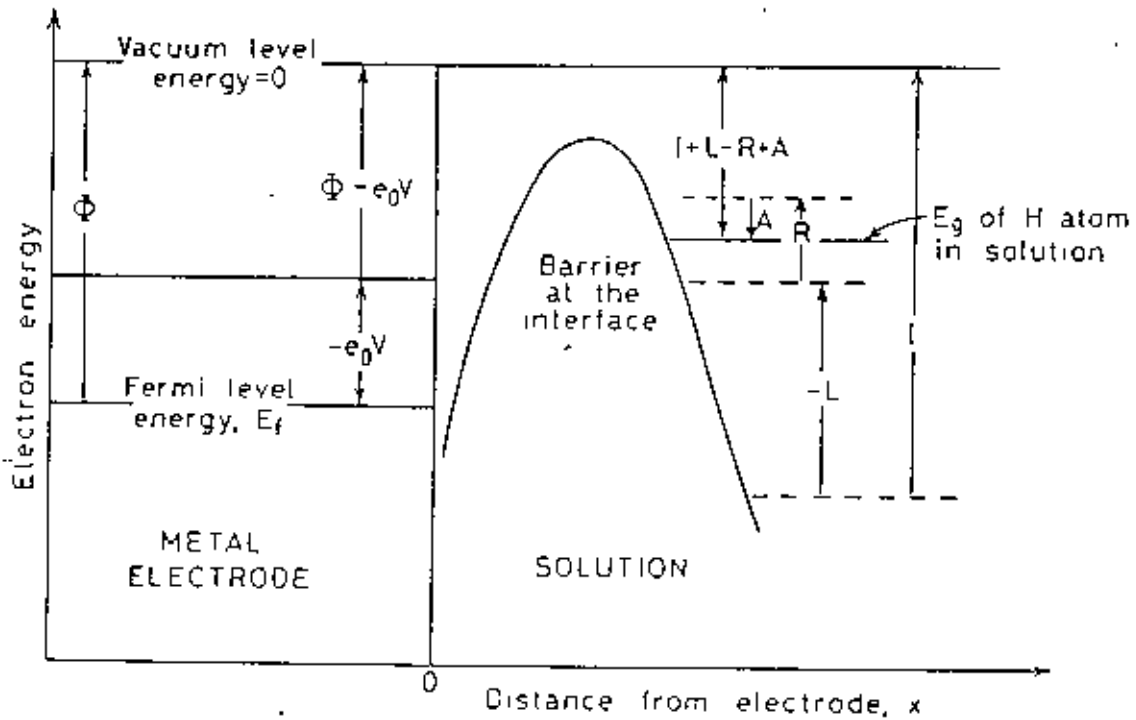


Fig.3.13 The schematic diagram of the potential energy barrier at the interface of a metal electrode and solution of H^+ . The diagram shows the effect of the cathodic potential on the work function and also the effect of solvation energy L , repulsion energy R , and the attraction energy A on the ground-state energy level E_g of hydrogen atom in solution.

large negative heat of adsorption is introduced. It will be seen that the effective level of the ground state of the electron in hydrogen atom is made lower on the curve for the energy scale in Fig. 3.13, and this has the effect of bringing levels in the proton close to the levels that are occupied by conduction electrons in the metal (i.e. it brings available levels in H_3O^+ closer to the Fermi level in the metal) and thus there is a greater overlap of conduction-electron levels near the Fermi level in the metal and the available distributed electron energy levels of $H^+ - H_2O$ of the H_3O^+ ion in solution (Fig. 3.13). It is therefore more likely that an electron will find a level equal to levels in the H_3O^+ in solution. Hence for a given electrode potential, when a large negative metal-hydrogen interaction is considered, the predicted current will be higher than if the metal-hydrogen interaction is neglected. Bulkr's addition of the chemical bonding term to Gurney's theory" made it not only the pioneering step toward the quantum mechanical treatment of charge transfer at the interface in solution but also a practical one.

CHAPTER 4

PRESENT WORK ON THE FACTORS AFFECTING ELECTROCATALYSIS

4.1 General :

The term "electrocatalysis" implies the influence of electrode material on the rate of the electrode reaction i.e. the kinetic and mechanistic effects of the bonds formed by reactants, products and/or intermediates with the electrode surface. Practically speaking if a material shows a lower overpotential because it is mainly a better conductor, this is as a whole regarded as a better electrocatalyst.

The main requisites needed for an electrode material to be useful as electrocatalysts are (i) high surface area (ii) high electrical conduction (iii) good electrocatalytic properties (iv) long-term mechanical and chemical stability at the support/active layer and at the active layer/solution interface (v) minimized gas bubble problems for gaseous fuels (vi) enhanced selectivity (vii) availability and low cost (viii) health safety.

It is inconceivable that all the requisites listed above can be optimized in a single electrocatalyst. More usually the choice is based on compromise between several factors depending on the type of application.

In this chapter we are going to discuss the progress that have been made so far for the development of new categories of electrodes and the studies made on these electrodes to draw conclusion about the success of various types of electrodes.

4.2 Recent Studies on Electrocatalysis on Various types of Electrode :

Electrocatalysis is greatly influenced by the nature of the electrode materials. Various types of electrode materials have been catagorised and their performance as electrocatalyst are discussed in the following sections.

4.2.1 Noble Metal Electrode :

The noble metals have long been found as the best electrocatalysts. Because of their good conductivity and incorrodability in oxidative conditions, these metals have been used as electrodes in the oxygen evolution reaction (the cathodic reaction in many fuel cells) as well as the anodic reactions (the organic fuel oxidations). However due to the high cost and limited availability in nature, extensive research is going on to find suitable substitutes for the noble metals.

The present state of achievements with the noble metals as electrocatalysts for various fuel cell reactions are shortly given.

The electrocatalytic hydrogen-evolution reaction on noble metal electrods has received most attention²². The exchange current densities for the hydrogen evolution reaction on a number of metals in acid solution²¹ are shown in Table 4.1. It may be seen that for this reaction the electrocatalytic activity of the metals varies by a factor of 10^9 from Hg to Pt. The noble metals have the highest catalytic activity for this reaction. The other transition metals have an intermediate catalytic power. The exchange current densities for the oxygen-dissolution reaction on some metals²³ are shown in Table 4.2. In this case, the catalytic activity varies by some 10^7 times from Ru to Au.

A knowledge of electrocatalysis is particularly important in the case of electroorganic oxidation. For example, the electrochemical reactivity of ethylene in its oxidation to CO_2 is low²³ (Table 4.3) compared with that of hydrogen evolution. Hence, the rate at which it can be converted to CO_2 with high efficiency, and the corresponding power, is relatively small. The products of the overall reaction here depend on the type of catalyst²⁴ : complete oxidation to CO_2 occurs on Pt, Rh and Ir, whereas partial oxidation to aldehydes occurs on Pd and Au.

TABLE 4.1 Exchange Current Densities for the Hydrogen-electrode Reaction on Some Metals in H_2SO_4 at 25°C

<i>Metal</i>	<i>Normality of H_2SO_4 electrolyte</i>	<i>i_0 amp cm^{-2}</i>
Pt	0.5	1×10^{-3}
Rh	0.5	6×10^{-4}
Ir	1.0	2×10^{-4}
Pd	1.0	1×10^{-3}
Au	2.0	4×10^{-6}
Ni	0.5	6×10^{-6}
Nb	1.0	4×10^{-7}
W	0.5	3×10^{-7}
Cd	0.5	2×10^{-11}
Mn	0.1	1×10^{-11}
Pb	0.5	5×10^{-12}
Hg	0.25	8×10^{-13}
Ti	2.0	6×10^{-9}

TABLE 4.2 Exchange Current Densities for the Oxygen-electrode Reaction on Some Metals at 25°C

<i>Metal</i>	<i>i_0 in 0.1 N $HClO_4$ (pH ~ 1), amp cm^{-2}</i>	<i>i_0 in 0.1 N NaOH (pH ~ 12), amp cm^{-2}</i>
Pt	1×10^{-10}	1×10^{-10}
Pd	4×10^{-11}	1×10^{-11}
Rh	2×10^{-12}	3×10^{-13}
Ir	4×10^{-13}	3×10^{-14}
Au	2×10^{-12}	4×10^{-15}
Ag		4×10^{-10}
Ru		1×10^{-8}
Ni		5×10^{-10}
Fe		6×10^{-11}
Cu		1×10^{-8}
Re		4×10^{-10}

TABLE 4.3 Exchange Current Densities for the Oxidation of Ethylene on Some Metals in 1N H_2SO_4 at 80°C

<i>Metal</i>	<i>i_0, amp cm^{-2}</i>
Pt	10^{-10}
Pd	10^{-10}
Rh	5×10^{-11}
Ir	8×10^{-11}
Au	2×10^{-10}
Ru	5×10^{-11}

In some cases, the electrocatalyst may also function as a chemical catalyst and may interfere with or aid the following electrocatalysis. An example is the electrooxidation of propane to CO_2 using platinum as a catalyst²³. The metal also catalyzes the chemical cracking of propane to inert products, mainly methane at open circuit and low overpotentials. The efficiency of the electrochemical energy conversion is thereby reduced at low current densities.

The oxidation of butanol in alkaline medium on different noble metal electrodes e.g. Pt, Rh, Pd and Au was investigated²³. The highest catalytic activity was reached with gold. The electronic structure of electrode was found to influence its catalytic activity. Oxidation of formic acid on three low index planes Pt (100), Pt (110) and Pt(111) was reported to show quite different voltammograms on different crystal planes.

Electrocatalytic oxidation of the four butanol isomers on different noble metal electrodes (Pt, Au, Pd, Rh) both in acid and in alkaline aqueous solutions were investigated²⁴. The electrochemical reactivity of the different isomers was expressed as the maximum current density determined from cyclic voltammograms. In acid medium the relative electrocatalytic activity of the metal electrodes were found as follows :



The electrochemical reactivity of the four isomers on a Pt electrode decreases according to the series:



In alkaline medium the electrocatalytic activity of platinum was comparable to that in acid medium, with the same sequence for the reactivity of the butanols. However Rh, Pd and above all Au electrodes were found much more active in alkaline than in acid

medium. Au electrodes was found to give highest current densities with s-BuOH.

Combined capacity and electroreflectance measurements have been employed to investigate the adsorption of aniline on a polycrystalline gold electrode in neutral aqueous solution⁶⁵. Thermodynamic analysis of capacity potential curves allowed the calculation of different adsorption parameters. The Frumkin isotherm was obeyed, indicating repulsive interaction in the adsorbed layer. The standard Gibbs energy of adsorption was found to be fairly large (-47 KJ mol^{-1}) showing the presence of chemical interaction between the adsorbate and the electrode. This was confirmed by electroreflectance spectra, where line shape was electric field-dependent and drastically perturbed when the applied potential was close to that of oxidation and polymerization of aniline. At this latter potential, the surface concentration of adsorbed species was about $2.6 \times 10^{-10} \text{ mol cm}^{-2}$; this value is compatible with a monolayer of flat orientated molecules. In the negative region, the aniline lies flat on the electrode, but the interaction between π -electrons and the gold electrode is weaker than in the positive region.

The electroreduction and-oxidation of toluene adsorbed on porous Pt electrode was studied using differential electrochemical mass spectrometry (DEMS)⁶⁶. Part of the toluene starts being desorbed at potentials where hydrogen adsorption begins. At potentials below 0.1V, hydrogenation to methylcyclo-hexane occurs as well. The oxidation in the first positive sweep after the adsorption is not complete. Quantification of the evolved CO_2 and oxidation charge shows that adsorbed intermediates are formed, which are in a higher oxidation state than toluene and which can be oxidized in subsequent sweeps only.

The adsorption of pyridine at an Ag(110) single crystal electrode has been studied⁶⁷. In the range of potential explored, adsorption, maximum coverage of the surface and beginning of

desorption are observed. At potentials close to the potential of zero charge the pyridine molecules assumed a tilted orientation with the nitrogen atom facing the metal. The adsorption isotherms have been determined for the first time for a silver face.

Change in adsorption profiles of 1,4-naphthohydroquinone (NHQ) on smooth polycrystalline platinum electrodes in aqueous 1M HClO₄, brought about by varying levels of surface active organic impurities (typified by hydroquinone (HQ) and benzene) have been studied by thin-layer electrochemical techniques⁸⁸. 10^{-5} M HQ is sufficient to alter the adsorption profile of NHQ; above 10^{-4} M HQ, the packing density transitions prominent from pure NHQ solutions were completely suppressed. Similar results were obtained when benzene was used as the contaminant. Packing density measurements indicated that the subject surface-active impurities inhibited formation of flat, but not edge, adsorbed NHQ; this is in agreement with data from a previous study⁸⁹ which showed that low levels of iodine, a surface active anion, enforced formation of edge-adsorbed NHQ even at (low) concentrations where flat-adsorbed species would have formed from pure NHQ solutions. The presence of surface active impurities may help account for the profound differences in adsorption measurements reported in the literature for various aromatic compounds.

4.2.2 Alloy Electrode :

Preparation and characterization of low overvoltage transition metal alloy electrocatalyst for hydrogen evolution in solution has been reported⁹⁰. The transition metal electrode prepared by thermal decomposition of solutions containing nickel or cobalt and molybdenum, tungsten or vanadium on a metallic substrate and curing the oxide coated substrate in an atmosphere of hydrogen at elevated temperature gave active hydrogen evolution electrocatalyst. Electrocatalyst of alloys based on nickel and molybdenum exhibit the highest activity for hydrogen evolution. The most stable electrode performance was obtained using a nickel to molybdenum

atomic ratio of 6:4 . The nickel-molybdenum alloy exhibits low overpotentials (under 100 mV) for both hydrogen evolution and oxidation at current densities of 200 mA cm⁻². X-ray diffraction and thermogravimetric measurement were employed to identify the active component of the nickel-molybdenum system responsible for its electrocatalytic activity. The result indicated that the major phase present in the electrocatalyst before and after hydrogen evolution was a face-centred cubic nickel-molybdenum alloy in which the molybdenum is randomly substituted on the nickel lattice.

The oxidation rate of ethylene-glycol was found to be increased (by a factor of eight) when alloying gold and platinum electrode than that for a pure gold and platinum electrode²³.

The formation of a bridge-type adsorbed CO species during the electro-oxidation of formaldehyde on Pd-Au alloy electrodes, but not on pure Au electrode in alkaline media was investigated by means of infrared reflectance spectroscopy²¹. The CO species is probably formed from HCHO which is predominant in the solution at lower pH, but not from HOCH₂O⁻. The species acts as a catalytic poison in formaldehyde electro-oxidation but the effect is weaker at higher pH where oxidation of HOCH₂O⁻ takes place more readily. The rate of CO formation is faster at lower pH and on electrodes of higher Pd content. No CO species was detected in the HCOO⁻ system. In mixed solutions of HCOO⁻ and HCHO, the oxidation of formate on both Pd and Pd Au alloy electrodes is suppressed greatly by the CO species originating from HCHO. The poisoning effect becomes less pronounced on the alloy electrode of higher Au content. The long term behaviour of mechanically treated mild steel and stainless steel cathodes under conditions of the chlorine-caustic production process by membrane cell was compared with other electrodes coated by different electrocatalysts in order to reduce hydrogen overvoltage²². At current densities of 3 kA m⁻² initially a reduction of the electrode potential by 200 to 300 mV were possible using electrocatalytically active coatings. The results of long term tests under technical conditions revealed the technically important

relations between the selection of the basis material (mild steel or stainless steel), the addition of precoating layers (e.g. galvanic nickel deposition) and selection of different electrocatalysts. It was possible to operate electrodes coated with raney nickel for longer than 1 year under a constant overvoltage which was about 200 mV lower compared to mild steel cathodes⁹².

The catalytic effect of foreign metal adatoms, obtained by the underpotential deposition of metals, on the oxidation and reduction of some organic molecules was investigated⁹³. Striking catalytic effects of lead, bismuth, thallium and tin adatoms were observed on the oxidation of formic acid, methanol, formaldehyde and carbon monoxide on platinum metal. This enhanced catalytic effects shown by the inclusion of these adatoms was attributed to decrease in the bond strength with the adsorbed organic molecules. The reduction of organic molecules on electrodes modified by adatoms has received much less attention than the oxidation. In this study the reductive hydrogenation of several molecules including ethylene, vinyl alcohols etc. were enhanced in the presence of some adatoms, while reduction of allyl alcohol, acrylic and maleinic acid was inhibited.

The electrocatalytic activity of a metal electrode was found to be greatly modified by under potential deposition of foreign metal adatoms. Oxidation of ethylene glycol on platinum was found to be modified by the under potential deposition of several metal adatoms like Bi, Cd, Cu, Pb, Re, Ru, and Tl. With Pb, Bi, Tl a pronounced enhancement on the rate of oxidation was reported⁹³.

Under potential deposition (UPD) of metals provides a relatively new and interesting method for modifying the electrocatalytic activity of metal electrode surfaces. Investigation of the electrocatalysis of oxygen and hydrogen peroxide reduction in acid solution on gold and silver single crystal surface of (111), (100) and (110) crystallographic orientation have been found to demonstrate negative and positive electrocatalytic effects caused by the UPD of Pb and Bi and their

dependence on the substrate and adsorbate structure⁹⁴. In absence of deposited metals oxygen reduction on the clean Ag and Au substrate was characterized by polarization curves. The complete 4 electron reduction of O_2 to H_2O for clean Ag electrode and the incomplete 2-electron reduction to H_2O_2 for Au electrode was found to take place. The polarization curves on silver were found to be nearly independent of the crystallographic orientation whereas a pronounced dependence was observed on the crystallographic orientation gold substrate. For the different gold single crystal surfaces, the half-wave potential were increased by the sequence (111), (110), (100) indicating increasing catalytic activity. The UPD of Pb on Ag surface results partial inhibition of oxygen reduction which was indicated by the gradual decrease of the cathodic current density. Positive catalytic effects were observed on Au (111) and Au (100) surfaces by UPD of Pb and Bi as well. The positive catalysis of oxygen reduction was indicated firstly by the shift of the polarization curves towards positive potentials and secondly by an increase of the limiting diffusion current density, due to further reduction of some of the H_2O_2 produced.

The electrocatalysis of the hydrogen peroxide reduction by UPD of Pb and Bi on gold and silver single crystal surfaces were also studied by using polarization curves, cyclic voltammograms and /or adsorption isotherms of UPD. It was reported that on silver, the hydrogen peroxide reduction was almost completely inhibited by the UPD of Pb, whereas positive catalysis was observed in the case of UPD of Pb and Bi on Au (100) and Au (111), respectively.

The effect of foreign metal adatoms on the O_2 reduction on the single crystal Au and Pt electrodes with the (100), (110) and (111) orientations were studied⁹⁵. A two electron reduction of O_2 and Au to HO_2^- in alkaline electrolytes, changes into four-electron reduction to OH^- on Au modified by foreign adatoms was found. The adsorbates of Pb and Tl was found to cause a doubling of diffusion-limited current density for all three planes of Au, as with polycrystalline electrodes. Small inhibition with Pb, but

considerable with Tl adsorbates was observed with the Au (100) surface in the potential region of a four-electron reduction of O_2 . The Tl adsorbates made all three surfaces investigated equally active.

The adsorption and electrocatalytic properties of the microdeposits of rhodium on gold, palladium on niobium, ruthenium and osmium on titanium, and palladium thin films on glassy carbon and nickel have been investigated⁹⁶. It was found that hydrogen adsorption on rhodium and ruthenium microdeposits was characterized by a high binding energy. The cathodic hydrogen evolution on ruthenium microdeposits and palladium films on glassy carbon and nickel is lower than that on the corresponding bulk metals. These results are consistent with the assumption of the predominant effect of the electronic interaction between microdeposits and thin films on the one hand and the support on the other, which affects the hydrogen adsorption parameters.

The effect of controlled amount of irreversibly absorbed bismuth on a Pt(111) oriented electrode surface on the electrocatalytic oxidation of formic acid has been studied in the whole range of coverage⁹⁷. The experimental method used in this work enables to maintain a constant surface coverage in heteroatoms while the electrode is cycled in the whole range of potential of oxidation of the organics. For a coverage range from 0 to up to 0.8, the electroactivity of the surface for the direct oxidation of formic acid is enhanced by a factor of 40, while in the whole range of coverage the accumulation of the blocking intermediate is lowered to an undetectable level.

4.2.3 Metal Oxides and Semi-conductor Electrodes :

By far the most studied alternate compounds are the oxides of transition metals with semi-conducting properties. These electrodes are not corroded in strong acidic or basic media and are stable at moderate temperatures ($\sim 100^\circ\text{C}$) and can operate at high anodic

potentials required for oxygen evolution reaction or oxidation of organic compounds in fuel cells. Only noble metals and their alloys have been found suitable at this working condition. Hence extensive research is going on to improve the stability and conductivity of these metal oxides.

The stability of anodically grown oxides has been found to be poorer⁹⁸ than that of the oxides prepared by the method of thermal decomposition. Investigation of the effect of the conditions of thermal preparation on the electrolytic properties of some of the most investigated oxides (RuO_2 , IrO_2 , Co_3O_4 , NiCo_2O_4) for Cl_2 and O_2 evolution shows that the activity of Co_3O_4 for Cl_2 evolution and activity of IrO_2 for O_2 evolution decreases steeply with the temperature of preparation⁹⁹. The surface area of Co_3O_4 was found to decrease with the temperature of preparation. It was reported that all of the activity variations is due not only to surface effects alone but other parameters such as non-stoichiometry co-vary with temperature¹⁰⁰.

The spinel and perovskite type electrodes are used for anodic oxygen evolution, catalytic activity of Ni, Co and Fe containing spinel and perovskite type oxide which were prepared with common ceramic technique was reported¹⁰¹. Some of these oxides found to show relatively high catalytic activity. The spinel type oxides prepared on the alloys by heating in air did not show high catalytic activity in comparison with the same alloy. The perovskite type electrode prepared by the plasma jet spraying method have been found to show a good even in 30% KOH at 75°C under a current density of 300 mA cm^2 .

The electrochemical oxidation of chloride ions on electrodes of various metal oxides, particularly RuO_2 and TiO_2 was investigated¹⁰². Three type of electrodes, viz the RuO_2 electrode consisting of pure RuO_2 , the RTO electrode consisting of RuO_2 , TiO_2 and eventually other metaloxides (with the RuO_2 content of the active mass of electrode higher than about 20%), and the MO

electrode consisting of one or more metaloxide doped with relatively small amount of RuO_2 were studied. The experimental results have been found to show a great variation in anodic Tafel slope, exchange current density and reaction order. For RTO electrodes the Tafel slope depends on various electrolytic conditions as potential range, temperature, chloride concentration, Chlorine concentration and p^{H} . Significantly higher slopes were found for MO electrodes and for RTO electrodes. An RuO_2 electrode found to behave similarly like on RTO electrode with a low minimum Tafel slope. The exchange current density or the current density at a fixed potential were used to indicate the catalytic activity of electrodes.

Mixed oxides of ruthenium and iridium ($\text{RuO}_2/\text{IrO}_2$) have been found to be the most promising anode materials¹⁰³. While the overvoltage of RuO_2 is about 50 mV lower than that of IrO_2 , the stability of RuO_2 is worse than that of IrO_2 , however, increases the cost of the catalyst. In order to optimize the anode catalyst with respect to performance and cost investigation of the factors influencing the corrosion of ruthenium and iridium compounds and the stabilization of ruthenium by iridium was performed¹⁰³. It has been reported that on ruthenium the stability of the hexavalent oxide appears to be most important for low corrosion rate. Corrosion occurs via RuO_4 . A thermal treatment of low temperature RuO_2 produced, by reactive sputtering, stabilizes the hexavalent state and thus increases the stability of RuO_2 during oxygen evolution. O_2 evolution and corrosion on iridium occurs on an oxide with Ir in the tetravalent state. Thermal treatment of IrO_2 have been found with no positive effect on corrosion rate.

Cobalt containing mixed oxides like the spinel Ni_2CoO_4 or the perovskite $\text{Sr}_{0.5}\text{CoO}_3$ are repeatedly reported to be efficient electrocatalysts for anodic oxygen-evolution¹⁰⁴. Long term performance-testing-especially of cobalt containing perovskite-revealed that most of these mixed oxides decomposed and where loosing the alkaline-earth component rapidly. However, the residual

oxide-cover always contained cobalt. Since the electrode kinetic characteristics (Tafel slope) of differently activated anodes become very similar to each other and to Co_3O_4 -activated anodes¹⁰⁴ reported that activated anodes very likely the Co_3O_4 content of coatings of aged electrodes to be responsible for the observed residual catalytic activity.

Engineering optimization of titanium anode electrocatalyst by interrelating composition, structure and surface properties in function of thermal processing (both temperature and time dependence) with steady state polarization characteristics (electrocatalytic activity), corrosion stability and the life time of the catalytic coating was studied¹⁰⁵. They worked with proper rutile structure of mixed oxide, viz $\text{RuO}_2/\text{TiO}_2$, at 40 mol% RuO_2 , with maximal diffraction peak of rutile phase, the total amount of the catalyst being between 5 and 10 g m^{-2} as accounted on both metals and the processing temperature about 500°C any further increase in precious metal was not found to bring any improvement neither in the electrode activity nor in its life time. It was also found that the corrosion resistivity decreases with further increase of ruthenium content in the coating. The author¹⁰⁵ reported another electrocatalyst (14% Ru, 17% Pd, 34% Sn and 35% Ti, all in atm.%) and optimized to provide a high catalytic activity, advanced corrosion stability and prolonged life time along with at the same time anodic selectivity and thereby the optimization of Faradaic yields for the chlorate cell process even at higher p^H values.

Metal anodes for electrolysis are generally covered with metal oxides, at least in aqueous electrolytes. These passive layers are able to undergo redox transitions¹⁰⁶. On anodic polarization the author reported higher oxidation states. In the presence of electrophores in the electrolyte, two different mechanisms are possible :

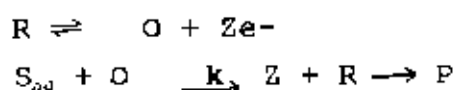
(A) direct electron exchange (B) redox catalysis.

The author reported various examples of anodic oxidation via mechanism (B). (i) Anodic oxidation of cyclohexanone oxime with PbO_2 ,

anode. aliphatic alcohols were oxidized directly. (ii) Anodic oxidation of isopropanol on Ti/CrO₂ electrodes. The oxidation potential was found about $U_a = 1.8V$. (iii) In the case of Ti/VO₂ electrodes, oxidation potential was much lower ($U_a = 1.0$), thus allowing only the conversion of easily oxidizable materials, e.g. hydroquinone.

Long term behaviour was found to govern by the ratio of anodic dissolution rate of oxide in the high valency state and the rate of chemical step.

If a layer, at least a monolayer, of a redox system modifies the electrode, the redox system can serve as an electron transfer mediator as well as a new surface for adsorptive interference with the reaction:



Obviously, the redox system itself exhibits typical catalyst behaviour. It plays only a temporary role. It is virtually not consumed in the overall process. The starting conditions are recovered again and again. This type of electrocatalysis is named redox catalysis.

Heterogeneous redox catalysis was investigated with Titanium/chromium (III) oxide + TiO₂ composite anodes¹⁰ fabricated by a ceramic method. Surface of α -Cr₂O₃ could be anodically stripped in 1M H₂SO₄ as H₂CrO₄ at $U_a = 1.8V$. Conversion of Cr₂O₃ decreased with increasing thickness of porous Cr₂O₃ layer. The electrodes were used for the anodic oxidation of aliphatic alcohol and ether in 1M H₂SO₄. Validity of model of heterogeneous redox catalysis was reported (i) by using current-voltage curve. A large amplification of anodic peak in the presence of oxidizable starting material (aliphatic alcohol, ether, and other organic substances etc.) showed that the peak current densities for various starting materials is of following order : Secondary alcohol < primary alcohol < ether (ii) coincidence of anodic current voltage curve with basic (stripping)

curve at low current densities. (iii) reaction limitation at high current densities. The author¹⁰⁷ also reported the life time of Ti/Cr₂O₃ electrode measured galvanostatically in 1M H₂SO₄/1M isopropanol for three current densities. Long term behaviour of Ti/Cr₂O₃ electrode was improved by either modifying an interlayer of TiO₂ eventually present or the chromic oxide layer itself.

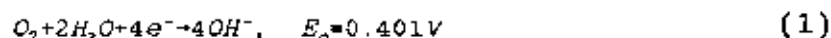
4.2.4 Non-metal electrodes :

In the investigation of O₂ reduction on various catalysts namely carbon, graphite, Pt, transition metal, macrocycles and heat treated macrocycles showed that the latter catalyst offer considerable promise as oxygen reduction catalysts combining high activity with good stability¹⁰⁸.

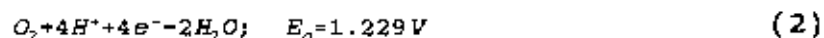
Oxygen reduction is considered to proceed by the following two overall pathways^{109,110}.

(i) Direct 4-electron Pathway

Alkaline solution :

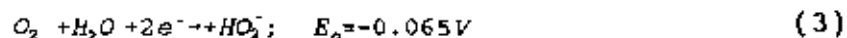


Acid solutions :

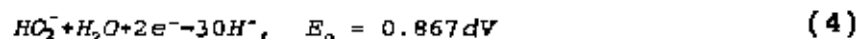


(ii) Peroxide Pathway

Alkaline solution :



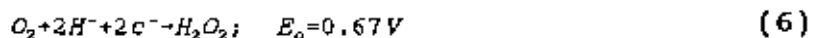
followed by either the further reduction reaction



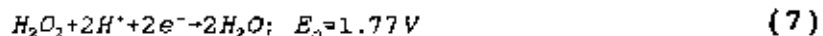
or the decomposition reaction



Acid solutions :



followed by either



The current densities for the reduction of O_2^- to O_2 and HO_2^- are far lower on the basal plane of graphite than the current densities found for O_2 reduction on ordinary pyrolytic graphite and glassy carbon in alkaline solutions. This implies that the O_2 reduction on carbon and graphite involves a strong interaction of O_2 with functional groups on the surface. It is reported that surface quinone groups are involved in the O_2 reduction to peroxi^{111,112}. Such evidence was further supported by other workers¹¹³.

The attachment of transition metal complexes to electrode surface play some catalytic role for O_2 reduction. Face-to-face porphyrins as O_2 electroreduction catalysts was involved by the workers^{114,115}. When the Co-Co distance is such ($\sim 4\text{\AA}$) as to permit formation of an -O-O- bridge between the Co-Co centres, the face-to-face porphyrin on a graphite catalyzes the 4-electron reduction in acid electrolytes while with the distance significantly less or greater, only the peroxide pathway catalyzed. It has been proposed that the formation of this bridge favours the rupture of O-O bond¹¹⁵. Recently it has been proposed that the 4-electron reduction is favoured by the cis-configuration rather than the trans-configuration since the catalytic activity for the staggered Co-Co-4 complex is much less for the 4-electron process¹¹⁶.

Planar bi-cobalt complexes have also been found to catalyze the 4-electron reduction of O_2 in alkaline solution when adsorptively attached to graphite¹¹⁷.

Some water soluble transition metal macrocycles such as the tetrasulfonated phthalocyanines (TsPc) are reported to form μ -O-bridged dimer complexes spontaneously in aqueous electrolytes^{118,119}. Fe-TsPc at p^H greater than 4 was found to catalyze the O_2 reduction via 4-electron pathway, on the otherhand Co-TsPc catalyzes the reduction of O_2 to the peroxide^{120,121}.

A number of the transition metal macrocycles on carbon, graphite or metal substrate have been found to catalyze the reduction of O_2 ^{120,122-125}. In most instances the peroxide pathway is involved with the macrocycle catalyzing reactions (3), (4) and or (5). While the results with transition metal complexes are exciting fundamental developments, it is difficult to translate the in to practical electrode, principally because of catalyst stability problem. Heat treatment of such macrocycles as cobalt tetramethoxyphenyl porphyrin (Co-TMPP) at temperatures of 450-900°C, results in high catalytic activity for O_2 reduction in alkaline solution with long term stability. The heat treated Fe-TMPP on a high area carbon support has been found also to have high catalytic activity for O_2 reduction in acid electrolytes although the long term stability has not yet been established.

In the electrochemical studies of thermally treated iron and cobalt porphyrins preadsorbed on high surface area carbon showed that μ -oxo and Co tetramethoxy phenyl porphyrin (TMPP) preadsorbed on a nominally metal free carbon substrate generate γ - Fe_2O_3 and a mixture of Co oxides respectively as the only metal containing species upon heat treatment of these specimen at 900°C in an inert gas flowing atmosphere¹²⁶. Oxygen reduction measurements of Mossbauer characterized samples conducted on gas fed Teflon bonded electrodes and thin film coatings in a rotating disc arrangement was found to exhibit noticeable improvement in the catalytic activity. Similar experiment was conducted on metal free tetramethoxy phenyl porphyrin which showed that the activity of pyrolyzed materials does not exceed that of carbon itself. The author concluded that the presence of MeN₄ centre is not essential

for the high activity of the materials studied and also that the metal centre is indeed necessary to achieve high catalytic activity.

Potential dependent adsorption of organic adsorbates was studied on flow through carbon fiber electrodes¹³⁷. Adsorbates included low molecular weight aromatic compounds, amino acids, a peptide and a protein. Factors which were found to influence electroadsorption included: pore distribution and surface functionalization of the adsorbent, as well as the solubility and ionization of the adsorbate. The impacts of electrochemical, thermal and chemical oxidative pretreatments on the adsorption tendencies of carbon fibers were determined. Separation of binary mixtures were demonstrated based on size exclusion phenomena and on differences in the potential dependence of adsorption of various adsorbates.

4.3 Phenomena of Oxidation of Organic Compounds used in Fuel Cells:

The oxidation of organic compounds on noble metal electrodes in aqueous solution is a very complex successive reaction due to the occurrence of one or several adsorbed intermediates and reaction products. Hence a complete analysis of the mechanistic and kinetic aspects of the complex multistep organic reaction has to be undertaken. This involves the elucidation of the mechanism of the complete reaction, identification of the rate determining step, catalytic role of the electrode material, role of the structure of the adsorbed species.

The study of the catalysis of electrochemical oxidation of organic compounds commenced with increasing interest in the potential application of relatively cheap organic compounds in electrochemical energy generators. A study of the electrochemical oxidation of ethylene on the platinum metals, gold and palladium shows that the noble metals were found to fall into one group and Au, Pd into another²⁴. There was complete oxidation to CO₂ in the case of former group but not so with the latter metals.

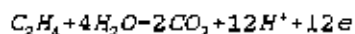
The practical usefulness of electrochemical generators (fuel cells) depends on energy conversion efficiency. The principle characteristic of electrocatalysis is the potential dependence of the rate of electrochemical reaction.

A knowledge of rate determining step and the reaction sequence allows one to choose appropriate electrode and organic fuels.

The mechanism of oxidation of several olefins (ethylene¹²⁸, propylene, allene, 1-butene, 2-butene¹²⁹) and of acetylene¹³⁰ has been studied on platinum at 90°C¹³¹.

Apart from small differences in i_0 and coulombic efficiency, the electrochemical behaviour and main reaction products were similar for all olefines studied (Table 4.3).

(i) The oxidation of ethylene (as representative of olefins) : the overall reaction yields CO_2 with 100 \pm 5% efficiency in alkaline solution. Thus branching reactions leading to products other than CO_2 and water (or proton) was neglected and half-cell reaction was presented as



The negative pressure effect of the hydrocarbons on current density, $di/dp < 0$ points to the facts that the rate determining step (r.d.s) involves a substance which will adsorb on the surface of the electrode if it is free of ethylene and its intermediate oxidized species.

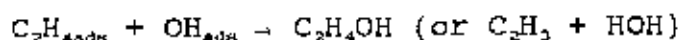
It can be concluded that the (r.d.s.) is one of the two following steps:

- a) $\text{H}_2\text{O} \rightarrow \text{OH} + \text{H}^+ + \text{e}$
- b) $\text{OH}^- \rightarrow \text{OH} + \text{e}$

The reaction sequence may be represented by



or r.d.s $OH^- \rightarrow OH_{ads} + e$



Which is consistent with the observed negative pressure effect.

The question of whether H_2O or OH^- takes part in the rate-determining charge transfer can be discussed in terms $\log i$ Vs p^H relationship. The value of $(d \log i / dp^H)_v$ is constant over the whole p^H range, suggesting that the same mechanism applies in both acidic and alkaline solutions. Hence it can be concluded that the discharge occurs from neutral water molecules.

Often with organic compound oxidation on metals, the working potential range is so positive that dissolution or passivation of the metal electrode occurs disrupting the normal electrochemical process. Hence, any advancement in producing electrode materials described in the previous section which are stable in anodic potential region can be considered as significant progress to study the mechanism of organic oxidation reaction in fuel cell phenomena.

Recent work in this area have been discussed in section 4.2 under the different category of electrodes. Oxidation of ethylene-glycol on smooth gold was investigated⁸³ by fast Fourier transform infra-red spectroscopy (FTIRS). The transmission spectra was found to show some characteristic bands which may be assigned to different compound e.g. glycolaldehyde, glycolate and formate. Adsorbed intermediate on platinum for the electrooxidation of methanol was detected by using electromodulated infra-red reflectance spectroscopy (EMIRS). The spectrum displayed two bands: a weaker band assigned to bridge-bonded CO and an intense band assigned to linearly bonded CO. Similar results were obtained with the adsorption of other organic fuel i.e. formic acid.

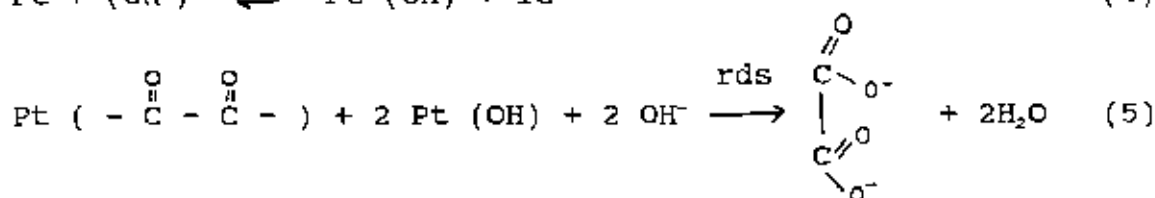
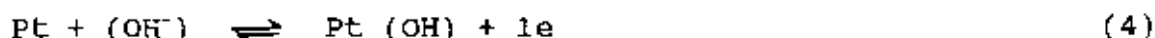
The same author²³ also reported the fact that the supporting electrolyte can modify the reaction rate or even the reaction path by specify adsorption of its constituting ions. Absolutely no oxidation of methanol on a palladium electrode in sulphuric acid medium was found. In perchloric acid a small oxidation current was observed on the cathodic sweep whereas in sodium hydroxide oxidation occurred at an higher rate both in anodic and cathodic sweeps.

Water molecules of the solvent are usually dissociated on noble metal surfaces into adsorbed hydrogen H_{ads} or adsorbed hydroxyl OH_{ads} , or even adsorbed oxygen depending on the solution p^H and the electrode potential²³. In the case of ethylene-glycol oxidation on a platinum electrode in acid medium, the effect of the lower potential limit, which controls the hydrogen adsorption as particularly drastic, leading to a decrease of the oxidation rate, when the lower limit was made more negative.

The electrocatalytic oxidation of ethylene glycol (EG) at polycrystalline platinum in 1M KOH was studied under potentiodynamic and potentiostatic conditions¹³². EG electroadsorption processes were clearly distinguished from the oxidation of EG electroadsorbed residues by using the flux technique after adsorption. The maximum adsorption potential was between 0.3 and 0.4 V in the H-adatoms potential region. An electroadsorbed residue which oxidizes at more positive potentials was formed. The average number of electrons per site released during the oxidation process $(\epsilon_{ps})_{ox}$ and the average number of electron per site released during the adsorption process $(\epsilon_{ps})_{ad}$ values were independently determined by the potentiostatic i/t transient at 0.35 V and the potentiodynamic oxidation profiles at low sweep rates respectively. The experimental values obtained allowed to postulate a plausible reaction pathway sequence.

A plausible reaction pathway for EG electroadsorption from alkaline solution which satisfied the experimental facts would be the electroadsorption through a single C and the electrooxidation

alkaline solution¹²⁵. The rate determining step for the oxidation of strongly adsorbed intermediates would be :



where the rds is a chemical surface reaction between the adsorbed residue and $\text{Pt} (\text{OH})_{\text{ads}}$. The $\text{Pt} (\text{OH})_{\text{ads}}$ formation at lower positive potentials in alkaline solutions than in acidic solution would account for the high activity of Pt electrocatalyst in the former medium.

The comparison of EG with electroadsorbed 1,3,dioxolane and adsorbed CO electrooxidation showed similar surface oxidation behaviour.

Antimony irreversibly adsorbed on the surface of Pt (100) was used as an electrode for the study of formic acid oxidation¹²⁶. The adsorbed antimony undergoes a surface redox reaction at nearly 0.66 V (RHE). In the most part of the potential range where the oxidation of the formic acid occurs the adatoms are in a zero valency state. The enhancement of the formic acid oxidation with increasing amount of adsorbed antimony is shown to be due to inhibition of the formation of the poisoning intermediate. A maximum of the oxidation current is obtained for an antimony coverage at $\theta_{\text{sb}} = 0.9$, where no poison is detected at the surface. For coverage below 0.7, the poisoning intermediate has been isolated on the modified Pt (100) electrode. The sequence for the oxidation of the two surface species shows that the antimony is oxidized first, forming an oxygenated species followed by poison oxidation. Because of the high regulation of both surface processes a clear example of a surface process involving an oxygen adsorbing adatom was observed.

4.4 Conclusion :

Direct conversion of chemical compounds (fuels) to electricity has a great future. These power generators are intrinsically much more efficient, pollution and noise free and has a great potential for future. These power generators known as fuel cells are already in use in developed countries as the power sources in space crafts, weather satellites, as underground power generators, as well as power sources in automobiles etc.

As such it is very important for a country like Bangladesh to start research work in this area which may help us to supply a fraction of our energy requirements.

With this aim, this work was launched to analyse the present state of developments of the power sources known as fuel cells.

An attempt was made to analyse the factors which influenced the performance of typical fuel cells and the current trend of research which is going on around the laboratories of the world and make an assessment of what has to be done in near future.

After a thorough literature survey and analysis we may make the following observations:

The role of electrocatalysts in the overall performance of the fuel cells is indispensable and of prime importance.

The electrodes composed of noble metals are at present widely used are extremely good catalysts. They have appropriate electronic characteristics and are non-corrodable in wide range of acidic and basic solution compositions. Moreover, the noble metals can be used at high anodic potentials required for oxygen reduction and oxidation of many organic fuels. Fuel cells using noble metal electrodes are well developed and are used for power sources where other advantages outweigh the factor of price of the electrodes.

Extensive research work is continuing to develop other materials having the characteristics of good catalysts.

Thus alloys of noble metals with other less expensive transition metals, inorganic oxides and compounds having semiconducting properties, inorganic and organic polymers including macrocyclic compounds are developed and studied from the point of view of electrocatalysts. It has been found that electronic and geometric factors of these compounds profoundly influence the rate and mechanism of electrochemical reaction.

As far the stability of electrodes in the anodic potential range where dissolution or passivation of the electrodes may occur, only a few have been developed. Thus inorganic oxide electrodes such as TiO_2 , RuO_2 , IrO_2 and quite a few other compounds have been used as electrodes for O_2 reduction reaction which is often the half cell reaction in a fuel cells.

Organic compounds can be used as cheap and highly efficient fuels for producing electrical energy provided suitable electrodes are developed which can be used in high anodic potentials. Scanty work has been done in this area. Systematic work keeping in view the electrocatalytic phenomena should be started in this area.

Proper research for the development of suitable electrode material as well as elaborate studies to understand the mechanism of the complicated multistep organic reactions are to be pursued so that cheap organic compounds can be used as fuel in fuel cells.

As in chemical catalysis, the phenomena of adsorption of active compound on the electrode (catalyst) surface is of immense importance. Already work has been done to understand the nature of adsorption, bond making and breaking in case of hydrogen evolution and oxygen reduction processes. It has been found that the geometric and electronic structures are very important for such phenomena. Research work is in progress to understand the behaviour of other prospective which can be used as power sources.

Simultaneously, theoretical work is continuing to understand the quantum mechanical aspects of charge transfer process. The rate process is enhanced by tunnelling through the potential energy barrier in addition to climbing over the energy barrier. A composite number forces are acting on the ions or molecules on the electrode-electrolyte interface and a mathematical expression for the condition for tunnelling has been developed here.

In conclusion, it may be said that judging the importance of development of fuel cells as future energy converters, much more research work in the above area should be embarked upon in collaboration with physicists, material scientists and engineers to produce novel materials having the properties of noble metals which can be used in fuel cells.

REFERENCES

REFERENCES

1. Chang, S.L., "Energy Conversion", Prentice-Hall, Inc., Englewood Cliffs, N.J., 1963.
2. Angrist, S.W., "Direct Energy Conversion", Allyn and Bacon, Inc., Englewood Cliffs, J.J., 1964.
3. Sutton, G.W., "Direct Energy Conversion", McGraw-Hill Book Company, New York, 1966.
4. TRW, Inc., "Advanced Solar Thermionic Power Systems", Office Tech. Serv., Dept. Comm. Tech. Doc. Rept. ASD-7DR-62-877 (AD 295917), 1962.
5. Avco Everett Research Laboratory (Via J. Klepeis), private communication, 1969.
6. Altman, M., Private communication, University of Pennsylvania, 1969.
7. Morrill, C.C., Proc. Ann. Power Sources Conf., 19, 38, 1965.
8. Gileadi, E., and S. Srinivasan, *J. Electroanal Chem.*, 7, 452, 1964.
9. Grubb, W.T., *Nature*, 198, 883, 1963.
10. Shropshire, J. a., and B.L. Tarmy, Fuel Cells, *Advan. Chem. Ser. 47*, Chap 12, American Chemical Society, Washington, D.C., 1965.
11. Bockris, J. O'M., *J. Electrochem. Soc.*, 98, 153C, 1951.
12. Langmuir, I., *J. Am. Chem. Soc.*, 40, 1361 1918.
13. Henry, W., *Phil. Trans, roy, Soc. London*, 29, 274, 1803.
14. Frumkin, a. N., *Z. Physik*, 35, 792, 1926.
15. Temkin, M.I., *Zh. Fiz. Khim.*, 15, 296, 1941.
16. Bailey, D.N., D. M. Hercules, and D. K. Roe, *R. Electrochem. Soc.*, 116, 190, 1969.
17. Wilson, H. A., "Modern Physics", Chap. 4, Blackie and Son Ltd., Glasgow, 1928.
18. Bockris, J. O'M, Chap. 4 in J. O'M Bockris and B.E. Conway (eds), "Modern Aspects of Electrochemistry", Vol. 1, Butterworth and Co. (Publishers), Ltd., London, 1954.
19. Moser, J., *Mol. Chem.*, 8, 373, 1887; Rigollof, H., *Compt. Rend., Acad. Sci. Paris*, 116, 873, 1893.
20. Thompson, G.E. *Phys. Rev.* 5, 43, 1915; Stora, C., *J. Chim. Phys.*, 29, 168, 1932.

21. Fisenberg, M., and H.P. Silverman, *Electrochim. Acta*, 5, 1, 1961.
22. Bockris, J. O'M., Chap. 4, in J.O'M. Bockris and B.E. Conway (eds), "Modern Aspects of Electrochemistry", vol. 1, Butterworth and Co. (Publishers), Ltd., London.
23. Piersma, B.J., and E. Gileadi, Chap. 2, in J.O'M Bockris (ed), "Modern Aspect of Electrochemistry", Vol. 4, Plenum Press, New York, 1967.
24. Dahms, H., and J.O'M Bockris, *J. Electrochem. Soc.* 111, 728, 1964.
25. Grubb, W.T., *Nature*, 198, 883, 1963.
26. Adlhart, O.J., and K.O. Hever, Engelhard report on Fuel Cell Catalysis, Contract No. Da 36-039 SC-90691, 1964.
27. Gerischer, H., *Ber. Bunsenges, Physik, Chem.*, 67, 164, 1963.
28. Allen, M.J., "Organic Electrode Reactions", Reinhold Publishing Corporation, New York, 1958.
29. Shropshire, J. A. and B.L. Tarny, *Advan. Chem. Ser.*, 47, 153, 1965.
30. Bockris, J.O'M., and Srinivasan, *Nature*, 215, 197, 1967.
31. Schwan, H.P., *Advan. Biol. Med. Phys.*, 5, 147, 1957.
32. Sherman, A., and H. Eyring, *J. Amer. Chem. Soc.*, 54, 2661, 1932.
33. Damjanovic, A., Private Communication, 1968.
34. Conway, B.E, and J.O'M. Bockris, *Electrochim. Acta*, 3, 349, 1961.
35. Drazic, D., and J.O'M Bockris, *Electrochim, Acta*, 7, 293, 1962.
36. Herring, C., Chap. 1, in R. Gomer and C.S. Smith (eds), "Structures and Properties of Solid Surfaces", The University of Chicago Press, Chicago, 1953.
37. Pauling, L., *Phys. Rev.* 54, 899, 1938; *Proc. Roy. Soc., Ser. A* 196, 343, 1949.
38. Smith, J.O., et al., Monsanto Research Corporation Annual Technical Report for period 15 May - 15 November, 1963, under USAERDL Contract No. DA-44-009-AMC 202 (T).
39. Sepa, D.B., A. Damjanovic, and J.O'M. Bockris, *Electrochim. Acta.*, 12, 746, 1967; A. Damjanovic, D. Septa and J.O'M. Bockris, *J. Res. Inst. Cat.*, 16, 1, 1968.
40. Bowden, F. P., and E.K. Rideal, *Proc. Roy. Soc., Ser. A*, 120, 59, 1928.
41. Gileadi, E., *J. Electroanal. Chem.*, 11, 137, 1966.

42. Eyring, H., S. Glasston, and K.J. Laidler, *J. Chem. Phys.*, **7**, 1053, 1939.
43. Horiuti, J., and M. Polanyi, *Acta Physicochim, USSR*, **2**, 505, 1935.
44. Bockris, J.O'M., and A.K.N. Reddy, "Essentials of Modern Electrochemistry", plenum Press, New York, 1969.
45. G. Gouy, *J. Physique*, **4**, 457, 1910.
46. D.L. Chapman, *Phil. Mag. Ser. 6*, **25**, 475, 1913.
47. W. H. Brattain and P.J. Boddy, *J. Electrochem. Soc.*, **109**, 574, 1962.
48. K. Bohnenkamp and J.J. Engell, *Z. Elektrochem.*, **61**, 1184, 1957.
49. H.U. Harten and R. Memming, *Phys. Lett.*, **3**, 95, 1962.
50. R. Memming, *Surf. Sci.*, **7**, 89, 1963.
51. P.J. Body and W.H. Brattain, *J. Electrochem. Soc.*, **110**, 570, 1963.
52. M. Hofmann-Perez and H. Gerischer, *Z. Electrochem.*, **65**, 771, 1961.
53. R. Memming and G. Schwandt, *Electrochim. Acta*, **13**, 1299, 1968.
54. W. H. Brattain and C.G.B. Garrett, *Bell. Syst. Tech. J.*, **34**, 129, 1955.
55. E. A. Efinov and J.G. Erusarlimchik, *Zh. Fiz. Khim*, **32**, 1103, 1958.
56. R. Memming and G. Schwandt, *Angew. Chem.* **79**, 833, 1967.
57. H.U. Harten and W. Schultz, *Z. Phys.*, **141**, 319, 1955.
58. Y.V. Pleskov, *Dokl. Akad. Nauk USSR*, **126**, 111, 1959.
59. H. Gerischer, A. Maurer, and W. Mandt, *Surf. Sci.*, **4**, 431, 1966.
60. H. Gerischer, and W. Mandt, *Surf. Sci.*, **1**, 440, 1966.
61. F. Beck and H. Gerischer, *Z. Electrochem.*, **63**, 500, 1959.
62. R. Memming and G. Schwandt, *Surf. Sci.*, **4**, 109, 1966.
63. F. Mollers and R. Memming, *Ber. Bunsenges*, **76**, 471, 1972.
64. R. W. Gurney, *Proc. Roy. Soc. A134*, 137, 1931.
65. N. S. Hush, *J. Chem. Phys.*, **28**, 962, 1958; *Trans. Faraday Soc.*, **57**, 557, 1961.
66. R. A. Marcus, *J. Chem. Phys.* **28**, 962, 1965.
67. V.G. Levich, *Advances in Electrochemistry and Electrochemical Engineering*, Vol. 4 (P. Delahay, ed), Interscience, new York, 1966.
68. R.R. Dogonadze and Y.A. Chizmadzhev, *Dokl. Akad. Nauk, USSR*, **144**, 463, 1962; **145**, 563, 1963.

69. A. M. Kuznetsov and R.R. Dogonadze, *izv. Akad. Maik*, 10, 1787, 1964.
70. H. Gerischer, *Z. Phys. chem. NF*, 26, 223, 1960; 27, 48, 1961.
71. R. Memming, Proceedings of the symposium on Electrocatalysis (M. Brister, ed), electrochem. Society, Binceton, 1974, p. 178.
72. H. Gerischer, in *Physical Chemistry*, Vol. 9A (M. Eyring, D. Henderson, and W. Jost, eds), Academic, New York, 1970.
73. K. H. Beckmann and R. Memming, *J. Electrochem. Soc.*, 116, 368, 1969.
74. R. Memming and g. Neumann, *Phys. Lett.*, 24A, 19, 1967; *Surf. Sci.*, 10, 1, 1968.
75. U. Plitt, Ph. D. Thesis, Gottingen, 1974.
76. D. Park, *Introduction to Quantum Theory*, McGraw-Hill, New York, 1974.
77. C. Eckart, *Phys. Rev.*, 35, 1303, 1930.
78. R. W. Gurney, *Proc. Roy. Soc.*, A134, 137, 1931.
79. D.B. Matthews and S.U.M. Khan, *Aust. J. Chem.*, 28, 253, 1975.
80. J.A.V. Butler, *Proc. Roy. Soc.*, A125, 423, 1936.
81. Mathews, D.B., Doctoral dissertation, University of Pennsylvania, Philadelphia, 1965.
82. Damjanovic, A., and V. Brusic, *Electrochim. Acta*, 12, 615, 1967.
83. C. Lany, *Electrochim. Acta*, 29, 1581, 1984.
84. J. M. Leger, and C. Lamy, *Electrochim. Acta*, 29, 1611, 1984.
85. C. Guyen Van Huong, *Electroanal. Chem.*, 264, 247, 1989.
86. J. Zhu, Th. hartung, *Electronal. Chem.* 244, 241, 1989.
87. A. Hamelin, S. Morin, *Electroanal. Chem.*, 272, 241, 1989.
88. Dian Song, Manuel P. Soriaga, *Electronal Chem*, 184, 171, 1985.
89. M. P. Soriaga, J.H. White, D. Song, *Electroanal Che.*, 171, 359, 1984.
90. D. E. Brown, N.M. Mahmood, A.K. Turner, *Electrochi. Acta*, 29, 1551, 1984.
91. Katsunori Nishimura, Michio Enyo, *Electroanal. Chem.*, 260, 181, 1989.
92. M. Kau and J. Russow, *Electrochim. Acta*, 29, 1609, 1984.
93. R. R. Adzic, *Electrochim. Acta*, 29, 1597, 1984.
94. K. Juttner, *Electrochim. Acta*, 29, 1597, 1984.
95. N. M. Markovic, R.R. Adzic, *Electrochim. Acta*, 29, 1609, 1984.
96. v. S. Bagotzky and A.M. Skundin; *Electrochim. Acta*, 30, 485, 1985.
97. J. Clavilier, A. aldaz, *Electroanal. Chem*, 258, 89, 1989.

98. M. M. Pecherskii, V.V. Losev, *Elektrokhimiya*, 18, 415, 1982.
99. S. Trasatti, *Electrochim. Acta*, 29, 1503, 1984.
100. G. Lody, E. Sivieri, S. Trasatti, *J. Appl. Electrochem*, 8, 135, 1978.
101. Y. Matsumoto, *Electrochim. Acta*, 29, 1607, 1984.
102. L.J.J. Janseen, *Electrochim. Acta*, 29, 1607, 1984.
103. R. Kotz, *Electrochim. Acta*, 29, 1607, 1984.
104. H. Tamura, Y. Matsumoto, Physico-chemie and electrochemical properties perovskite oxides, in *Electrodes of conductive metallic oxides* (Edited by S. Trasatti) Part A, pp. 261-300.
105. M. Spasojevic and N. Kratajic, *Electrochim. Acta*, 29, 1608, 1984.
106. F. Beck, W. Gabriel, H. Schulz, *Electrochim. Acta*, 29, 1611, 1984.
107. F. Beck, and H. Schulz, *Electrochim. Acta*, 29, 1569, 1984.
108. E. Yeager, *Electrochim. Acta*, 29, 1527, 1984.
109. E. Yeager, Mechanism of Electrochemical Reaction on non-metallic surfaces, in *Electrocatalysis on Non-metallic surfaces*, pp 203-219. NBS Special Publication 455, 1976.
110. M. Tarasevich, A. Sadkowski and E. Yeager, *Oxygen Electrochemistry*, Vol. 7, Kinetics and Mechanism of Electrode Process, Chap. 6, pp. 301-398, Plenum Press, New York, 1983.
111. V. A. Garten and P.E. Weiss, *Austral. J. Chem.*, 8, 81, 1955.
112. V. A. Garten and P.E. Weiss, *Rev. Pure appl. Chem.*, 7, 69, 1957.
113. Z.W. Zhang, D. Tryk and E. Yeager, National Meeting, The Electrochem. Soc., Washington, October 1983.
114. J. P. Collman, M. Marrocco, F. Anson, *J. Electroanal. Chem*, 101, 117, 1979.
115. J. P. Collman, M. Marrocco, F. Anson, *J. An. Chem. Soc.*, 103, 6027, 1980.
116. H.Y. Liu, M. Weaver, C. Wang, C. Chang, *J. Electroanal. Chem.*, 145, 439, 1983.
117. S. Sarnagapani, F. Urbach and E. Yeager, to be published.
118. D. Venderschmitt, S. Fallat, *Helv. Chim. Acta*, 48, 951, 1965.
119. J. Veprek-Siska, D.M. Wagnerova, *Chimia*, 26, 75, 1972.
120. J. Zagal, P. Bindra, E. Yeager, *J. electrochem. Soc.*, 127, 1506, 1980.
121. J. Zagal, R. Sen, E. Yeager, *Inorg. Chem.*, 16, 3379, 1977.
122. R. Jasinski, *J. electrochem. Soc.*, 122, 526, 1965.
123. A. Kozawa, R. J. Brood, *J. electrochem. Soc.*, 117, 1470, 1970.

124. M. Behret, S. Sandstede, *ber. Bunsenges, Phys. Chem.* 81, 54, 1977.
125. A. J. Appleby, J. Fleish and M. Savy, *J. Catal.*, 44, 281, 1976.
126. D. Scherson, C. Fierro, E.B. Yeager, *electrochim. Acta*, 29, 1609, 1984.
127. F.E. Woodard, R.E.W. Jansson, *Electroanal. Chem.* 214, 303, 1986.
128. H. Wroblowa, J.O'M Bockris, *Electroanal. Chem.* 6, 401, 1963.
129. H. Wroblowa, J.O'M Bockris, to be published.
130. E. Justi and A. Windsel, *Fuel cells*, Franz Steiner Publisher, Wiesbaden, 1962, p.66.
131. J.O'M. Bockris, H. Wroblowa, *Electroanal. Chem.* 7, 428, 1964.
132. E. Santos and M.C. Giordano, *Electrochim. Acta*, 30, 871, 1985.
133. J. March, *Advanced Organic Chemistry: Reaction mechanisms and structure*, Kogakvsha Co. Ltd., Tokyo, 1968.
134. D. J. Cram and G.S. Hammond, *Quimica Organica*, McGraw-Hill, New York- Toronto - London, 1963.
135. E. Santos and M.C. Giordano, *Electrochim. Acta*, 29, 1327, 1984.
136. J. Clavilier, J. M. Fellu, A. Aldaz, *Electroanal. Chem.*, 258, 89, 1989.
137. L. V. Azeroff, J. J. Brophy, *Electronic Processes in Materials*, Chap. 8, pp. 194, McGraw-Hill Book Co. Ltd., 1963.
138. R. A. Smith, *Semiconductors*, Chap. 3, pp. 45, Syndics of the Cambridge University Press, London, 1959.
139. J.O'M Bockris, S. Srinivasan, *Fuel Cells : Their Electrochemistry*, Chap. 1,2, 3,6,10, pp. 1 -515, McGraw-Hill Bok Co. Ltd., New York.
140. Allen. J. Bard, *Electroanalytical Chemistry*, Vol. 11, pp. 2, Marcel Dekker Inc., New York and Basel, 1979.
141. J.O'M. Bockris and S.U.M. Khan, *Quantum Electrochemistry*, Chap. 8, pp. 235, Plenum Press, New York and London, 1979.

